Supplementary Materials: From extracellular-space compression to extracranial electromagnetic response: multiscale forward modelling of ischemia-associated tissue change

Jiawei Tang[1], Yuhao Liu[1], Shuzhong Tan[1], Wen Yang[1] and Degang Xu[1,*]

Description: Analytical equations, physiological anchors, numerical verification, material provenance, raw complex voltages and additional forward-model comparisons.

Sections S1–S8 preserve historical numerical records, with explicit direct replacements for selected S5b rows and supersession notices for the affected head-reference records. Sections S9–S11 add the major-revision analyses and supersede the original unequal-effect sensitivity interpretation. Tables retain existing numerical records and their original denominators. Display rounding does not replace the full-precision CSV companions. These are benchmark and reference forward calculations, not tissue calibration or hardware measurements.

S1. Physiological anchors and analytical benchmark

Perez-Pinzon et al. [1] supplies these anchors. "Matched" refers to corresponding regional reference/ischemic conditions; it does not establish longitudinal tracking of the same cell or animal. The controlled ϕ = 0.20 to 0.05 RVE span is not the measured CA1 pair. Under fixed local volume and effective cell number, $P = 1 - \phi$, $V/V_0 = P/P_0$ and $\frac{R}{R_0} = \left(\frac{P}{P_0}\right)^{1/3}$. These are geometric assumptions, not observations of isotropic cell deformation, neurite morphology or macroscopic swelling.

Table S1a. Independent regional ECS anchors and model-derived geometry

Table S1a, column panel 1/2. First column is repeated for alignment.

Row	region	phi_ecs_normal	phi_ecs_ischemia	p_normal
1	CA3	0.2	0.17	0.8
2	cortex	0.18	0.09	0.82
3	CA1	0.14	0.05	0.86

Table S1a, column panel 2/2. First column is repeated for alignment.

Row	region	p_ischemia	derived_volume_ratio	derived_radius_ratio
1	CA3	0.83	1.0375	1.012346926
2	cortex	0.91	1.10975609756	1.03532296317
3	CA1	0.95	1.10465116279	1.03373300987

Units: All fractions and V/V0/R/R0 dimensionless. Denominator: Each region has its own normal state. ECS anchors are literature evidence; derived ratios assume fixed local volume and effective cell number.

Full records: Table_S1a.csv.

Table S1b. Recorded single-shell benchmark features

Table S1b, column panel 1/2. First column is repeated for alignment.

Row	region	phi_ECS_normal	phi_ECS_ischemia	max_relative_contrast
1	CA3	0.2	0.17	15.889037875
2	cortex	0.18	0.09	51.5032189973
3	CA1	0.14	0.05	65.3051153532

Table S1b, column panel 2/2. First column is repeated for alignment.

Row	region	f_max_relative	beta_shift_percent
1	CA3	1000	-0.15982773285
2	cortex	1000	-0.326764381485
3	CA1	1000	-0.218356218852

Units: Hz; conductivity contrast percent; beta shift percent. Denominator: Same-region normal conductivity and beta frequency. Benchmark quantities, not measured ischemic conductivity or a regional severity ranking.

Full records: Table_S1b.csv.

The single-shell benchmark uses the 5 μm normal equivalent radius, 5 nm membrane, $\sigma_i = \sigma_e = 1\ \mathrm{S\,m^{-1}}$, $\varepsilon_{r,i} = \varepsilon_{r,e} = 80$, $\sigma_m = 10^{-7}\ \mathrm{S\,m^{-1}}$ and $\varepsilon_{r,m} = 5$ described in Methods 2.2. The shell and mixing formulas are given in S2. No earlier pilot severity series is included.

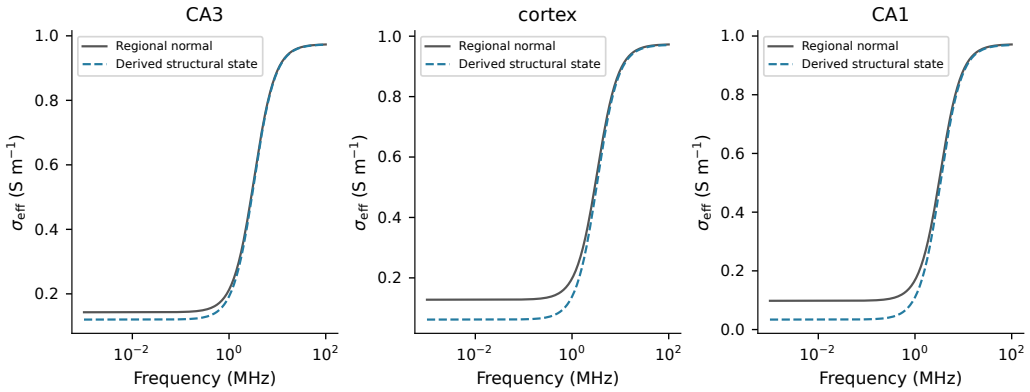


Figure S1. Three independent regional paired benchmark spectra. Lines connect the 201 frozen points per region; no new peak extraction, smoothing or fitting was performed. The ischemic ECS anchor defines a derived structural state under benchmark electrical properties.

S2. Analytical equations, branch selection and model-form comparison

The time convention is $\exp(+j\omega t)$, $\gamma = \sigma + j\omega\varepsilon_0\varepsilon_r = j\omega\varepsilon_0\varepsilon^*$, with $\varepsilon^* = \varepsilon_r - j\sigma/(\omega\varepsilon_0)$. Set $v = (1 - d_m/R)^3$. The coated-cell admittivity is

$$\gamma_c = \gamma_m \frac{2(1-v)\gamma_m + (1+2v)\gamma_i}{(2+v)\gamma_m + (1-v)\gamma_i}. \tag{S1}$$

M1, ECS-host Maxwell–Garnett:

$$\gamma_{M1} = \gamma_e \frac{\gamma_c + 2\gamma_e + 2P(\gamma_c - \gamma_e)}{\gamma_c + 2\gamma_e - P(\gamma_c - \gamma_e)}. \tag{S2}$$

M2, symmetric Bruggeman:

$$P\frac{\gamma_c - \gamma}{\gamma_c + 2\gamma} + (1-P)\frac{\gamma_e - \gamma}{\gamma_e + 2\gamma} = 0. \tag{S3}$$

Writing $a = P(2\gamma_c - \gamma_e) + (1-P)(2\gamma_e - \gamma_c)$, the roots are $[a \pm \sqrt{a^2 + 8\gamma_c\gamma_e}]/4$. The implemented branch selection is performed in complex-permittivity space: at the first sampled frequency select the root nearest the linear mixture; at subsequent frequencies select the root nearest the preceding selected ε^* value. This describes the actual numerical continuation, not a claim that sign selection on the square root alone identifies the physical branch. The archived branch was not re-solved.

M3, host/inclusion-swapped Maxwell–Garnett comparator:

$$\gamma_{M3} = \gamma_c \frac{\gamma_e + 2\gamma_c + 2(1-P)(\gamma_e - \gamma_c)}{\gamma_e + 2\gamma_c - (1-P)(\gamma_e - \gamma_c)}. \tag{S4}$$

Citations: Pauly and Schwan [2] for the shell-model tradition; Garnett [3], Bruggeman [4], and Markel [5] for effective-medium theory and expressions. M3 is the same MG construction with host/inclusion exchanged, not a separate classical theory. High occupancy is not a dilute-sphere validation regime.

Table S2a. Analytical model-form comparison

Table S2a, column panel 1/2. First column is repeated for alignment.

Row	region	model_short	max_relative_contrast	f_max_relative
1	CA3	M1	15.889037875	1000
2	CA3	M2	43.0269586426	42169.6503429
3	CA3	M3	13.5260591697	149623.565609
4	cortex	M1	51.5032189973	1000
5	cortex	M2	74.1490163206	63095.734448
6	cortex	M3	39.1960372926	158489.319246
7	CA1	M1	65.3051153532	1000
8	CA1	M2	69.3603367008	94406.0876286
9	CA1	M3	43.5039429964	167880.401812

Table S2a, column panel 2/2. First column is repeated for alignment.

Row	region	max_absolute_contrast	f_max_absolute	beta_shift_percent
1	CA3	0.0227132134455	1000	-0.15982773285
2	CA3	0.0199420532471	1188502.22744	0.390511775311
3	CA3	0.0210455269647	1496235.65609	0.394009552152
4	cortex	0.0657965727608	1000	-0.326764381485

Table S2a continued

Row	region	max_absolute_contrast	f_max_absolute	beta_shift_percent
5	cortex	0.058452040129	1333521.43216	1.16322588712
6	cortex	0.0611689165316	1584893.19246	1.14187842701
7	CA1	0.0639968552179	1000	-0.218356218852
8	CA1	0.0576359331231	1496235.65609	1.15344709573
9	CA1	0.0596766746996	1678804.01812	1.13598018281

Units: Hz; percent; $\mathrm{S\,m^{-1}}$. Denominator: Same-region normal under each model. No analytical model is treated as ground truth.

Full records: Table_S2a.csv.

Table S2b. Sign-agreement summary

Table S2b, column panel 1/2. First column is repeated for alignment.

Row	pair_id	region	frequency_band	frequency_points
1	CA3_pair	CA3	overall 1 kHz-100 MHz	201
2	CA3_pair	CA3	1 kHz-100 kHz	81
3	CA3_pair	CA3	100 kHz-1 MHz	40
4	CA3_pair	CA3	1-10 MHz	40
5	CA3_pair	CA3	10-100 MHz	40
6	cortex_pair	cortex	overall 1 kHz-100 MHz	201
7	cortex_pair	cortex	1 kHz-100 kHz	81
8	cortex_pair	cortex	100 kHz-1 MHz	40
9	cortex_pair	cortex	1-10 MHz	40
10	cortex_pair	cortex	10-100 MHz	40
11	CA1_pair	CA1	overall 1 kHz-100 MHz	201
12	CA1_pair	CA1	1 kHz-100 kHz	81
13	CA1_pair	CA1	100 kHz-1 MHz	40
14	CA1_pair	CA1	1-10 MHz	40
15	CA1_pair	CA1	10-100 MHz	40

Table S2b, column panel 2/2. First column is repeated for alignment.

Row	pair_id	sign_agreement_fraction
1	CA3_pair	1
2	CA3_pair	1
3	CA3_pair	1
4	CA3_pair	1
5	CA3_pair	1
6	cortex_pair	1
7	cortex_pair	1
8	cortex_pair	1
9	cortex_pair	1
10	cortex_pair	1
11	CA1_pair	1
12	CA1_pair	1
13	CA1_pair	1

Table S2b continued

Row	pair_id	sign_agreement_fraction
14	CA1_pair	1
15	CA1_pair	1

Units: Counts; fraction. Denominator: Number of frequencies within each recorded band. Band summaries overlap the overall row; do not sum all band counts.

Full records: Table_S2b.csv.

Table S2c. Frequency-resolved model contrasts and sign agreement

pair_id	frequency_hz	contrast_M1_s_per_m	contrast_M2_s_per_m	contrast_M3_s_per_m	sign_agreement
CA3_pair	1000	-0.0227132134455	$-4.4141388448 \times 10^{-5}$	$-1.15897360581 \times 10^{-5}$	True
CA3_pair	1059.25372518	-0.0227132131687	$-4.42519968119 \times 10^{-5}$	$-1.15956814125 \times 10^{-5}$	True
CA3_pair	1122.0184543	-0.022713212858	$-4.4376099076 \times 10^{-5}$	$-1.16023522074 \times 10^{-5}$	True
CA3_pair	1188.50222744	-0.0227132125095	$-4.45153411335 \times 10^{-5}$	$-1.16098369592 \times 10^{-5}$	True
CA3_pair	1258.92541179	-0.0227132121184	$-4.46715695493 \times 10^{-5}$	$-1.16182349849 \times 10^{-5}$	True
CA3_pair	1333.52143216	-0.0227132116796	$-4.48468560035 \times 10^{-5}$	$-1.16276577198 \times 10^{-5}$	True
CA3_pair	1412.53754462	-0.0227132111873	$-4.5043524709 \times 10^{-5}$	$-1.16382301959 \times 10^{-5}$	True
CA3_pair	1496.23565609	-0.0227132106349	$-4.52641831599 \times 10^{-5}$	$-1.16500927013 \times 10^{-5}$	True
CA3_pair	1584.89319246	-0.0227132100151	$-4.55117566153 \times 10^{-5}$	$-1.16634026414 \times 10^{-5}$	True
CA3_pair	1678.80401812	-0.0227132093197	$-4.57895267697 \times 10^{-5}$	$-1.16783366273 \times 10^{-5}$	True
CA3_pair	1778.27941004	-0.0227132085394	$-4.61011751154 \times 10^{-5}$	$-1.16950928193 \times 10^{-5}$	True
CA3_pair	1883.64908949	-0.0227132076639	$-4.64508315625 \times 10^{-5}$	$-1.17138935562 \times 10^{-5}$	True
CA3_pair	1995.26231497	-0.0227132066816	$-4.68431289487 \times 10^{-5}$	$-1.17349883049 \times 10^{-5}$	True
CA3_pair	2113.48903984	-0.0227132055794	$-4.72832641484 \times 10^{-5}$	$-1.1758656971 \times 10^{-5}$	True
CA3_pair	2238.72113857	-0.0227132043428	$-4.77770665705 \times 10^{-5}$	$-1.17852136115 \times 10^{-5}$	True
CA3_pair	2371.37370566	-0.0227132029552	$-4.83310749311 \times 10^{-5}$	$-1.18150106026 \times 10^{-5}$	True
CA3_pair	2511.88643151	-0.0227132013983	$-4.89526232878 \times 10^{-5}$	$-1.18484433137 \times 10^{-5}$	True
CA3_pair	2660.7250598	-0.0227131996515	$-4.96499374395 \times 10^{-5}$	$-1.18859553538 \times 10^{-5}$	True
CA3_pair	2818.38293126	-0.0227131976915	$-5.04322429216 \times 10^{-5}$	$-1.19280444557 \times 10^{-5}$	True
CA3_pair	2985.38261892	-0.0227131954924	$-5.13098859682 \times 10^{-5}$	$-1.19752690798 \times 10^{-5}$	True
CA3_pair	3162.27766017	-0.0227131930249	$-5.22944689704 \times 10^{-5}$	$-1.20282558222 \times 10^{-5}$	True
CA3_pair	3349.65439158	-0.0227131902564	$-5.33990021305 \times 10^{-5}$	$-1.2087707727 \times 10^{-5}$	True
CA3_pair	3548.13389234	-0.0227131871501	$-5.46380732035 \times 10^{-5}$	$-1.21544136119 \times 10^{-5}$	True
CA3_pair	3758.37404288	-0.0227131836647	$-5.60280374252 \times 10^{-5}$	$-1.22292585318 \times 10^{-5}$	True
CA3_pair	3981.07170553	-0.022713179754	$-5.75872299551 \times 10^{-5}$	$-1.23132355179 \times 10^{-5}$	True
CA3_pair	4216.96503429	-0.0227131753662	$-5.9336203413 \times 10^{-5}$	$-1.24074587485 \times 10^{-5}$	True
CA3_pair	4466.83592151	-0.022713170443	$-6.12979933573 \times 10^{-5}$	$-1.25131783258 \times 10^{-5}$	True

Table S2c continued

pair_id	frequency_hz	contrast_M1_s_per_m	contrast_M2_s_per_m	contrast_M3_s_per_m	sign_agreement
CA3_pair	4731.51258961	-0.022713164919	$-6.34984148491 \times 10^{-5}$	$-1.26317968538 \times 10^{-5}$	True
CA3_pair	5011.87233627	-0.022713158721	$-6.59663935606 \times 10^{-5}$	$-1.27648880386 \times 10^{-5}$	True
CA3_pair	5308.84444231	-0.0227131517668	$-6.87343352229 \times 10^{-5}$	$-1.29142175544 \times 10^{-5}$	True
CA3_pair	5623.4132519	-0.022713143964	$-7.18385375681 \times 10^{-5}$	$-1.30817664535 \times 10^{-5}$	True
CA3_pair	5956.62143529	-0.0227131352092	$-7.53196492911 \times 10^{-5}$	$-1.32697574297 \times 10^{-5}$	True
CA3_pair	6309.5734448	-0.0227131253861	$-7.92231809475 \times 10^{-5}$	$-1.34806842807 \times 10^{-5}$	True
CA3_pair	6683.43917569	-0.0227131143644	$-8.36000730955 \times 10^{-5}$	$-1.37173449611 \times 10^{-5}$	True
CA3_pair	7079.45784384	-0.0227131019979	$-8.8507327381 \times 10^{-5}$	$-1.39828786601 \times 10^{-5}$	True
CA3_pair	7498.94209332	-0.0227130881225	$-9.40087066419 \times 10^{-5}$	$-1.42808073959 \times 10^{-5}$	True
CA3_pair	7943.28234724	-0.022713072554	-0.000100175510454	$-1.46150826728 \times 10^{-5}$	True
CA3_pair	8413.95141645	-0.0227130550859	-0.00010708743283	$-1.49901378181 \times 10^{-5}$	True
CA3_pair	8912.50938134	-0.0227130354864	-0.000114833509	$-1.54109466872 \times 10^{-5}$	True
CA3_pair	9440.60876286	-0.0227130134955	-0.000123513158297	$-1.58830895094 \times 10^{-5}$	True
CA3_pair	10000	-0.0227129888213	-0.000133237330092	$-1.64128267397 \times 10^{-5}$	True
CA3_pair	10592.5372518	-0.0227129611364	-0.000144129759471	$-1.70071818867 \times 10^{-5}$	True
CA3_pair	11220.184543	-0.0227129300736	-0.000156328338735	$-1.76740344031 \times 10^{-5}$	True
CA3_pair	11885.0222744	-0.0227128952207	-0.000169986609899	$-1.8422223853 \times 10^{-5}$	True
CA3_pair	12589.2541179	-0.0227128561151	-0.000185275381912	$-1.92616667209 \times 10^{-5}$	True
CA3_pair	13335.2143216	-0.0227128122382	-0.00020238447434	$-2.02034873828 \times 10^{-5}$	True
CA3_pair	14125.3754462	-0.0227127630076	-0.000221524586466	$-2.12601649481 \times 10^{-5}$	True
CA3_pair	14962.3565609	-0.0227127077703	-0.000242929287112	$-2.2445697877 \times 10^{-5}$	True
CA3_pair	15848.9319246	-0.0227126457933	-0.000266857115723	$-2.3775788508 \times 10^{-5}$	True
CA3_pair	16788.0401812	-0.0227125762544	-0.000293593779207	$-2.52680498779 \times 10^{-5}$	True
CA3_pair	17782.7941004	-0.022712498231	-0.00032345442142	$-2.69422374979 \times 10^{-5}$	True
CA3_pair	18836.4908949	-0.0227124106879	-0.000356785932889	$-2.88205090575 \times 10^{-5}$	True
CA3_pair	19952.6231497	-0.0227123124638	-0.000393969257064	$-3.09277153736 \times 10^{-5}$	True
CA3_pair	21134.8903984	-0.0227122022555	-0.000435421636021	$-3.32917262822 \times 10^{-5}$	True
CA3_pair	22387.2113857	-0.0227120786011	-0.000481598722848	$-3.59437955931 \times 10^{-5}$	True

Table S2c continued

pair_id	frequency_hz	contrast_M1_s_per_m	contrast_M2_s_per_m	contrast_M3_s_per_m	sign_agreement
CA3_pair	23713.7370566	-0.0227119398603	-0.000532996470128	$-3.89189696922 \times 10^{-5}$	True
CA3_pair	25118.8643151	-0.0227117841925	-0.000590152683953	$-4.22565448898 \times 10^{-5}$	True
CA3_pair	26607.250598	-0.0227116095329	-0.000653648111357	$-4.60005791771 \times 10^{-5}$	True
CA3_pair	28183.8293126	-0.022711413565	-0.000724106906505	$-5.02004646691 \times 10^{-5}$	True
CA3_pair	29853.8261892	-0.0227111936894	-0.000802196298633	$-5.49115676884 \times 10^{-5}$	True
CA3_pair	31622.7766017	-0.0227109469901	-0.000888625264181	$-6.01959441742 \times 10^{-5}$	True
CA3_pair	33496.5439158	-0.0227106701954	-0.000984141988866	$-6.61231388958 \times 10^{-5}$	True
CA3_pair	35481.3389234	-0.0227103596348	-0.00108952989546	$-7.27710778011 \times 10^{-5}$	True
CA3_pair	37583.7404288	-0.0227100111904	-0.0012056020129	$-8.02270637414 \times 10^{-5}$	True
CA3_pair	39810.7170553	-0.0227096202422	-0.00133319347581	$-8.85888867765 \times 10^{-5}$	True
CA3_pair	42169.6503429	-0.0227091816075	-0.00147315197466	$-9.79660612753 \times 10^{-5}$	True
CA3_pair	44668.3592151	-0.0227086894717	-0.00162632602882	-0.000108481203068	True
CA3_pair	47315.1258961	-0.0227081373122	-0.00179355103146	-0.000120271560964	True
CA3_pair	50118.7233627	-0.0227075178114	-0.00197563311729	-0.000133490717996	True
CA3_pair	53088.4444231	-0.0227068227611	-0.00217333103176	-0.000148310478764	True
CA3_pair	56234.132519	-0.0227060429533	-0.00238733632937	-0.000164922960131	True
CA3_pair	59566.2143529	-0.0227051680595	-0.00261825239243	-0.000183542903329	True
CA3_pair	63095.734448	-0.022704186494	-0.00286657292906	-0.000204410225994	True
CA3_pair	66834.3917569	-0.0227030852622	-0.00313266076537	-0.000227792832867	True
CA3_pair	70794.5784384	-0.022701849789	-0.00341672787557	-0.000253989703586	True
CA3_pair	74989.4209332	-0.0227004637282	-0.00371881767521	-0.000283334275028	True
CA3_pair	79432.8234724	-0.0226989087472	-0.00403879062184	-0.000316198133883	True
CA3_pair	84139.5141645	-0.0226971642877	-0.00437631410883	-0.000352995032189	True
CA3_pair	89125.0938134	-0.0226952072966	-0.00473085749692	-0.000394185234182	True
CA3_pair	94406.0876286	-0.0226930119249	-0.00510169290505	-0.000440280196573	True
CA3_pair	100000	-0.0226905491916	-0.00548790208913	-0.000491847575812	True
CA3_pair	105925.372518	-0.0226877866063	-0.00588838939583	-0.000549516544424	True
CA3_pair	112201.84543	-0.0226846877489	-0.00630190041683	-0.000613983383463	True

Table S2c continued

pair_id	frequency_hz	contrast_M1_s_per_m	contrast_M2_s_per_m	contrast_M3_s_per_m	sign_agreement
CA3_pair	118850.222744	-0.0226812117985	-0.00672704561931	-0.000686017298732	True
CA3_pair	125892.541179	-0.0226773130074	-0.00716232792541	-0.000766466383786	True
CA3_pair	133352.143216	-0.0226729401142	-0.00760617298411	-0.000856263621851	True
CA3_pair	141253.754462	-0.0226680356887	-0.00805696074492	-0.000956432780678	True
CA3_pair	149623.565609	-0.022662535401	-0.0085130569134	-0.00106809400785	True
CA3_pair	158489.319246	-0.0226563672074	-0.00897284294197	-0.0011924688782	True
CA3_pair	167880.401812	-0.0226494504444	-0.00943474337197	-0.00133088457883	True
CA3_pair	177827.941004	-0.0226416948201	-0.00989724957379	-0.00148477684036	True
CA3_pair	188364.908949	-0.0226329992947	-0.0103589392037	-0.00165569113544	True
CA3_pair	199526.231497	-0.0226232508382	-0.0108184909807	-0.00184528156766	True
CA3_pair	211348.903984	-0.0226123230529	-0.0112746946599	-0.00205530676915	True
CA3_pair	223872.113857	-0.0226000746519	-0.0117264563175	-0.00228762201555	True
CA3_pair	237137.370566	-0.0225863477771	-0.0121727992555	-0.00254416666012	True
CA3_pair	251188.643151	-0.0225709661478	-0.0126128609727	-0.00282694589342	True
CA3_pair	266072.50598	-0.0225537330254	-0.0130458867322	-0.00313800576286	True
CA3_pair	281838.293126	-0.0225344289833	-0.0134712202896	-0.00347940035532	True
CA3_pair	298538.261892	-0.0225128094711	-0.0138882923383	-0.00385315007576	True
CA3_pair	316227.766017	-0.0224886021639	-0.0142966071878	-0.00426119007014	True
CA3_pair	334965.439158	-0.0224615040908	-0.0146957281311	-0.00470530806921	True
CA3_pair	354813.389234	-0.0224311785407	-0.0150852618799	-0.00518707129894	True
CA3_pair	375837.404288	-0.0223972517467	-0.0154648423746	-0.00570774263789	True
CA3_pair	398107.170553	-0.0223593093608	-0.0158341141953	-0.00626818691849	True
CA3_pair	421696.503429	-0.022316892738	-0.0161927157427	-0.00686876916966	True
CA3_pair	446683.592151	-0.0222694950595	-0.0165402622953	-0.00750924766091	True
CA3_pair	473151.258961	-0.0222165573432	-0.0168763290199	-0.00818866578186	True
CA3_pair	501187.233627	-0.0221574644058	-0.0172004339836	-0.00890524798716	True
CA3_pair	530884.444231	-0.0220915408653	-0.0175120212168	-0.00965630612832	True
CA3_pair	562341.32519	-0.0220180472988	-0.0178104438904	-0.0104381633211	True

Table S2c continued

pair_id	frequency_hz	contrast_M1_s_per_m	contrast_M2_s_per_m	contrast_M3_s_per_m	sign_agreement
CA3_pair	595662.143529	-0.0219361767084	-0.0180949477101	-0.0112461028785	True
CA3_pair	630957.34448	-0.0218450514802	-0.0183646546846	-0.0120743496037	True
CA3_pair	668343.917569	-0.0217437210731	-0.018618547514	-0.0129160897431	True
CA3_pair	707945.784384	-0.0216311607204	-0.0188554549447	-0.0137635340966	True
CA3_pair	749894.209332	-0.0215062714819	-0.0190740385721	-0.0146080262199	True
CA3_pair	794328.234724	-0.0213678820452	-0.0192727817283	-0.0154401945178	True
CA3_pair	841395.141645	-0.0212147527277	-0.019449981268	-0.0162501436426	True
CA3_pair	891250.938134	-0.0210455821877	-0.0196037432601	-0.0170276773845	True
CA3_pair	944060.876286	-0.0208590173932	-0.0197319837938	-0.0177625426206	True
CA3_pair	1000000	-0.020653667421	-0.0198324362985	-0.0184446822665	True
CA3_pair	1059253.72518	-0.0204281216565	-0.0199026669412	-0.0190644848126	True
CA3_pair	1122018.4543	-0.0201809729153	-0.0199400997657	-0.0196130189788	True
CA3_pair	1188502.22744	-0.0199108459132	-0.0199420532471	-0.0200822441297	True
CA3_pair	1258925.41179	-0.0196164313412	-0.0199057898	-0.0204651899849	True
CA3_pair	1333521.43216	-0.0192965255558	-0.0198285794571	-0.0207561023586	True
CA3_pair	1412537.54462	-0.0189500755611	-0.0197077783782	-0.0209505546329	True
CA3_pair	1496235.65609	-0.0185762285278	-0.0195409220171	-0.0210455269647	True
CA3_pair	1584893.19246	-0.0181743845913	-0.019325831657	-0.0210394565395	True
CA3_pair	1678804.01812	-0.0177442510964	-0.0190607316303	-0.0209322624116	True
CA3_pair	1778279.41004	-0.0172858958777	-0.018744372942	-0.0207253476984	True
CA3_pair	1883649.08949	-0.0167997966095	-0.0183761573319	-0.0204215804127	True
CA3_pair	1995262.31497	-0.0162868828364	-0.017956254234	-0.0200252523982	True
CA3_pair	2113489.03984	-0.0157485670561	-0.0174857018495	-0.0195420141424	True
CA3_pair	2238721.13857	-0.0151867612851	-0.0169664829281	-0.0189787821038	True
CA3_pair	2371373.70566	-0.0146038759377	-0.01640156609	-0.0183436149577	True
CA3_pair	2511886.43151	-0.014002798645	-0.0157949048292	-0.0176455560451	True
CA3_pair	2660725.0598	-0.0133868518046	-0.0151513887714	-0.0168944413196	True
CA3_pair	2818382.93126	-0.0127597291225	-0.0144767452238	-0.016100675046	True

Table S2c continued

pair_id	frequency_hz	contrast_M1_s_per_m	contrast_M2_s_per_m	contrast_M3_s_per_m	sign_agreement
CA3_pair	2985382.61892	-0.0121254130441	-0.0137773932426	-0.0152749790208	True
CA3_pair	3162277.66017	-0.011488076598	-0.0130602568849	-0.0144281246351	True
CA3_pair	3349654.39158	-0.0108519745889	-0.0123325484109	-0.013570660089	True
CA3_pair	3548133.89234	-0.0102213300885	-0.0116015353542	-0.0127126469351	True
CA3_pair	3758374.04288	-0.00960022263079	-0.0108743070871	-0.0118634204949	True
CA3_pair	3981071.70553	-0.00899248436786	-0.0101575564871	-0.0110313873951	True
CA3_pair	4216965.03429	-0.0084016096907	-0.00945739055912	-0.0102238706457	True
CA3_pair	4466835.92151	-0.00783068258058	-0.00877918066303	-0.00944700872612	True
CA3_pair	4731512.58961	-0.00728232440051	-0.00812745884791	-0.00870571061376	True
CA3_pair	5011872.33627	-0.00675866316425	-0.00750586231639	-0.00800366424179	True
CA3_pair	5308844.44231	-0.0062613237315	-0.00691712385962	-0.00734339205332	True
CA3_pair	5623413.2519	-0.0057914370352	-0.00636310269982	-0.00672634456351	True
CA3_pair	5956621.43529	-0.00534966545571	-0.00584484786053	-0.00615302133395	True
CA3_pair	6309573.4448	-0.00493624086199	-0.00536268504488	-0.00562310849316	True
CA3_pair	6683439.17569	-0.00455101162766	-0.00491631794201	-0.00513562271189	True
CA3_pair	7079457.84384	-0.00419349504488	-0.00450493567753	-0.00468905306463	True
CA3_pair	7498942.09332	-0.00386293191958	-0.00412731948554	-0.00428149414786	True
CA3_pair	7943282.34724	-0.00355834064833	-0.00378194331897	-0.00391076587653	True
CA3_pair	8413951.41645	-0.00327856866771	-0.00346706478519	-0.00357451730295	True
CA3_pair	8912509.38134	-0.00302233976163	-0.00318080431641	-0.0032703134386	True
CA3_pair	9440608.76286	-0.0027882962613	-0.00292121175121	-0.00299570533264	True
CA3_pair	10000000	-0.00257503564487	-0.00268632047134	-0.00274828455765	True
CA3_pair	10592537.2518	-0.00238114142471	-0.0024741899102	-0.00252572380715	True
CA3_pair	11220184.543	-0.00220520849778	-0.00228293766096	-0.00232580557983	True
CA3_pair	11885022.2744	-0.00204586333502	-0.00211076261299	-0.00214644098032	True
CA3_pair	12589254.1179	-0.0019017795113	-0.00195596058891	-0.00198568057228	True
CA3_pair	13335214.3216	-0.00177168914255	-0.00181693389099	-0.00184171903428	True
CA3_pair	14125375.4462	-0.0016543908147	-0.00169219603678	-0.00171289513666	True

Table S2c continued

pair_id	frequency_hz	contrast_M1_s_per_m	contrast_M2_s_per_m	contrast_M3_s_per_m	sign_agreement
CA3_pair	14962356.5609	-0.00154875457379	-0.001580372801	-0.00159768831294	True
CA3_pair	15848931.9246	-0.00145372450902	-0.00148020050912	-0.00149471286215	True
CA3_pair	16788040.1812	-0.00136831940938	-0.00139052236002	-0.00140271060411	True
CA3_pair	17782794.1004	-0.00129163191671	-0.00131028340334	-0.00132054262274	True
CA3_pair	18836490.8949	-0.00122282653944	-0.00123852466247	-0.00124718057562	True
CA3_pair	19952623.1497	-0.00116113683362	-0.00117437678109	-0.00118169792029	True
CA3_pair	21134890.3984	-0.00110586200555	-0.001117053477	-0.00112326130566	True
CA3_pair	22387211.3857	-0.00105636314197	-0.00106584501138	-0.00107112229748	True
CA3_pair	23713737.0566	-0.00101205923285	-0.00102011182101	-0.00102460954635	True
CA3_pair	25118864.3151	-0.000972423115266	-0.000979278414397	-0.000983121461357	True
CA3_pair	26607250.598	-0.000936977437123	-0.000942827596683	-0.000946119419159	True
CA3_pair	28183829.3126	-0.000905290714073	-0.000910295060963	-0.000913121514844	True
CA3_pair	29853826.1892	-0.00087697353269	-0.000881264363827	-0.000883696844468	True
CA3_pair	31622776.6017	-0.000851674936268	-0.000855362288237	-0.000857460298198	True
CA3_pair	33496543.9158	-0.000829079016611	-0.000832254586727	-0.000834067836242	True
CA3_pair	35481338.9234	-0.000808901724862	-0.000811642090837	-0.000813212215822	True
CA3_pair	37583740.4288	-0.000790887906578	-0.000793257168254	-0.000794619135726	True
CA3_pair	39810717.0553	-0.000774808560335	-0.000776860506371	-0.000778043764725	True
CA3_pair	42169650.3429	-0.000760458314768	-0.000762238199668	-0.000763267620827	True
CA3_pair	44668359.2151	-0.000747653115913	-0.000749199117894	-0.000750095769809	True
CA3_pair	47315125.8961	-0.00073622811457	-0.000737572532342	-0.000738354313195	True
CA3_pair	50118723.3627	-0.000726035742131	-0.000727205978236	-0.000727888137923	True
CA3_pair	53088444.4231	-0.000716943962566	-0.000717963332319	-0.000718558902001	True
CA3_pair	56234132.519	-0.000708834688033	-0.000709723085956	-0.00071024323259	True
CA3_pair	59566214.3529	-0.000701602345585	-0.000702376795389	-0.000702831114999	True
CA3_pair	63095734.448	-0.000695152582835	-0.000695827692167	-0.000696224453	True
CA3_pair	66834391.7569	-0.000689401100834	-0.000689989438105	-0.000690335782771	True
CA3_pair	70794578.4384	-0.000684272603099	-0.00068478501046	-0.000685087124415	True

Table S2c continued

pair_id	frequency_hz	contrast_M1_s_per_m	contrast_M2_s_per_m	contrast_M3_s_per_m	sign_agreement
CA3_pair	74989420.9332	-0.000679699850301	-0.000680145704259	-0.000680408956637	True
CA3_pair	79432823.4724	-0.0006756228109	-0.000676010239901	-0.000676239301581	True
CA3_pair	84139514.1645	-0.000671987898668	-0.000672323965264	-0.000672522908149	True
CA3_pair	89125093.8134	-0.000668747288775	-0.000669038142586	-0.000669210523326	True
CA3_pair	94406087.6286	-0.000665858304765	-0.000666109311291	-0.000666258242131	True
CA3_pair	100000000	-0.000663282869446	-0.000663498718877	-0.000663626927768	True
cortex_pair	1000	-0.0657965727608	$-7.63094144903 \times 10^{-5}$	$-3.16762538674 \times 10^{-5}$	True
cortex_pair	1059.25372518	-0.0657965719918	$-7.64248737432 \times 10^{-5}$	$-3.16915888735 \times 10^{-5}$	True
cortex_pair	1122.0184543	-0.0657965711289	$-7.65544201587 \times 10^{-5}$	$-3.17087950278 \times 10^{-5}$	True
cortex_pair	1188.50222744	-0.0657965701608	$-7.66997723726 \times 10^{-5}$	$-3.17281006432 \times 10^{-5}$	True
cortex_pair	1258.92541179	-0.0657965690745	$-7.68628586587 \times 10^{-5}$	$-3.17497618911 \times 10^{-5}$	True
cortex_pair	1333.52143216	-0.0657965678558	$-7.70458424923 \times 10^{-5}$	$-3.17740661996 \times 10^{-5}$	True
cortex_pair	1412.53754462	-0.0657965664883	$-7.72511512263 \times 10^{-5}$	$-3.18013360681 \times 10^{-5}$	True
cortex_pair	1496.23565609	-0.0657965649539	$-7.74815082623 \times 10^{-5}$	$-3.18319333458 \times 10^{-5}$	True
cortex_pair	1584.89319246	-0.0657965632323	$-7.77399691393 \times 10^{-5}$	$-3.18662640336 \times 10^{-5}$	True
cortex_pair	1678.80401812	-0.0657965613006	$-7.80299620171 \times 10^{-5}$	$-3.19047836705 \times 10^{-5}$	True
cortex_pair	1778.27941004	-0.0657965591333	$-7.83553330885 \times 10^{-5}$	$-3.19480033781 \times 10^{-5}$	True
cortex_pair	1883.64908949	-0.0657965567015	$-7.87203975177 \times 10^{-5}$	$-3.19964966428 \times 10^{-5}$	True
cortex_pair	1995.26231497	-0.065796553973	$-7.91299965776 \times 10^{-5}$	$-3.2050906924 \times 10^{-5}$	True
cortex_pair	2113.48903984	-0.0657965509115	$-7.95895617348 \times 10^{-5}$	$-3.21119561924 \times 10^{-5}$	True
cortex_pair	2238.72113857	-0.0657965474765	$-8.01051865278 \times 10^{-5}$	$-3.21804545085 \times 10^{-5}$	True
cortex_pair	2371.37370566	-0.0657965436223	$-8.06837071784 \times 10^{-5}$	$-3.22573107702 \times 10^{-5}$	True
cortex_pair	2511.88643151	-0.0657965392979	$-8.13327929959 \times 10^{-5}$	$-3.2343544772 \times 10^{-5}$	True
cortex_pair	2660.7250598	-0.0657965344458	$-8.20610477549 \times 10^{-5}$	$-3.24403007344 \times 10^{-5}$	True
cortex_pair	2818.38293126	-0.0657965290017	$-8.28781233733 \times 10^{-5}$	$-3.25488624844 \times 10^{-5}$	True
cortex_pair	2985.38261892	-0.0657965228933	$-8.37948473716 \times 10^{-5}$	$-3.26706704876 \times 10^{-5}$	True
cortex_pair	3162.27766017	-0.0657965160395	$-8.4823365772 \times 10^{-5}$	$-3.2807340958 \times 10^{-5}$	True
cortex_pair	3349.65439158	-0.0657965083495	$-8.59773032942 \times 10^{-5}$	$-3.29606872982 \times 10^{-5}$	True

Table S2c continued

pair_id	frequency_hz	contrast_M1_s_per_m	contrast_M2_s_per_m	contrast_M3_s_per_m	sign_agreement
cortex_pair	3548.13389234	-0.0657964997211	$-8.72719429191 \times 10^{-5}$	$-3.31327441558 \times 10^{-5}$	True
cortex_pair	3758.37404288	-0.0657964900399	$-8.87244271402 \times 10^{-5}$	$-3.33257944125 \times 10^{-5}$	True
cortex_pair	3981.07170553	-0.0657964791775	$-9.03539834913 \times 10^{-5}$	$-3.3542399466 \times 10^{-5}$	True
cortex_pair	4216.96503429	-0.0657964669896	$-9.21821772381 \times 10^{-5}$	$-3.37854332039 \times 10^{-5}$	True
cortex_pair	4466.83592151	-0.0657964533146	$-9.42331944603 \times 10^{-5}$	$-3.4058120121 \times 10^{-5}$	True
cortex_pair	4731.51258961	-0.065796437971	$-9.65341591155 \times 10^{-5}$	$-3.43640780842 \times 10^{-5}$	True
cortex_pair	5011.87233627	-0.0657964207552	$-9.91154880895 \times 10^{-5}$	$-3.47073663116 \times 10^{-5}$	True
cortex_pair	5308.84444231	-0.0657964014387	-0.000102011288685	$-3.5092539201 \times 10^{-5}$	True
cortex_pair	5623.4132519	-0.0657963797654	-0.000105259803506	$-3.55247067195 \times 10^{-5}$	True
cortex_pair	5956.62143529	-0.0657963554474	-0.000108903908224	$-3.60096021545 \times 10^{-5}$	True
cortex_pair	6309.5734448	-0.0657963281623	-0.000112991668339	$-3.65536581207 \times 10^{-5}$	True
cortex_pair	6683.43917569	-0.0657962975479	-0.00011757696167	$-3.71640918293 \times 10^{-5}$	True
cortex_pair	7079.45784384	-0.065796263198	-0.000122720174036	$-3.78490007449 \times 10^{-5}$	True
cortex_pair	7498.94209332	-0.0657962246569	-0.000128488976359	$-3.86174698945 \times 10^{-5}$	True
cortex_pair	7943.28234724	-0.065796181413	-0.000134959192233	$-3.94796922451 \times 10^{-5}$	True
cortex_pair	8413.95141645	-0.0657961328927	-0.000142215765891	$-4.04471037367 \times 10^{-5}$	True
cortex_pair	8912.50938134	-0.0657960784521	-0.000150353841437	$-4.1532534752 \times 10^{-5}$	True
cortex_pair	9440.60876286	-0.0657960173689	-0.000159479965182	$-4.2750380018 \times 10^{-5}$	True
cortex_pair	10000	-0.0657959488325	-0.000169713423938	$-4.41167891737 \times 10^{-5}$	True
cortex_pair	10592.5372518	-0.0657958719335	-0.000181187733155	$-4.56498805117 \times 10^{-5}$	True
cortex_pair	11220.184543	-0.0657957856517	-0.000194052289804	$-4.73699806975 \times 10^{-5}$	True
cortex_pair	11885.0222744	-0.0657956888422	-0.000208474205901	$-4.92998936132 \times 10^{-5}$	True
cortex_pair	12589.2541179	-0.0657955802206	-0.000224640339479	$-5.14652018436 \times 10^{-5}$	True
cortex_pair	13335.2143216	-0.0657954583455	-0.000242759540583	$-5.38946047485 \times 10^{-5}$	True
cortex_pair	14125.3754462	-0.0657953215999	-0.000263065130459	$-5.66202975314 \times 10^{-5}$	True
cortex_pair	14962.3565609	-0.0657951681695	-0.000285817632376	$-5.96783962428 \times 10^{-5}$	True
cortex_pair	15848.9319246	-0.0657949960187	-0.00031130777242	$-6.31094142397 \times 10^{-5}$	True
cortex_pair	16788.0401812	-0.0657948028634	-0.000339859767962	$-6.69587962754 \times 10^{-5}$	True

Table S2c continued

pair_id	frequency_hz	contrast_M1_s_per_m	contrast_M2_s_per_m	contrast_M3_s_per_m	sign_agreement
cortex_pair	17782.7941004	-0.065794586141	-0.000371834920111	$-7.12775171221 \times 10^{-5}$	True
cortex_pair	18836.4908949	-0.0657943429762	-0.00040763552427	$-7.61227524356 \times 10^{-5}$	True
cortex_pair	19952.6231497	-0.0657940701429	-0.000447709109432	$-8.15586304693 \times 10^{-5}$	True
cortex_pair	21134.8903984	-0.0657937640218	-0.000492553012104	$-8.76570742434 \times 10^{-5}$	True
cortex_pair	22387.2113857	-0.0657934205516	-0.000542719284087	$-9.4498744879 \times 10^{-5}$	True
cortex_pair	23713.7370566	-0.0657930351762	-0.000598819924713	-0.000102174098029	True
cortex_pair	25118.8643151	-0.0657926027833	-0.000661532416885	-0.000110784566689	True
cortex_pair	26607.250598	-0.0657921176374	-0.00073160553213	-0.000120443885157	True
cortex_pair	28183.8293126	-0.0657915733035	-0.000809865352385	-0.000131279570551	True
cortex_pair	29853.8261892	-0.0657909625618	-0.000897221434943	-0.00014343458007	True
cortex_pair	31622.7766017	-0.0657902773121	-0.000994673021631	-0.000157069164173	True
cortex_pair	33496.5439158	-0.0657895084667	-0.00110331516366	-0.000172362937931	True
cortex_pair	35481.3389234	-0.0657886458298	-0.00122434459957	-0.00018951719516	True
cortex_pair	37583.7404288	-0.0657876779629	-0.00135906518591	-0.000208757492391	True
cortex_pair	39810.7170553	-0.065786592033	-0.00150889263881	-0.000230336532384	True
cortex_pair	42169.6503429	-0.0657853736433	-0.00167535830158	-0.000254537379727	True
cortex_pair	44668.3592151	-0.0657840066425	-0.00186011160987	-0.000281677043974	True
cortex_pair	47315.1258961	-0.0657824729115	-0.00206492088485	-0.00031211046884	True
cortex_pair	50118.7233627	-0.0657807521242	-0.00229167204977	-0.000346234969072	True
cortex_pair	53088.4444231	-0.0657788214786	-0.00254236484007	-0.000384495159698	True
cortex_pair	56234.132519	-0.0657766553967	-0.00281910606708	-0.00042738842528	True
cortex_pair	59566.2143529	-0.0657742251864	-0.00312409950527	-0.000475470979562	True
cortex_pair	63095.734448	-0.0657714986643	-0.00345963200878	-0.00052936456813	True
cortex_pair	66834.3917569	-0.0657684397314	-0.00382805552832	-0.000589763868324	True
cortex_pair	70794.5784384	-0.0657650078987	-0.00423176479917	-0.000657444641303	True
cortex_pair	74989.4209332	-0.0657611577551	-0.00467317060435	-0.000733272690462	True
cortex_pair	79432.8234724	-0.0657568383717	-0.00515466868422	-0.000818213677851	True
cortex_pair	84139.5141645	-0.0657519926348	-0.00567860455756	-0.000913343845291	True

Table S2c continued

pair_id	frequency_hz	contrast_M1_s_per_m	contrast_M2_s_per_m	contrast_M3_s_per_m	sign_agreement
cortex_pair	89125.0938134	-0.065746556498	-0.00624723473235	-0.00101986167872	True
cortex_pair	94406.0876286	-0.0657404581466	-0.00686268500287	-0.00113910054199	True
cortex_pair	100000	-0.0657336170612	-0.00752690673995	-0.00127254228866	True
cortex_pair	105925.372518	-0.0657259429705	-0.00824163226513	-0.00142183183642	True
cortex_pair	112201.84543	-0.0657173346807	-0.00900833054412	-0.00158879265574	True
cortex_pair	118850.222744	-0.0657076787658	-0.00982816452462	-0.00177544308215	True
cortex_pair	125892.541179	-0.0656968481056	-0.0107019514727	-0.00198401330591	True
cortex_pair	133352.143216	-0.0656847002517	-0.0116301276254	-0.00221696282289	True
cortex_pair	141253.754462	-0.0656710756046	-0.0126127183785	-0.00247699804204	True
cortex_pair	149623.565609	-0.06565579538	-0.0136493150757	-0.00276708963616	True
cortex_pair	158489.319246	-0.0656386593422	-0.0147390592654	-0.00309048908936	True
cortex_pair	167880.401812	-0.0656194432805	-0.0158806350634	-0.00345074373419	True
cortex_pair	177827.941004	-0.0655978962007	-0.0170722700025	-0.00385170938209	True
cortex_pair	188364.908949	-0.0655737372044	-0.0183117444871	-0.00429755942862	True
cortex_pair	199526.231497	-0.0655466520252	-0.0195964096939	-0.00479278906264	True
cortex_pair	211348.903984	-0.0655162891887	-0.0209232134796	-0.00534221292562	True
cortex_pair	223872.113857	-0.0654822557631	-0.0222887335801	-0.00595095426134	True
cortex_pair	237137.370566	-0.0654441126653	-0.0236892171004	-0.00662442327659	True
cortex_pair	251188.643151	-0.0654013694854	-0.0251206250299	-0.00736828211757	True
cortex_pair	266072.50598	-0.0653534787947	-0.0265786802595	-0.00818839357979	True
cortex_pair	281838.293126	-0.0652998299031	-0.0280589173608	-0.00909075044539	True
cortex_pair	298538.261892	-0.0652397420324	-0.0295567322142	-0.0100813822284	True
cortex_pair	316227.766017	-0.0651724568786	-0.0310674294712	-0.0111662361623	True
cortex_pair	334965.439158	-0.0650971305428	-0.0325862658186	-0.0123510295555	True
cortex_pair	354813.389234	-0.0650128248196	-0.0341084870875	-0.0136410712445	True
cortex_pair	375837.404288	-0.0649184978451	-0.0356293574281	-0.015041050876	True
cortex_pair	398107.170553	-0.0648129941283	-0.0371441790403	-0.0165547962126	True
cortex_pair	421696.503429	-0.0646950340094	-0.0386483013003	-0.0181850006421	True

Table S2c continued

pair_id	frequency_hz	contrast_M1_s_per_m	contrast_M2_s_per_m	contrast_M3_s_per_m	sign_agreement
cortex_pair	446683.592151	-0.0645632026254	-0.0401371185365	-0.0199329255824	True
cortex_pair	473151.258961	-0.0644159384996	-0.041606056151	-0.0217980854675	True
cortex_pair	501187.233627	-0.0642515219251	-0.0430505452476	-0.0237779263389	True
cortex_pair	530884.444231	-0.0640680633734	-0.04446598638	-0.0258675125273	True
cortex_pair	562341.32519	-0.0638634922344	-0.045847703472	-0.0280592391425	True
cortex_pair	595662.143529	-0.0636355462881	-0.0471908893772	-0.0303425906778	True
cortex_pair	630957.34448	-0.063381762411	-0.0484905449518	-0.0327039674742	True
cortex_pair	668343.917569	-0.0630994691467	-0.0497414139063	-0.0351266016086	True
cortex_pair	707945.784384	-0.0627857819088	-0.0509379161239	-0.0375905815603	True
cortex_pair	749894.209332	-0.0624376017388	-0.0520740825697	-0.0400730005891	True
cortex_pair	794328.234724	-0.0620516187019	-0.0531434954123	-0.0425482371972	True
cortex_pair	841395.141645	-0.0616243211734	-0.0541392375093	-0.044988367789	True
cortex_pair	891250.938134	-0.0611520124222	-0.0550538559875	-0.0473637024486	True
cortex_pair	944060.876286	-0.0606308360326	-0.0558793452275	-0.0496434256793	True
cortex_pair	1000000	-0.0600568117927	-0.0566071550917	-0.051796316113	True
cortex_pair	1059253.72518	-0.0594258836919	-0.0572282306343	-0.0537915136741	True
cortex_pair	1122018.4543	-0.0587339815835	-0.0577330896777	-0.055599300178	True
cortex_pair	1188502.22744	-0.0579770978344	-0.0581119443977	-0.0571918601339	True
cortex_pair	1258925.41179	-0.057151379872	-0.0583548722607	-0.0585439922917	True
cortex_pair	1333521.43216	-0.0562532389094	-0.058452040129	-0.0596337484291	True
cortex_pair	1412537.54462	-0.05527947425	-0.0583939829512	-0.0604429828681	True
cortex_pair	1496235.65609	-0.0542274114344	-0.0581719350784	-0.0609578029958	True
cortex_pair	1584893.19246	-0.053095051114	-0.0577782078898	-0.0611689165316	True
cortex_pair	1678804.01812	-0.0518812239582	-0.0572066022202	-0.0610718747081	True
cortex_pair	1778279.41004	-0.0505857452369	-0.0564528383588	-0.0606672116818	True
cortex_pair	1883649.08949	-0.0492095611087	-0.0555149806724	-0.0599604796561	True
cortex_pair	1995262.31497	-0.0477548772924	-0.0543938289009	-0.058962177161	True
cortex_pair	2113489.03984	-0.0462252599342	-0.0530932447427	-0.0576875657499	True

Table S2c continued

pair_id	frequency_hz	contrast_M1_s_per_m	contrast_M2_s_per_m	contrast_M3_s_per_m	sign_agreement
cortex_pair	2238721.13857	-0.0446256983513	-0.0516203813837	-0.056156369219	True
cortex_pair	2371373.70566	-0.042962620143	-0.0499857858993	-0.0543923503573	True
cortex_pair	2511886.43151	-0.0412438510478	-0.048203350434	-0.0524227638666	True
cortex_pair	2660725.0598	-0.0394785148981	-0.0462900977309	-0.0502776905846	True
cortex_pair	2818382.93126	-0.0376768729281	-0.0442657993107	-0.0479892670088	True
cortex_pair	2985382.61892	-0.0358501062161	-0.0421524391481	-0.0455908342512	True
cortex_pair	3162277.66017	-0.0340100497047	-0.039973550315	-0.0431160404022	True
cortex_pair	3349654.39158	-0.0321688905048	-0.0377534647524	-0.040597938115	True
cortex_pair	3548133.89234	-0.0303388464858	-0.0355165252231	-0.0380681234536	True
cortex_pair	3758374.04288	-0.0285318430301	-0.0332863121902	-0.0355559616253	True
cortex_pair	3981071.70553	-0.0267592060188	-0.0310849362479	-0.0330879398171	True
cortex_pair	4216965.03429	-0.0250313875853	-0.0289324391512	-0.0306871775425	True
cortex_pair	4466835.92151	-0.0233577381422	-0.0268463346401	-0.0283731119667	True
cortex_pair	4731512.58961	-0.0217463340781	-0.0248413059552	-0.0261613614413	True
cortex_pair	5011872.33627	-0.0202038658714	-0.0229290622749	-0.0240637568451	True
cortex_pair	5308844.44231	-0.0187355867579	-0.0211183431586	-0.0220885189895	True
cortex_pair	5623413.2519	-0.0173453179974	-0.0194150499043	-0.0202405524433	True
cortex_pair	5956621.43529	-0.0160355035854	-0.01782247628	-0.0185218221469	True
cortex_pair	6309573.4448	-0.0148073051347	-0.0163416084651	-0.0169317789532	True
cortex_pair	6683439.17569	-0.0136607266224	-0.0149714647746	-0.0154678030963	True
cortex_pair	7079457.84384	-0.0125947586679	-0.0137094490064	-0.0141256395839	True
cortex_pair	7498942.09332	-0.0116075327521	-0.012551696098	-0.0128998056424	True
cortex_pair	7943282.34724	-0.0106964770805	-0.0114933942718	-0.0117839566727	True
cortex_pair	8413951.41645	-0.00985846739031	-0.0105290732519	-0.0107712030287	True
cortex_pair	8912509.38134	-0.00908996768154	-0.00965285292631	-0.00985437484854	True
cortex_pair	9440608.76286	-0.00838715747027	-0.00885865072052	-0.00902623595072	True
cortex_pair	10000000	-0.00774604359389	-0.00814034884641	-0.00827965044629	True
cortex_pair	10592537.2518	-0.00716255579093	-0.00749192454325	-0.00760770731929	True

Table S2c continued

pair_id	frequency_hz	contrast_M1_s_per_m	contrast_M2_s_per_m	contrast_M3_s_per_m	sign_agreement
cortex_pair	11220184.543	-0.00663262620814	-0.00690754756747	-0.00700380899061	True
cortex_pair	11885022.2744	-0.00615225366329	-0.00638164968472	-0.00646173000558	True
cortex_pair	12589254.1179	-0.00571755394199	-0.00590897094766	-0.00597565167753	True
cortex_pair	13335214.3216	-0.00532479766652	-0.00548458726227	-0.00554017794826	True
cortex_pair	14125375.4462	-0.00497043738477	-0.00510392328275	-0.00515033702305	True
cortex_pair	14962356.5609	-0.00465112552575	-0.00476275412801	-0.00480157260131	True
cortex_pair	15848931.9246	-0.00436372478938	-0.00445719884895	-0.00448972781561	True
cortex_pair	16788040.1812	-0.00410531240939	-0.00418370804034	-0.00421102435084	True
cortex_pair	17782794.1004	-0.00387317957248	-0.00393904750748	-0.00396203865799	True
cortex_pair	18836490.8949	-0.00366482711041	-0.00372027947937	-0.00373967670996	True
cortex_pair	19952623.1497	-0.00347795841623	-0.00352474250744	-0.00354114836481	True
cortex_pair	21134890.3984	-0.00331047037952	-0.00335003090023	-0.00336394209718	True
cortex_pair	22387211.3857	-0.00316044299263	-0.00319397431174	-0.00320580062076	True
cortex_pair	23713737.0566	-0.00302612815309	-0.00305461791842	-0.00306469774249	True
cortex_pair	25118864.3151	-0.00290593807738	-0.00293020347771	-0.00293881665221	True
cortex_pair	26607250.598	-0.00279843364733	-0.00281915145297	-0.00282652975108	True
cortex_pair	28183829.3126	-0.0027023129322	-0.00272004430873	-0.00272638004935	True
cortex_pair	29853826.1892	-0.00261640006462	-0.00263161102055	-0.00263706411384	True
cortex_pair	31622776.6017	-0.00253963459623	-0.00255271280119	-0.00255741651114	True
cortex_pair	33496543.9158	-0.00247106141671	-0.00248233001479	-0.00248639567055	True
cortex_pair	35481338.9234	-0.002409821287	-0.00241955023072	-0.00242307107828	True
cortex_pair	37583740.4288	-0.0023551420116	-0.00236355735579	-0.00236661170763	True
cortex_pair	39810717.0553	-0.0023063302554	-0.00231362177646	-0.00231627558858	True
cortex_pair	42169650.3429	-0.00226276399623	-0.00226909143896	-0.00227140042099	True
cortex_pair	44668359.2151	-0.00222388559336	-0.00222938379479	-0.00223139513982	True
cortex_pair	47315125.8961	-0.00218919544521	-0.00219397854034	-0.00219573234479	True
cortex_pair	50118723.3627	-0.00215824620469	-0.00216241108216	-0.00216394151312	True
cortex_pair	53088444.4231	-0.00213063751767	-0.00213426666274	-0.00213560291947	True

Table S2c continued

pair_id	frequency_hz	contrast_M1_s_per_m	contrast_M2_s_per_m	contrast_M3_s_per_m	sign_agreement
cortex_pair	56234132.519	-0.00210601124875	-0.00210917508587	-0.00211034219331	True
cortex_pair	59566214.3529	-0.00208404715837	-0.00208680598486	-0.00208782545002	True
cortex_pair	63095734.448	-0.00206445899561	-0.00206686458107	-0.00206775493725	True
cortex_pair	66834391.7569	-0.0020469909727	-0.00204908788473	-0.00204986514397	True
cortex_pair	70794578.4384	-0.00203141458804	-0.002033241294	-0.00203391932418	True
cortex_pair	74989420.9332	-0.00201752576728	-0.00201911555199	-0.00201970639211	True
cortex_pair	79432823.4724	-0.00200514229307	-0.0020065240255	-0.00200703815001	True
cortex_pair	84139514.1645	-0.0019941014969	-0.00199530027238	-0.00199574681341	True
cortex_pair	89125093.8134	-0.00198425818777	-0.00198529586758	-0.00198568280248	True
cortex_pair	94406087.6286	-0.00197548279512	-0.00197637846115	-0.00197671277111	True
cortex_pair	100000000	-0.00196765970468	-0.00196843004375	-0.00196871784845	True
CA1_pair	1000	-0.0639968552179	$-5.1096960909 \times 10^{-5}$	$-2.92042775191 \times 10^{-5}$	True
CA1_pair	1059.25372518	-0.0639968545093	$-5.11465183793 \times 10^{-5}$	$-2.92176603348 \times 10^{-5}$	True
CA1_pair	1122.0184543	-0.0639968537141	$-5.12021226235 \times 10^{-5}$	$-2.92326760965 \times 10^{-5}$	True
CA1_pair	1188.50222744	-0.063996852822	$-5.12645114202 \times 10^{-5}$	$-2.92495240528 \times 10^{-5}$	True
CA1_pair	1258.92541179	-0.063996851821	$-5.13345125606 \times 10^{-5}$	$-2.92684277638 \times 10^{-5}$	True
CA1_pair	1333.52143216	-0.0639968506979	$-5.14130548285 \times 10^{-5}$	$-2.92896380677 \times 10^{-5}$	True
CA1_pair	1412.53754462	-0.0639968494377	$-5.15011803207 \times 10^{-5}$	$-2.9313436409 \times 10^{-5}$	True
CA1_pair	1496.23565609	-0.0639968480238	$-5.16000582685 \times 10^{-5}$	$-2.93401385734 \times 10^{-5}$	True
CA1_pair	1584.89319246	-0.0639968464373	$-5.17110005454 \times 10^{-5}$	$-2.93700988773 \times 10^{-5}$	True
CA1_pair	1678.80401812	-0.0639968446573	$-5.18354790655 \times 10^{-5}$	$-2.94037148692 \times 10^{-5}$	True
CA1_pair	1778.27941004	-0.06399684266	$-5.1975145303 \times 10^{-5}$	$-2.9441432605 \times 10^{-5}$	True
CA1_pair	1883.64908949	-0.0639968404191	$-5.21318521914 \times 10^{-5}$	$-2.94837525659 \times 10^{-5}$	True
CA1_pair	1995.26231497	-0.0639968379047	$-5.23076786919 \times 10^{-5}$	$-2.95312362993 \times 10^{-5}$	True
CA1_pair	2113.48903984	-0.0639968350835	$-5.25049573565 \times 10^{-5}$	$-2.95845138696 \times 10^{-5}$	True
CA1_pair	2238.72113857	-0.0639968319181	$-5.27263052496 \times 10^{-5}$	$-2.96442922174 \times 10^{-5}$	True
CA1_pair	2371.37370566	-0.0639968283664	$-5.29746586374 \times 10^{-5}$	$-2.97113645397 \times 10^{-5}$	True
CA1_pair	2511.88643151	-0.0639968243814	$-5.32533119037 \times 10^{-5}$	$-2.97866208135 \times 10^{-5}$	True

Table S2c continued

pair_id	frequency_hz	contrast_M1_s_per_m	contrast_M2_s_per_m	contrast_M3_s_per_m	sign_agreement
CA1_pair	2660.7250598	-0.0639968199102	$-5.3565961204 \times 10^{-5}$	$-2.98710596033 \times 10^{-5}$	True
CA1_pair	2818.38293126	-0.0639968148933	$-5.39167534378 \times 10^{-5}$	$-2.996580131 \times 10^{-5}$	True
CA1_pair	2985.38261892	-0.0639968092643	$-5.43103411802 \times 10^{-5}$	$-3.00721030345 \times 10^{-5}$	True
CA1_pair	3162.27766017	-0.0639968029485	$-5.47519443012 \times 10^{-5}$	$-3.01913752556 \times 10^{-5}$	True
CA1_pair	3349.65439158	-0.063996795862	$-5.52474190807 \times 10^{-5}$	$-3.0325200542 \times 10^{-5}$	True
CA1_pair	3548.13389234	-0.0639967879109	$-5.58033357302 \times 10^{-5}$	$-3.04753545465 \times 10^{-5}$	True
CA1_pair	3758.37404288	-0.0639967789895	$-5.64270653398 \times 10^{-5}$	$-3.06438295608 \times 10^{-5}$	True
CA1_pair	3981.07170553	-0.0639967689796	$-5.71268773904 \times 10^{-5}$	$-3.0832860944 \times 10^{-5}$	True
CA1_pair	4216.96503429	-0.0639967577484	$-5.79120491106 \times 10^{-5}$	$-3.10449567733 \times 10^{-5}$	True
CA1_pair	4466.83592151	-0.0639967451467	$-5.87929881096 \times 10^{-5}$	$-3.12829311112 \times 10^{-5}$	True
CA1_pair	4731.51258961	-0.0639967310073	$-5.97813698862 \times 10^{-5}$	$-3.15499413294 \times 10^{-5}$	True
CA1_pair	5011.87233627	-0.0639967151427	$-6.08902920108 \times 10^{-5}$	$-3.18495299838 \times 10^{-5}$	True
CA1_pair	5308.84444231	-0.0639966973424	$-6.21344469825 \times 10^{-5}$	$-3.21856717946 \times 10^{-5}$	True
CA1_pair	5623.4132519	-0.06399667737	$-6.35303160091 \times 10^{-5}$	$-3.25628263551 \times 10^{-5}$	True
CA1_pair	5956.62143529	-0.0639966549607	$-6.50963862152 \times 10^{-5}$	$-3.29859972644 \times 10^{-5}$	True
CA1_pair	6309.5734448	-0.0639966298171	$-6.68533940852 \times 10^{-5}$	$-3.34607984684 \times 10^{-5}$	True
CA1_pair	6683.43917569	-0.0639966016055	$-6.8824598269 \times 10^{-5}$	$-3.39935286856 \times 10^{-5}$	True
CA1_pair	7079.45784384	-0.0639965699516	$-7.10360852488 \times 10^{-5}$	$-3.45912549017 \times 10^{-5}$	True
CA1_pair	7498.94209332	-0.0639965344354	$-7.35171117641 \times 10^{-5}$	$-3.52619060369 \times 10^{-5}$	True
CA1_pair	7943.28234724	-0.0639964945856	$-7.63004883425 \times 10^{-5}$	$-3.60143780219 \times 10^{-5}$	True
CA1_pair	8413.95141645	-0.0639964498735	$-7.94230087784 \times 10^{-5}$	$-3.68586516715 \times 10^{-5}$	True
CA1_pair	8912.50938134	-0.0639963997057	$-8.29259309459 \times 10^{-5}$	$-3.78059249092 \times 10^{-5}$	True
CA1_pair	9440.60876286	-0.0639963434166	$-8.68555149366 \times 10^{-5}$	$-3.88687610866 \times 10^{-5}$	True
CA1_pair	10000	-0.0639962802594	$-9.126362517 \times 10^{-5}$	$-4.00612553513 \times 10^{-5}$	True
CA1_pair	10592.5372518	-0.0639962093959	$-9.62084038513 \times 10^{-5}$	$-4.13992212531 \times 10^{-5}$	True
CA1_pair	11220.184543	-0.063996129886	-0.000101755023937	$-4.29004000409 \times 10^{-5}$	True
CA1_pair	11885.0222744	-0.0639960406746	-0.00010797653063	$-4.45846954002 \times 10^{-5}$	True
CA1_pair	12589.2541179	-0.0639959405781	-0.000114954781346	$-4.6474436709 \times 10^{-5}$	True

Table S2c continued

pair_id	frequency_hz	contrast_M1_s_per_m	contrast_M2_s_per_m	contrast_M3_s_per_m	sign_agreement
CA1_pair	13335.2143216	-0.0639958282684	-0.000122781495102	$-4.85946742599 \times 10^{-5}$	True
CA1_pair	14125.3754462	-0.0639957022553	-0.000131559423335	$-5.09735103095 \times 10^{-5}$	True
CA1_pair	14962.3565609	-0.0639955608669	-0.000141403655276	$-5.36424702752 \times 10^{-5}$	True
CA1_pair	15848.9319246	-0.0639954022273	-0.00015244307221	$-5.66369189147 \times 10^{-5}$	True
CA1_pair	16788.0401812	-0.0639952242316	-0.000164821966159	$-5.99965268966 \times 10^{-5}$	True
CA1_pair	17782.7941004	-0.0639950245184	-0.000178701839749	$-6.37657938105 \times 10^{-5}$	True
CA1_pair	18836.4908949	-0.0639948004381	-0.000194263405302	$-6.79946343753 \times 10^{-5}$	True
CA1_pair	19952.6231497	-0.0639945490177	-0.000211708802337	$-7.27390353982 \times 10^{-5}$	True
CA1_pair	21134.8903984	-0.0639942669218	-0.00023126405378	$-7.80617919161 \times 10^{-5}$	True
CA1_pair	22387.2113857	-0.0639939504081	-0.000253181782118	$-8.40333319282 \times 10^{-5}$	True
CA1_pair	23713.7370566	-0.0639935952776	-0.000277744207402	$-9.07326402124 \times 10^{-5}$	True
CA1_pair	25118.8643151	-0.0639931968195	-0.000305266449349	$-9.82482929157 \times 10^{-5}$	True
CA1_pair	26607.250598	-0.0639927497483	-0.000336100155633	-0.000106679615931	True
CA1_pair	28183.8293126	-0.0639922481337	-0.000370637477628	-0.000116137981537	True
CA1_pair	29853.8261892	-0.0639916853225	-0.00040931541321	-0.000126748259372	True
CA1_pair	31622.7766017	-0.0639910538501	-0.000452620533422	-0.000138650439577	True
CA1_pair	33496.5439158	-0.0639903453416	-0.000501094105617	-0.000152001447869	True
CA1_pair	35481.3389234	-0.0639895504011	-0.000555337619771	-0.000166977174375	True
CA1_pair	37583.7404288	-0.0639886584874	-0.000616018716535	-0.000183774740339	True
CA1_pair	39810.7170553	-0.0639876577742	-0.000683877504933	-0.000202615029246	True
CA1_pair	42169.6503429	-0.0639865349938	-0.000759733243801	-0.000223745511499	True
CA1_pair	44668.3592151	-0.0639852752616	-0.000844491343673	-0.000247443394565	True
CA1_pair	47315.1258961	-0.0639838618795	-0.000939150624226	-0.000274019133388	True
CA1_pair	50118.7233627	-0.063982276115	-0.00104481073619	-0.000303820338894	True
CA1_pair	53088.4444231	-0.063980496954	-0.00116267962527	-0.000337236125442	True
CA1_pair	56234.132519	-0.0639785008236	-0.00129408087896	-0.000374701941138	True
CA1_pair	59566.2143529	-0.0639762612807	-0.00144046075499	-0.000416704927872	True
CA1_pair	63095.734448	-0.0639737486639	-0.00160339464296	-0.000463789860599	True

Table S2c continued

pair_id	frequency_hz	contrast_M1_s_per_m	contrast_M2_s_per_m	contrast_M3_s_per_m	sign_agreement
CA1_pair	66834.3917569	-0.0639709297027	-0.00178459265944	-0.000516565717715	True
CA1_pair	70794.5784384	-0.06396776708	-0.00198590402208	-0.00057571293598	True
CA1_pair	74989.4209332	-0.0639642189412	-0.00220931979423	-0.000641991404197	True
CA1_pair	79432.8234724	-0.0639602383452	-0.00245697353864	-0.000716249249254	True
CA1_pair	84139.5141645	-0.0639557726488	-0.00273113937404	-0.000799432465793	True
CA1_pair	89125.0938134	-0.0639507628172	-0.00303422689483	-0.000892595436066	True
CA1_pair	94406.0876286	-0.0639451426533	-0.00336877239919	-0.000996912378702	True
CA1_pair	100000	-0.0639388379332	-0.00373742588046	-0.0011136897533	True
CA1_pair	105925.372518	-0.0639317654407	-0.00414293327815	-0.00124437963083	True
CA1_pair	112201.84543	-0.0639238318862	-0.00458811356391	-0.00139059401636	True
CA1_pair	118850.222744	-0.0639149326987	-0.00507583035921	-0.00155412007927	True
CA1_pair	125892.541179	-0.063904950675	-0.00560895794712	-0.00173693620454	True
CA1_pair	133352.143216	-0.0638937544716	-0.00619034174855	-0.00194122872512	True
CA1_pair	141253.754462	-0.0638811969202	-0.00682275357805	-0.00216940912737	True
CA1_pair	149623.565609	-0.0638671131495	-0.00750884226386	-0.00242413143539	True
CA1_pair	158489.319246	-0.0638513184896	-0.00825108049638	-0.00270830937431	True
CA1_pair	167880.401812	-0.0638336061385	-0.00905170903884	-0.00302513278246	True
CA1_pair	177827.941004	-0.0638137445648	-0.00991267967187	-0.00337808258613	True
CA1_pair	188364.908949	-0.063791474619	-0.0108355984295	-0.00377094346456	True
CA1_pair	199526.231497	-0.0637665063263	-0.0118216707984	-0.00420781311624	True
CA1_pair	211348.903984	-0.0637385153286	-0.0128716505816	-0.00469310678867	True
CA1_pair	223872.113857	-0.0637071389445	-0.0139857940664	-0.00523155545592	True
CA1_pair	237137.370566	-0.063671971813	-0.0151638209842	-0.00582819572527	True
CA1_pair	251188.643151	-0.0636325610867	-0.0164048835106	-0.00648834923694	True
CA1_pair	266072.50598	-0.0635884011393	-0.01770754425	-0.00721758900433	True
CA1_pair	281838.293126	-0.0635389277532	-0.0190697637835	-0.00802168985101	True
CA1_pair	298538.261892	-0.0634835117557	-0.0204888979572	-0.00890655986744	True
CA1_pair	316227.766017	-0.0634214520735	-0.0219617046683	-0.0098781496798	True

Table S2c continued

pair_id	frequency_hz	contrast_M1_s_per_m	contrast_M2_s_per_m	contrast_M3_s_per_m	sign_agreement
CA1_pair	334965.439158	-0.0633519681826	-0.0234843594758	-0.0109423363511	True
CA1_pair	354813.389234	-0.0632741919402	-0.0250524789471	-0.0121047789884	True
CA1_pair	375837.404288	-0.0631871587917	-0.0266611502606	-0.0133707436832	True
CA1_pair	398107.170553	-0.0630897983687	-0.0283049652374	-0.0147448963482	True
CA1_pair	421696.503429	-0.0629809245093	-0.0299780566923	-0.0162310633997	True
CA1_pair	446683.592151	-0.0628592247631	-0.0316741347986	-0.0178319621297	True
CA1_pair	473151.258961	-0.0627232494757	-0.0333865210812	-0.0195489050331	True
CA1_pair	501187.233627	-0.0625714005959	-0.0351081777012	-0.0213814852616	True
CA1_pair	530884.444231	-0.0624019203996	-0.0368317299109	-0.0233272536567	True
CA1_pair	562341.32519	-0.0622128803943	-0.0385494799349	-0.0253814012535	True
CA1_pair	595662.143529	-0.0620021707505	-0.040253411094	-0.0275364644411	True
CA1_pair	630957.34448	-0.0617674907005	-0.0419351817143	-0.029782072698	True
CA1_pair	668343.917569	-0.0615063404579	-0.0435861092497	-0.0321047605395	True
CA1_pair	707945.784384	-0.0612160153417	-0.0451971460565	-0.0344878655282	True
CA1_pair	749894.209332	-0.0608936029293	-0.0467588493722	-0.0369115325221	True
CA1_pair	794328.234724	-0.0605359842165	-0.0482613492155	-0.0393528405312	True
CA1_pair	841395.141645	-0.060139839926	-0.0496943191034	-0.0417860626381	True
CA1_pair	891250.938134	-0.0597016632586	-0.0510469556135	-0.0441830617635	True
CA1_pair	944060.876286	-0.0592177805231	-0.0523079738369	-0.0465138162647	True
CA1_pair	1000000	-0.0586843811895	-0.0534656265834	-0.0487470603742	True
CA1_pair	1059253.72518	-0.0580975589528	-0.0545077557129	-0.0508510163564	True
CA1_pair	1122018.4543	-0.0574533653622	-0.0554218840377	-0.0527941889652	True
CA1_pair	1188502.22744	-0.0567478774071	-0.056195355722	-0.0545461890704	True
CA1_pair	1258925.41179	-0.0559772801347	-0.0568155318357	-0.0560785525154	True
CA1_pair	1333521.43216	-0.0551379648616	-0.0572700455362	-0.0573655222153	True
CA1_pair	1412537.54462	-0.0542266428015	-0.057547118148	-0.0583847656165	True
CA1_pair	1496235.65609	-0.0532404729435	-0.0576359331231	-0.0591180049717	True
CA1_pair	1584893.19246	-0.0521772017853	-0.0575270595816	-0.0595515434225	True

Table S2c continued

pair_id	frequency_hz	contrast_M1_s_per_m	contrast_M2_s_per_m	contrast_M3_s_per_m	sign_agreement
CA1_pair	1678804.01812	-0.051035311082	-0.0572129110795	-0.0596766746996	True
CA1_pair	1778279.41004	-0.049814168194	-0.0566882188547	-0.0594899677481	True
CA1_pair	1883649.08949	-0.048514172025	-0.055950492698	-0.0589934196202	True
CA1_pair	1995262.31497	-0.0471368861091	-0.0550004375902	-0.0581944708654	True
CA1_pair	2113489.03984	-0.0456851493403	-0.0538422912483	-0.057105878107	True
CA1_pair	2238721.13857	-0.0441631543785	-0.0524840476302	-0.0557454394574	True
CA1_pair	2371373.70566	-0.0425764841223	-0.0509375349609	-0.0541355708422	True
CA1_pair	2511886.43151	-0.0409320979855	-0.0492183243148	-0.0523027358473	True
CA1_pair	2660725.0598	-0.0392382621095	-0.0473454560187	-0.0502767386237	True
CA1_pair	2818382.93126	-0.037504421016	-0.0453409853268	-0.0480898982955	True
CA1_pair	2985382.61892	-0.0357410123162	-0.0432293645238	-0.0457761332715	True
CA1_pair	3162277.66017	-0.0339592305618	-0.0410366939498	-0.0433699933857	True
CA1_pair	3349654.39158	-0.0321707506415	-0.0387898873323	-0.0409056852383	True
CA1_pair	3548133.89234	-0.0303874247592	-0.0365158053726	-0.0384161399213	True
CA1_pair	3758374.04288	-0.0286209694953	-0.034240414433	-0.035932171436	True
CA1_pair	3981071.70553	-0.0268826603952	-0.031988023939	-0.0334817682232	True
CA1_pair	4216965.03429	-0.0251830508161	-0.0297806472251	-0.0310895498856	True
CA1_pair	4466835.92151	-0.0235317295076	-0.0276375173972	-0.0287764076917	True
CA1_pair	4731512.58961	-0.0219371278988	-0.0255747743197	-0.026559332638	True
CA1_pair	5011872.33627	-0.0204063838071	-0.0236053232355	-0.0244514206725	True
CA1_pair	5308844.44231	-0.0189452637983	-0.0217388517726	-0.022462032855	True
CA1_pair	5623413.2519	-0.0175581422317	-0.0199819816083	-0.0205970799325	True
CA1_pair	5956621.43529	-0.0162480315198	-0.0183385246032	-0.0188593965472	True
CA1_pair	6309573.4448	-0.0150166555895	-0.0168098108102	-0.0172491699095	True
CA1_pair	6683439.17569	-0.0138645570395	-0.0153950568685	-0.0157643905901	True
CA1_pair	7079457.84384	-0.0127912279991	-0.0140917470152	-0.0144012981556	True
CA1_pair	7498942.09332	-0.0117952550615	-0.0128960042557	-0.0131548006259	True
CA1_pair	7943282.34724	-0.010874469663	-0.011802935163	-0.0120188532558	True

Table S2c continued

pair_id	frequency_hz	contrast_M1_s_per_m	contrast_M2_s_per_m	contrast_M3_s_per_m	sign_agreement
CA1_pair	8413951.41645	-0.0100260966797	-0.0108069375484	-0.0109867881882	True
CA1_pair	8912509.38134	-0.00924689560374	-0.00990196532322	-0.0100515916456	True
CA1_pair	9440608.76286	-0.00853329025175	-0.0090817489731	-0.00920612928661	True
CA1_pair	10000000	-0.0078814844285	-0.00833997309489	-0.0084433231471	True
CA1_pair	10592537.2518	-0.00728756223541	-0.00767041447254	-0.00775628530908	True
CA1_pair	11220184.543	-0.00674757273417	-0.00706704533017	-0.00713841429494	True
CA1_pair	11885022.2744	-0.00625759944907	-0.00652410688951	-0.0065834603755	True
CA1_pair	12589254.1179	-0.00581381573331	-0.00603615835827	-0.0060855657145	True
CA1_pair	13335214.3216	-0.00541252736499	-0.0055981061536	-0.00563928472393	True
CA1_pair	14125375.4462	-0.00505020391624	-0.00520521765651	-0.00523958931203	True
CA1_pair	14962356.5609	-0.00472350049016	-0.00485312320055	-0.00488186296909	True
CA1_pair	15848931.9246	-0.0044292713811	-0.00453780939299	-0.00456188692197	True
CA1_pair	16788040.1812	-0.00416457711261	-0.00425560629412	-0.004275820937	True
CA1_pair	17782794.1004	-0.00392668617014	-0.00400317046636	-0.00402018078197	True
CA1_pair	18836490.8949	-0.00371307258921	-0.00377746546041	-0.0037918138783	True
CA1_pair	19952623.1497	-0.00352141039958	-0.00357574093335	-0.00358787427987	True
CA1_pair	21134890.3984	-0.00334956577005	-0.00339551128796	-0.00340579779953	True
CA1_pair	22387211.3857	-0.00319558755385	-0.00323453447879	-0.00324327785566	True
CA1_pair	23713737.0566	-0.00305769680425	-0.0030907914376	-0.00309824242015	True
CA1_pair	25118864.3151	-0.00293427571529	-0.00296246642242	-0.00296883230458	True
CA1_pair	26607250.598	-0.00282385634396	-0.00284792848127	-0.00285338091401	True
CA1_pair	28183829.3126	-0.00272510938684	-0.00274571413712	-0.00275039552015	True
CA1_pair	29853826.1892	-0.00263683321508	-0.00265451133891	-0.00265854005037	True
CA1_pair	31622776.6017	-0.00255794331465	-0.00257314467876	-0.00257661935125	True
CA1_pair	33496543.9158	-0.00248746223333	-0.00250056184491	-0.00250356486043	True
CA1_pair	35481338.9234	-0.00242451009932	-0.00243582125894	-0.00243842160537	True
CA1_pair	37583740.4288	-0.00236829574809	-0.00237808083295	-0.0023803364393	True
CA1_pair	39810717.0553	-0.00231810847207	-0.00232658777473	-0.00232854742132	True

Table S2c continued

pair_id	frequency_hz	contrast_M1_s_per_m	contrast_M2_s_per_m	contrast_M3_s_per_m	sign_agreement
CA1_pair	42169650.3429	-0.00227331039147	-0.0022806693656	-0.00228237424787	True
CA1_pair	44668359.2151	-0.0022333294322	-0.0022397246352	-0.00224120964538	True
CA1_pair	47315125.8961	-0.00219765288845	-0.00220321685899	-0.0022045116379	True
CA1_pair	50118723.3627	-0.00216582154146	-0.00217066680704	-0.00217179660867	True
CA1_pair	53088444.4231	-0.00213742430257	-0.00214164667646	-0.00214263307996	True
CA1_pair	56234132.519	-0.00211209334619	-0.00211577464424	-0.00211663614141	True
CA1_pair	59566214.3529	-0.00208949969816	-0.00209270998138	-0.00209346246253	True
CA1_pair	63095734.448	-0.00206934924445	-0.00207214867412	-0.00207280583087	True
CA1_pair	66834391.7569	-0.00205137912674	-0.00205381950223	-0.0020543931623	True
CA1_pair	70794578.4384	-0.00203535449196	-0.00203748052876	-0.002037980935	True
CA1_pair	74989420.9332	-0.00202106556523	-0.00202291595978	-0.00202335200338	True
CA1_pair	79432823.4724	-0.00200832501698	-0.00200993333625	-0.00201031275222	True
CA1_pair	84139514.1645	-0.00199696559719	-0.00199836102399	-0.00199869055557	True
CA1_pair	89125093.8134	-0.00198683801153	-0.00198804597082	-0.00198833150807	True
CA1_pair	94406087.6286	-0.00197780901634	-0.00197885170305	-0.00197909840017	True
CA1_pair	100000000	-0.00196975971097	-0.00197065653622	-0.00197086891107	True

Units: Hz; S m^-1; dimensionless flags. Denominator: Existing model-specific normal states. 603 existing region/frequency comparisons; no model averaging.

Full records: Table_S2c.csv.

Table S2d. Occupancy-only and radius-only diagnostic summary

Table S2d, column panel 1/3. First column is repeated for alignment.

Row	pair_id	region	integration_metric	full_integrated_s_per_m_decade
1	CA3_pair	CA3	integral of absolute signed conductivity contrast over log10(f)	0.0802893452618
2	cortex_pair	cortex	integral of absolute signed conductivity contrast over log10(f)	0.233266312819
3	CA1_pair	CA1	integral of absolute signed conductivity contrast over log10(f)	0.227705414074

Table S2d, column panel 2/3. First column is repeated for alignment.

Row	pair_id	p_only_integrated_s_per_m_decade	r_only_integrated_s_per_m_decade	interaction_integrated_s_per_m_decade
1	CA3_pair	0.0852400988271	0.00482194654607	0.000128807019227
2	cortex_pair	0.248203441341	0.0138810258226	0.00105610269954
3	CA1_pair	0.242410670674	0.0137229556039	0.000982300995929

Table S2d, column panel 3/3. First column is repeated for alignment.

Row	pair_id	p_to_r_ratio	pair_dominant_contribution	diagnostic_status
1	CA3_pair	17.6775287765	P	MECHANISM DIAGNOSTIC ONLY
2	cortex_pair	17.88077081	P	MECHANISM DIAGNOSTIC ONLY
3	CA1_pair	17.6646108659	P	MECHANISM DIAGNOSTIC ONLY

Units: As encoded in column names. Denominator: Original integrated-contrast definition in source. Artificial structural decompositions, not independent physiological processes.

Full records: Table_S2d.csv.

Table S2e. Archived limiting, positivity and frequency-grid checks

Record 1: stage0_cell_swelling / tests

[0]/test: TEST 1: P -> 0 gives extracellular medium
[0]/status: PASS
[0]/value: $1.5000555264939538 \times 10^{-12}$
[0]/criterion: relative error < 1×10^{-10}
[1]/test: TEST 2: uniform medium has no beta dispersion
[1]/status: PASS
[1]/value: $8.881784197001252 \times 10^{-16}$
[1]/criterion: maximum relative identity/dispersion error < 1×10^{-10}
[2]/test: TEST 3: sigma_eff > 0
[2]/status: PASS
[2]/value: 0.0340023221934323
[2]/criterion: minimum sigma_eff > 0 S/m
[3]/test: TEST 4: legal volume fractions
[3]/status: PASS
[3]/value: 0.0
[3]/criterion: 0 < phi_ECS,P < 1 and phi_ECS+P=1
[4]/test: TEST 5: swelling geometry is monotonic
[4]/status: PASS
[4]/value: True
[4]/criterion: decreasing ECS implies increasing P and R/R0
[5]/test: TEST 6: 101 vs 201 point frequency-grid convergence
[5]/status: PASS
[5]/value/C_sigma_max: 0.0
[5]/value/f_beta_normal: 0.00017679993484498446
[5]/value/f_beta_severe: 0.00020455510730732485
[5]/criterion: C_sigma relative change < 0.005; each f_beta relative change < 0.01
[6]/test: AUDIT A/B: complex-property formulas and exp(jwt) sign agree
[6]/status: PASS
[6]/value: $7.905854143337271 \times 10^{-22}$
[6]/criterion: relative error < 1×10^{-10}
[7]/test: AUDIT F: beta peaks are interior to frequency grid
[7]/status: PASS
[7]/value[0]/phi_ecs: 0.2
[7]/value[0]/beta_grid_index: 70
[7]/value[1]/phi_ecs: 0.18
[7]/value[1]/beta_grid_index: 70
[7]/value[2]/phi_ecs: 0.15
[7]/value[2]/beta_grid_index: 70
[7]/value[3]/phi_ecs: 0.12
[7]/value[3]/beta_grid_index: 70
[7]/value[4]/phi_ecs: 0.08
[7]/value[4]/beta_grid_index: 70
[7]/value[5]/phi_ecs: 0.05
[7]/value[5]/beta_grid_index: 70
[7]/criterion: no beta-gradient maximum at first or last frequency point
[8]/test: AUDIT D/E: shell geometry and radius-volume relation are valid
[8]/status: PASS

[8]/value: $4.440892098500626 \times 10^{-16}$
[8]/criterion: dm < R and max |(R/R0)^3 - V/V0| is numerical roundoff
[9]/test: AUDIT G: all eight figures have PNG and PDF outputs
[9]/status: PASS
[9]/value/files: 16
[9]/value/expected: 16
[9]/criterion: 16 non-empty files generated directly from the in-memory spectra table
[10]/test: AUDIT G: raw CSV matches in-memory plotted data
[10]/status: PASS
[10]/value/rows: 606
[10]/value/roundtrip_max_abs_difference: $1.862645149230957 \times 10^{-9}$
[10]/criterion: same row count and rtol <= 1×10^{-12} for plotted numeric columns
[11]/test: AUDIT H: report preserves benchmark/pilot/clinical distinction
[11]/status: PASS
[11]/value/assumed pilot value: True
[11]/value/not an established clinical value: True
[11]/value/benchmark scale: True
[11]/value/not clinical detectability thresholds: True
[11]/value/cannot show that cerebral ischaemia is detectable: True
[11]/criterion: all required assumption and non-clinical disclaimer phrases are present
[12]/test: AUDIT I: GO/NO-GO is generated from coded rules
[12]/status: PASS
[12]/value: STRONG_GO
[12]/criterion: decision JSON, report, and coded evaluator agree

Record 2: stage0_cell_swelling / convergence

coarse_points: 101.0
fine_points: 201.0
coarse_c_sigma_max_fraction: 0.7621366142376721
fine_c_sigma_max_fraction: 0.7621366142376721
relative_change_c_sigma_max: 0.0
coarse_f_beta_normal_hz: 3306043.413235529
fine_f_beta_normal_hz: 3306627.921495584
relative_change_f_beta_normal: 0.00017679993484498446
coarse_f_beta_severe_hz: 3289229.256769716
fine_f_beta_severe_hz: 3289902.085413293
relative_change_f_beta_severe: 0.00020455510730732485

Record 3: results / row_count

: True

Record 4: results / finite_spectra

: True

Record 5: results / baseline_zero_relative

: True

Record 6: results / baseline_zero_absolute

: True

Record 7: results / four_figures

: True

Record 8: results / frequency_grid_unchanged

: True

Record 9: stage1BI_structural_mechanism / checks

structural_freeze_status_ready: True
three_independent_regional_pairs: True
frequency_grid_201_points: True
frequency_bounds_match_stage0: True
all_spectra_finite: True
all_conductivities_positive: True
beta_peaks_interior: True
diagnostic_absolute_metric_identity: True
all_seven_figures_present: True
grid_convergence_pass: True
electrical_parameters_identical_by_construction: True
stage1BII_parameters_remain_null: True
historical_stage1a_freeze_exists_and_was_not_overwritten: True
no_comsol_or_head_or_coil_model_called: True

Record 10: stage1BI_structural_mechanism / decomposition_max_abs_identity_error_s_per_m

: 0.0

Record 11: stage1BI_structural_mechanism / convergence_201_vs_401

coarse_points: 201
fine_points: 401
max_relative_contrast_largest_relative_change: 0.0
beta_frequency_largest_relative_change: $2.395971225899185 \times 10^{-5}$
pass: True

Record 12: stage1BI_structural_mechanism / structural_freeze_sha256

: 09d76e74fa4d765085359a88d0db756122a5e019d569d0d00a8d309df38c06cc

Record 13: stage1BI_structural_mechanism / stage0_single_shell_sha256

: e87cb2bf64c7b5ffb430447aeccaadd36721aa6897d832a9232ae9578a186763

Record 14: stage1BI_structural_mechanism / stage0_config_sha256

: 6bf365c3a1544138ec87a0f2694799791791735589f958e94b139aab89e6d55a

Record 15: stage1BI_structural_mechanism / model_name

: STRUCTURAL-ONLY ISCHEMIA MODEL

Units: Original units retained. Denominator: Original criterion and denominator retained within each record. These are archived test records, not newly executed calculations.

Full records: Table_S2e.csv.

All 603 frequency-resolved comparisons in Table S2c agree in sign. The 15 rows of Table S2b summarize these points by region and frequency band. This resolves a source-filename transcription in the V2 assembly plan: the 603 point records are in robustness_metrics.csv,

whereas sign_agreement.csv contains band summaries. The count and scientific conclusion are unchanged. Model magnitudes and regional rankings differ (Table S2a).

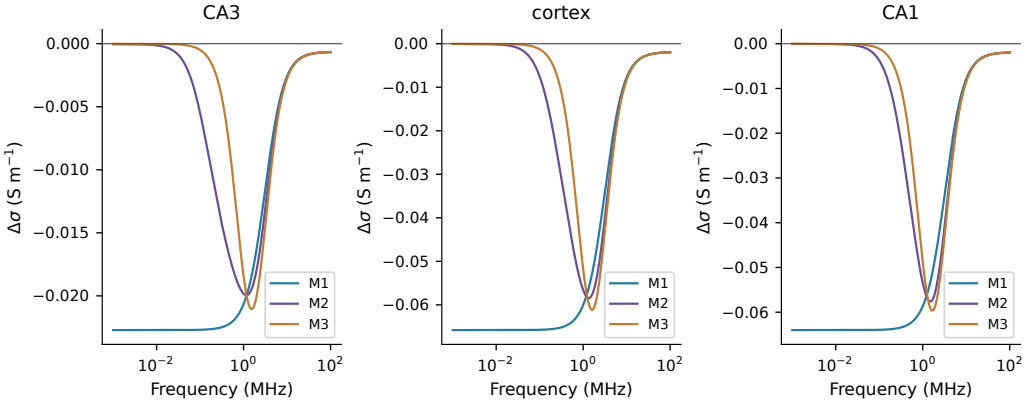


Figure S2. Signed conductivity contrasts from the three existing analytical comparators. The same sign across the 603 region/frequency points does not imply agreement in magnitude or model accuracy. No model is used as biological ground truth.

S3. Thin interface, homogeneous recovery and geometry checks

The nominal membrane surface admittance is $y_m = G_m + j\omega C_m$, with $G_m = 20\ \mathrm{S\,m^{-2}}$ and C_m approximately $0.008854\ \mathrm{F\,m^{-2}}$. For the normal from intracellular to extracellular space, normal total current is continuous and $j_n = y_m(u_i - u_e)$. The membrane has electrical thickness 5 nm but no separate volumetric mesh. Bulk equations and extraction are given in main Methods 2.3. Poignard [6] supports thin-membrane modelling for its stated smooth geometries; its asymptotic error estimates are not corner-error estimates for these cubes.

Table S3a. Homogeneous-medium recovery

Table S3a, column panel 1/3. First column is repeated for alignment.

Row	frequency_Hz	Y_real_S	Y_imag_S	gamma_real_S_per_m
1	1000	$8.68237807692 \times 10^{-6}$	$3.86417938211 \times 10^{-11}$	1.00000571419
2	1000000	$8.68237807692 \times 10^{-6}$	$3.86417938211 \times 10^{-8}$	1.00000571419
3	10000000	$8.68237807692 \times 10^{-6}$	$3.86417938211 \times 10^{-7}$	1.00000571419

Table S3a, column panel 2/3. First column is repeated for alignment.

Row	frequency_Hz	gamma_imag_S_per_m	epsilon_r_recovered	sigma_relative_error
1	1000	$4.45062565639 \times 10^{-6}$	80.0004571895	$5.71418831274 \times 10^{-6}$
2	1000000	0.00445062565639	80.0004571895	$5.71418831763 \times 10^{-6}$
3	10000000	0.0445062565639	80.0004571895	$5.7141883183 \times 10^{-6}$

Table S3a, column panel 3/3. First column is repeated for alignment.

Row	frequency_Hz	epsilon_r_relative_error	imaginary_sign
1	1000	$5.71486898355 \times 10^{-6}$	POSITIVE
2	1000000	$5.71486898568 \times 10^{-6}$	POSITIVE
3	10000000	$5.71486898693 \times 10^{-6}$	POSITIVE

Units: Hz; S; $\mathrm{S\,m^{-1}}$; relative errors dimensionless. Denominator: Reference sigma=1 $\mathrm{S\,m^{-1}}$; epsilon_r=80. Numerical recovery, not physiological validation.

Full records: Table_S3a.csv.

Table S3b. Thin-membrane slab benchmark

Table S3b, column panel 1/3. First column is repeated for alignment.

Row	frequency_Hz	Y_FEM_real_S	Y_FEM_imag_S	Y_expected_real_S
1	1000000	$1.63751746216 \times 10^{-6}$	$3.39492818964 \times 10^{-6}$	$1.63748482398 \times 10^{-6}$

Table S3b, column panel 2/3. First column is repeated for alignment.

Row	frequency_Hz	Y_expected_imag_S	complex_relative_error	real_relative_error
1	1000000	$3.39492739884 \times 10^{-6}$	$8.66171552923 \times 10^{-6}$	$1.99318990811 \times 10^{-5}$

Table S3b, column panel 3/3. First column is repeated for alignment.

Row	frequency_Hz	imag_relative_error
1	1000000	$2.32935564184 \times 10^{-7}$

Units: Hz; S; dimensionless relative errors. Denominator: Independent slab complex admittance. The recorded 1 MHz relative complex error is $8.661715529 \times 10^{-6}$.

Full records: Table_S3b.csv.

Table S3c. Geometry-volume and membrane-selection checks

Table S3c, column panel 1/3. First column is repeated for alignment.

Row	topology_short	phi_ECS	target_cell_volume_m3	fem_cell_volume_m3
1	A	0.2	$5.23598775598 \times 10^{-16}$	$5.23598775598 \times 10^{-16}$
2	B	0.2	$5.23598775598 \times 10^{-16}$	$5.23598775598 \times 10^{-16}$
3	A	0.15	$5.56323699073 \times 10^{-16}$	$5.56323699073 \times 10^{-16}$
4	B	0.15	$5.56323699073 \times 10^{-16}$	$5.56323699073 \times 10^{-16}$
5	A	0.1	$5.89048622548 \times 10^{-16}$	$5.89048622548 \times 10^{-16}$
6	B	0.1	$5.89048622548 \times 10^{-16}$	$5.89048622548 \times 10^{-16}$
7	A	0.05	$6.21773546023 \times 10^{-16}$	$6.21773546023 \times 10^{-16}$
8	B	0.05	$6.21773546023 \times 10^{-16}$	$6.21773546023 \times 10^{-16}$

Table S3c, column panel 2/3. First column is repeated for alignment.

Row	topology_short	target_ECS_volume_m3	fem_ECS_volume_m3	measured_phi_ECS
1	A	$1.308996939 \times 10^{-16}$	$1.308996939 \times 10^{-16}$	0.2
2	B	$1.308996939 \times 10^{-16}$	$1.308996939 \times 10^{-16}$	0.2
3	A	$9.81747704247 \times 10^{-17}$	$9.81747704247 \times 10^{-17}$	0.15
4	B	$9.81747704247 \times 10^{-17}$	$9.81747704247 \times 10^{-17}$	0.15
5	A	$6.54498469498 \times 10^{-17}$	$6.54498469498 \times 10^{-17}$	0.1
6	B	$6.54498469498 \times 10^{-17}$	$6.54498469498 \times 10^{-17}$	0.1
7	A	$3.27249234749 \times 10^{-17}$	$3.27249234749 \times 10^{-17}$	0.05
8	B	$3.27249234749 \times 10^{-17}$	$3.27249234749 \times 10^{-17}$	0.05

Table S3c, column panel 3/3. First column is repeated for alignment.

Row	topology_short	fem_membrane_area_m2
1	A	$3.89777708972 \times 10^{-10}$
2	B	$3.97201184602 \times 10^{-10}$
3	A	$4.05853807284 \times 10^{-10}$
4	B	$4.11436433986 \times 10^{-10}$
5	A	$4.2161754996 \times 10^{-10}$
6	B	$4.2534773458 \times 10^{-10}$
7	A	$4.37091885625 \times 10^{-10}$
8	B	$4.38960513809 \times 10^{-10}$

Units: m; m^3; m^2; dimensionless fractions. Denominator: Target volume and target phi; B/A membrane area. B changes membrane area. These geometries are model abstractions.

Full records: Table_S3c.csv.

Table S3d. Limited orthogonal-direction check

Table S3d, column panel 1/2. First column is repeated for alignment.

Row	topology_short	phi_ECS	frequency_Hz	axis
1	A	0.1	1000000	x
2	A	0.1	1000000	y
3	A	0.1	1000000	z
4	B	0.1	1000000	x
5	B	0.1	1000000	y
6	B	0.1	1000000	z

Table S3d, column panel 2/2. First column is repeated for alignment.

Row	topology_short	sigma_eff_S_per_m	epsilon_r_eff	sigma_directional_spread_percent
1	A	0.207158468049	4763.66454104	0.0255713805866
2	A	0.207140107907	4763.69925365	0.0255713805866
3	A	0.207193082573	4763.62323716	0.0255713805866
4	B	0.213972793954	4875.9006474	0.000605522656313
5	B	0.213971806218	4875.72586931	0.000605522656313
6	B	0.21397310187	4875.80798483	0.000605522656313

Units: Hz; $\mathrm{S\,m^{-1}}$; dimensionless epsilon and spread. Denominator: Recorded directional spread at phi0.10, 1 MHz. One-point direction check, not full anisotropic characterization.

Full records: Table_S3d.csv.

S4. RVE mesh, domain size, boundary and topology comparisons

The following finite comparisons retain their original cases and normalization. Domain-size checks concern configured regular domains, not statistical representative-volume convergence of random tissue. Bottleneck geometry changes membrane area; the aligned/staggered comparison preserves cellular shape, volume and area. No all-state numerical bound is inferred.

Table S4a. Tested domain-size dependence

Table S4a, column panel 1/4. First column is repeated for alignment.

Row	phi_ECS	frequency_Hz	sigma_single_S_per_m	sigma_T3A_S_per_m
1	0.2	100000	0.143039117101	0.143510004616
2	0.2	1000000	0.267220850914	0.268085809877
3	0.2	3000000	0.554145876319	0.556130655836
4	0.1	100000	0.0710104637849	0.0709770111792
5	0.1	1000000	0.207158468049	0.207414831762
6	0.1	3000000	0.491483959978	0.493040297535
7	0.05	100000	0.0367832779665	0.0372529435456
8	0.05	1000000	0.164680819978	0.166079697416
9	0.05	3000000	0.44924808126	0.451289644355

Table S4a, column panel 2/4. First column is repeated for alignment.

Row	phi_ECS	D_size_sigma	D_size_sigma_percent	epsilon_single
1	0.2	0.00329201916803	0.329201916803	5952.39326162
2	0.2	0.00323686927911	0.323686927911	4670.73447923
3	0.2	0.00358169139478	0.358169139478	2150.10625519
4	0.1	0.000471094032646	0.0471094032646	6578.16071755
5	0.1	0.00123752466348	0.123752466348	4763.66454104
6	0.1	0.00316660905304	0.316660905304	2340.56703986
7	0.05	0.0127684536308	1.27684536308	6850.42409936
8	0.05	0.00849447699901	0.849447699901	4594.4316884
9	0.05	0.00454440025429	0.454440025429	2479.95006048

Table S4a, column panel 3/4. First column is repeated for alignment.

Row	phi_ECS	epsilon_T3A	D_size_epsilon	D_size_epsilon_percent
1	0.2	5966.67427857	0.00239920588585	0.239920588585
2	0.2	4683.78940874	0.00279504852324	0.279504852324
3	0.2	2151.32848079	0.000568448930566	0.0568448930566
4	0.1	6591.10392057	0.00196760212671	0.196760212671
5	0.1	4776.23862113	0.00263958135271	0.263958135271
6	0.1	2341.67732922	0.00047436768232	0.047436768232
7	0.05	6845.52970993	0.000714465172169	0.0714465172169
8	0.05	4607.21359012	0.00278204195437	0.278204195437
9	0.05	2480.65003762	0.000282254528804	0.0282254528804

Table S4a, column panel 4/4. First column is repeated for alignment.

Row	phi_ECS	size_validation_status
1	0.2	PASS
2	0.2	PASS
3	0.2	PASS
4	0.1	PASS
5	0.1	PASS
6	0.1	PASS
7	0.05	PASS
8	0.05	PASS
9	0.05	PASS

Units: Hz; $\mathrm{S\,m^{-1}}$; dimensionless epsilon; percent difference. Denominator: Single-domain conductivity or epsilon. Nine existing comparisons only.

Full records: Table_S4a.csv.

Table S4b. Selected lateral-boundary comparisons

Table S4b, column panel 1/4. First column is repeated for alignment.

Row	phi_ECS	frequency_Hz	sigma_side_insulation_S_per_m	sigma_yz_periodic_S_per_m
1	0.1	100000	0.0710104637849	0.0709327132987
2	0.1	1000000	0.207158468049	0.207066098444

Table S4b, column panel 2/4. First column is repeated for alignment.

Row	phi_ECS	D_BC_sigma	D_BC_sigma_percent	epsilon_side_insulation
1	0.1	0.00109491590494	0.109491590494	6578.16071755
2	0.1	0.000445888625352	0.0445888625352	4763.66454104

Table S4b, column panel 3/4. First column is repeated for alignment.

Row	phi_ECS	epsilon_yz_periodic	D_BC_epsilon	D_BC_epsilon_percent
1	0.1	6578.58135454	$6.39444677947 \times 10^{-5}$	0.00639444677947
2	0.1	4764.05164573	$8.12619557214 \times 10^{-5}$	0.00812619557214

Table S4b, column panel 4/4. First column is repeated for alignment.

Row	phi_ECS	boundary_validation_status
1	0.1	PASS
2	0.1	PASS

Units: Hz; $\mathrm{S\,m^{-1}}$; dimensionless epsilon; recorded percent difference. Denominator: Insulating-side reference. Opposite x faces driven; only lateral treatment changes.

Full records: Table_S4b.csv.

Table S4c. Same-frequency finite prescribed effects

frequency_Hz	ECS_endpoint_percent	max_topology_percent	finite_effect_ratio
100000	74.284462382	6.52716371405	See S9
1000000	38.3727656675	6.44280856562	See S9
3000000	18.9296355962	5.29472917418	See S9

Units: Hz; percent; dimensionless ratio. Denominator: ECS=abs(R_σ(.05)-1); topology=max(abs(T_kappa),abs(T_arrangement)) at the same f. Unequal finite prescribed perturbations, not sensitivity derivatives or universal dominance.

Full records: Table_S4c.csv.

Table S4d. Stage2B coarse, medium and fine meshes

Table S4d, column panel 1/3. First column is repeated for alignment.

Row	case	phi_ECS	frequency_Hz	mesh_label
1	M1_B_phi005_kappa030	0.05	1000000	coarse
2	M1_B_phi005_kappa030	0.05	1000000	medium
3	M1_B_phi005_kappa030	0.05	1000000	fine
4	M2_T3B_phi005	0.05	1000000	coarse
5	M2_T3B_phi005	0.05	1000000	medium
6	M2_T3B_phi005	0.05	1000000	fine

Table S4d, column panel 2/3. First column is repeated for alignment.

Row	case	mesh_elements	sigma_eff_S_per_m	epsilon_r_eff
1	M1_B_phi005_kappa030	148362	0.174744194345	4706.95901019
2	M1_B_phi005_kappa030	360433	0.175290889954	4702.28966894
3	M1_B_phi005_kappa030	845892	0.175393406662	4703.39679414
4	M2_T3B_phi005	122637	0.161098285762	4615.1341105
5	M2_T3B_phi005	277320	0.160480556255	4601.59122949
6	M2_T3B_phi005	779163	0.160014671152	4591.18881553

Table S4d, column panel 3/3. First column is repeated for alignment.

Row	case	medium_to_fine_sigma_change
1	M1_B_phi005_kappa030	0.000584495795578
2	M1_B_phi005_kappa030	0.000584495795578
3	M1_B_phi005_kappa030	0.000584495795578
4	M2_T3B_phi005	0.00291151492785
5	M2_T3B_phi005	0.00291151492785
6	M2_T3B_phi005	0.00291151492785

Units: Hz; $S\,m^{-1}$; dimensionless epsilon and change. Denominator: Original medium-to-fine metric. Only the two recorded 1 MHz cases.

Full records: Table_S4d.csv.

Table S4e. Earlier Stage2A mesh checks

Table S4e, column panel 1/3. First column is repeated for alignment.

Row	topology	phi_ECS	frequency_Hz	mesh_label
1	TOPOLOGY_B_CONSTRICTED_CONNECTED	0.05	1000	coarse
2	TOPOLOGY_B_CONSTRICTED_CONNECTED	0.05	1000	fine
3	TOPOLOGY_B_CONSTRICTED_CONNECTED	0.05	1000	medium
4	TOPOLOGY_B_CONSTRICTED_CONNECTED	0.05	3000000	coarse
5	TOPOLOGY_B_CONSTRICTED_CONNECTED	0.05	3000000	fine
6	TOPOLOGY_B_CONSTRICTED_CONNECTED	0.05	3000000	medium

Table S4e, column panel 2/3. First column is repeated for alignment.

Row	topology	mesh_elements	sigma_eff_S_per_m	epsilon_r_eff
1	TOPOLOGY_B_CONSTRICTED_CONNECTED	200682	0.0332440887567	7209.0336692
2	TOPOLOGY_B_CONSTRICTED_CONNECTED	1230163	0.0330477919504	7196.6162652
3	TOPOLOGY_B_CONSTRICTED_CONNECTED	545864	0.0333383461392	7206.34063543
4	TOPOLOGY_B_CONSTRICTED_CONNECTED	200682	0.457081806163	2470.7121735
5	TOPOLOGY_B_CONSTRICTED_CONNECTED	1230163	0.456845037753	2470.60979158
6	TOPOLOGY_B_CONSTRICTED_CONNECTED	545864	0.456579963981	2470.70222023

Table S4e, column panel 3/3. First column is repeated for alignment.

Row	topology	medium_to_fine_sigma_change
1	TOPOLOGY_B_CONSTRICTED_CONNECTED	0.00879193954326
2	TOPOLOGY_B_CONSTRICTED_CONNECTED	0.00879193954326
3	TOPOLOGY_B_CONSTRICTED_CONNECTED	0.00879193954326
4	TOPOLOGY_B_CONSTRICTED_CONNECTED	0.000580226882157
5	TOPOLOGY_B_CONSTRICTED_CONNECTED	0.000580226882157
6	TOPOLOGY_B_CONSTRICTED_CONNECTED	0.000580226882157

Units: Hz; S m^-1; dimensionless epsilon/change. Denominator: Original medium-to-fine metric. Maximum recorded relative sigma change 0.008791939543; not a global error bound.

Full records: Table_S4e.csv.

Table S4f. Bottleneck–geometry sweep

Table S4f, column panel 1/2. First column is repeated for alignment.

Row	phi_ECS	frequency_Hz	kappa	sigma_eff_S_per_m	sigma_A_S_per_m	T_kappa
1	0.05	1000	0.3	0.0315219188864	0.0337023125559	-0.0646956693524
2	0.05	1000	0.6	0.0333383461506	0.0337023125559	-0.0107994489906
3	0.05	1000	0.9	0.0339605445797	0.0337023125559	0.00766214553957
4	0.05	100000	0.3	0.0352778744936	0.0367832779665	-0.0409263001029
5	0.05	100000	0.6	0.036726301818	0.0367832779665	-0.00154896876121
6	0.05	100000	0.9	0.0371078082263	0.0367832779665	0.00882276615274
7	0.05	1000000	0.3	0.175290889954	0.164680819978	0.0644280856562
8	0.05	1000000	0.6	0.17080071762	0.164680819978	0.037162176158
9	0.05	1000000	0.9	0.166641797232	0.164680819978	0.0119077452596
10	0.05	3000000	0.3	0.462787841638	0.44924808126	0.0301387160972
11	0.05	3000000	0.6	0.456579979532	0.44924808126	0.0163203774882
12	0.05	3000000	0.9	0.450790865607	0.44924808126	0.00343414788202
13	0.05	10000000	0.3	0.838183605149	0.834570799708	0.0043289382303
14	0.05	10000000	0.6	0.836309680707	0.834570799708	0.00208356319142
15	0.05	10000000	0.9	0.834653678717	0.834570799708	$9.93073427171 \times 10^{-5}$
16	0.1	1000	0.3	0.0638950847783	0.0687467793878	-0.0705734094419
17	0.1	1000	0.6	0.0672720888869	0.0687467793878	-0.0214510485297
18	0.1	1000	0.9	0.068798167594	0.0687467793878	0.000747499833576
19	0.1	100000	0.3	0.066582362643	0.0710104637849	-0.0623584315029
20	0.1	100000	0.6	0.0697277527818	0.0710104637849	-0.0180636899797
21	0.1	100000	0.9	0.0711015090226	0.0710104637849	0.00128213833312
22	0.1	1000000	0.3	0.218826672775	0.207158468049	0.0563250193713
23	0.1	1000000	0.6	0.213972793954	0.207158468049	0.0328942667402
24	0.1	1000000	0.9	0.20916567635	0.207158468049	0.0096892408974
25	0.1	3000000	0.3	0.512999428896	0.491483959978	0.0437765434286
26	0.1	3000000	0.6	0.503620535829	0.491483959978	0.0246937374132

Table S4f continued

Row	phi_ECS	frequency_Hz	kappa	sigma_eff_S_per_m	sigma_A_S_per_m	T_kappa
27	0.1	3000000	0.9	0.495015120847	0.491483959978	0.00718469198629
28	0.1	10000000	0.3	0.847677421199	0.840458011313	0.00858985194816
29	0.1	10000000	0.6	0.844686499631	0.840458011313	0.00503117140996
30	0.1	10000000	0.9	0.841927608618	0.840458011313	0.00174856719229
31	0.15	1000	0.3	0.0971007606061	0.104352951005	-0.0694967447388
32	0.15	1000	0.6	0.102399894989	0.104352951005	-0.0187158676106
33	0.15	1000	0.9	0.104355262507	0.104352951005	$2.21508125457 \times 10^{-5}$
34	0.15	100000	0.3	0.0993518082397	0.106269337011	-0.0650943062816
35	0.15	100000	0.6	0.104470238115	0.106269337011	-0.0169296143808
36	0.15	100000	0.9	0.106303795393	0.106269337011	0.000324255164061
37	0.15	1000000	0.3	0.248580706145	0.238004516115	0.0444369300335
38	0.15	1000000	0.6	0.244791218588	0.238004516115	0.0285150155317
39	0.15	1000000	0.9	0.240024035438	0.238004516115	0.0084852142984
40	0.15	3000000	0.3	0.551619203982	0.525069146293	0.050564878695
41	0.15	3000000	0.6	0.540601333487	0.525069146293	0.0295812224031
42	0.15	3000000	0.9	0.529526498141	0.525069146293	0.00848907592327
43	0.15	10000000	0.3	0.856512744177	0.846754939202	0.0115237650509
44	0.15	10000000	0.6	0.853196832403	0.846754939202	0.00760774210225
45	0.15	10000000	0.9	0.848901536165	0.846754939202	0.0025350864386
46	0.2	1000	0.3	0.131719998504	0.141345324261	-0.0680979424479
47	0.2	1000	0.6	0.138641265084	0.141345324261	-0.0191308710812
48	0.2	1000	0.9	0.141385397615	0.141345324261	0.000283513832777
49	0.2	100000	0.3	0.133702719752	0.143039117101	-0.0652716371405
50	0.2	100000	0.6	0.140468514037	0.143039117101	-0.0179713292143
51	0.2	100000	0.9	0.143107431428	0.143039117101	0.000477591922952
52	0.2	1000000	0.3	0.275556359181	0.267220850914	0.0311933303058
53	0.2	1000000	0.6	0.273246545326	0.267220850914	0.0225494918971
54	0.2	1000000	0.9	0.26924854924	0.267220850914	0.00758809920545

Table S4f continued

Row	phi_ECS	frequency_Hz	kappa	sigma_eff_S_per_m	sigma_A_S_per_m	T_kappa
55	0.2	3000000	0.3	0.5834863997	0.554145876319	0.0529472917418
56	0.2	3000000	0.6	0.571737691275	0.554145876319	0.0317458194821
57	0.2	3000000	0.9	0.559323121137	0.554145876319	0.00934274717119
58	0.2	10000000	0.3	0.864910924253	0.85366218427	0.0131770391035
59	0.2	10000000	0.6	0.861588189912	0.85366218427	0.00928470979246
60	0.2	10000000	0.9	0.856431111151	0.85366218427	0.00324358620075

Table S4f, column panel 2/2. First column is repeated for alignment.

Row	phi_ECS	minimum_gap_m	membrane_area_m2
1	0.05	$2.20779815847 \times 10^{-8}$	$4.40358372173 \times 10^{-10}$
2	0.05	$4.41559631695 \times 10^{-8}$	$4.38960513809 \times 10^{-10}$
3	0.05	$6.62339447542 \times 10^{-8}$	$4.37559560471 \times 10^{-10}$
4	0.05	$2.20779815847 \times 10^{-8}$	$4.40358372173 \times 10^{-10}$
5	0.05	$4.41559631695 \times 10^{-8}$	$4.38960513809 \times 10^{-10}$
6	0.05	$6.62339447542 \times 10^{-8}$	$4.37559560471 \times 10^{-10}$
7	0.05	$2.20779815847 \times 10^{-8}$	$4.40358372173 \times 10^{-10}$
8	0.05	$4.41559631695 \times 10^{-8}$	$4.38960513809 \times 10^{-10}$
9	0.05	$6.62339447542 \times 10^{-8}$	$4.37559560471 \times 10^{-10}$
10	0.05	$2.20779815847 \times 10^{-8}$	$4.40358372173 \times 10^{-10}$
11	0.05	$4.41559631695 \times 10^{-8}$	$4.38960513809 \times 10^{-10}$
12	0.05	$6.62339447542 \times 10^{-8}$	$4.37559560471 \times 10^{-10}$
13	0.05	$2.20779815847 \times 10^{-8}$	$4.40358372173 \times 10^{-10}$
14	0.05	$4.41559631695 \times 10^{-8}$	$4.38960513809 \times 10^{-10}$
15	0.05	$6.62339447542 \times 10^{-8}$	$4.37559560471 \times 10^{-10}$
16	0.1	$4.49448747547 \times 10^{-8}$	$4.28130496607 \times 10^{-10}$

Table S4f continued

Row	phi_ECS	minimum_gap_m	membrane_area_m2
17	0.1	$8.98897495094 \times 10^{-8}$	$4.2534773458 \times 10^{-10}$
18	0.1	$1.34834624264 \times 10^{-7}$	$4.2255223573 \times 10^{-10}$
19	0.1	$4.49448747547 \times 10^{-8}$	$4.28130496607 \times 10^{-10}$
20	0.1	$8.98897495094 \times 10^{-8}$	$4.2534773458 \times 10^{-10}$
21	0.1	$1.34834624264 \times 10^{-7}$	$4.2255223573 \times 10^{-10}$
22	0.1	$4.49448747547 \times 10^{-8}$	$4.28130496607 \times 10^{-10}$
23	0.1	$8.98897495094 \times 10^{-8}$	$4.2534773458 \times 10^{-10}$
24	0.1	$1.34834624264 \times 10^{-7}$	$4.2255223573 \times 10^{-10}$
25	0.1	$4.49448747547 \times 10^{-8}$	$4.28130496607 \times 10^{-10}$
26	0.1	$8.98897495094 \times 10^{-8}$	$4.2534773458 \times 10^{-10}$
27	0.1	$1.34834624264 \times 10^{-7}$	$4.2255223573 \times 10^{-10}$
28	0.1	$4.49448747547 \times 10^{-8}$	$4.28130496607 \times 10^{-10}$
29	0.1	$8.98897495094 \times 10^{-8}$	$4.2534773458 \times 10^{-10}$
30	0.1	$1.34834624264 \times 10^{-7}$	$4.2255223573 \times 10^{-10}$
31	0.15	$6.86751727893 \times 10^{-8}$	$4.15588909438 \times 10^{-10}$
32	0.15	$1.37350345579 \times 10^{-7}$	$4.11436433986 \times 10^{-10}$
33	0.15	$2.06025518368 \times 10^{-7}$	$4.07254443763 \times 10^{-10}$
34	0.15	$6.86751727893 \times 10^{-8}$	$4.15588909438 \times 10^{-10}$
35	0.15	$1.37350345579 \times 10^{-7}$	$4.11436433986 \times 10^{-10}$
36	0.15	$2.06025518368 \times 10^{-7}$	$4.07254443763 \times 10^{-10}$
37	0.15	$6.86751727893 \times 10^{-8}$	$4.15588909438 \times 10^{-10}$
38	0.15	$1.37350345579 \times 10^{-7}$	$4.11436433986 \times 10^{-10}$
39	0.15	$2.06025518368 \times 10^{-7}$	$4.07254443763 \times 10^{-10}$
40	0.15	$6.86751727893 \times 10^{-8}$	$4.15588909438 \times 10^{-10}$
41	0.15	$1.37350345579 \times 10^{-7}$	$4.11436433986 \times 10^{-10}$
42	0.15	$2.06025518368 \times 10^{-7}$	$4.07254443763 \times 10^{-10}$
43	0.15	$6.86751727893 \times 10^{-8}$	$4.15588909438 \times 10^{-10}$
44	0.15	$1.37350345579 \times 10^{-7}$	$4.11436433986 \times 10^{-10}$

Table S4f continued

Row	phi_ECS	minimum_gap_m	membrane_area_m2
45	0.15	$2.06025518368 \times 10^{-7}$	$4.07254443763 \times 10^{-10}$
46	0.2	$9.33553041572 \times 10^{-8}$	$4.02705519568 \times 10^{-10}$
47	0.2	$1.86710608314 \times 10^{-7}$	$3.97201184602 \times 10^{-10}$
48	0.2	$2.80065912471 \times 10^{-7}$	$3.9164274895 \times 10^{-10}$
49	0.2	$9.33553041572 \times 10^{-8}$	$4.02705519568 \times 10^{-10}$
50	0.2	$1.86710608314 \times 10^{-7}$	$3.97201184602 \times 10^{-10}$
51	0.2	$2.80065912471 \times 10^{-7}$	$3.9164274895 \times 10^{-10}$
52	0.2	$9.33553041572 \times 10^{-8}$	$4.02705519568 \times 10^{-10}$
53	0.2	$1.86710608314 \times 10^{-7}$	$3.97201184602 \times 10^{-10}$
54	0.2	$2.80065912471 \times 10^{-7}$	$3.9164274895 \times 10^{-10}$
55	0.2	$9.33553041572 \times 10^{-8}$	$4.02705519568 \times 10^{-10}$
56	0.2	$1.86710608314 \times 10^{-7}$	$3.97201184602 \times 10^{-10}$
57	0.2	$2.80065912471 \times 10^{-7}$	$3.9164274895 \times 10^{-10}$
58	0.2	$9.33553041572 \times 10^{-8}$	$4.02705519568 \times 10^{-10}$
59	0.2	$1.86710608314 \times 10^{-7}$	$3.97201184602 \times 10^{-10}$
60	0.2	$2.80065912471 \times 10^{-7}$	$3.9164274895 \times 10^{-10}$

Units: Hz; S m^-1; m; m^2; T_kappa fraction. Denominator: sigma_A at matching phi,f. Membrane area is not fixed.

Full records: Table_S4f.csv.

Table S4g. Fixed-area arrangement comparisons

Table S4g, column panel 1/2. First column is repeated for alignment.

Row	phi_ECS	frequency_Hz	sigma_aligned_S_per_m	sigma_staggered_S_per_m
1	0.2	100000	0.143510004616	0.136413163513
2	0.2	1000000	0.268085809877	0.264510355914
3	0.2	3000000	0.556130655836	0.548747596511
4	0.1	100000	0.0709770111792	0.0678788847648
5	0.1	1000000	0.207414831762	0.201340545407
6	0.1	3000000	0.493040297535	0.488124499921
7	0.05	100000	0.0372529435456	0.0361475594962
8	0.05	1000000	0.166079697416	0.160480556255
9	0.05	3000000	0.451289644355	0.447339482884

Table S4g, column panel 2/2. First column is repeated for alignment.

Row	phi_ECS	T_arrangement	membrane_area_equal
1	0.2	-0.0494518909825	True
2	0.2	-0.0133369758157	True
3	0.2	-0.0132757639718	True
4	0.1	-0.0436497164776	True
5	0.1	-0.0292856894749	True
6	0.1	-0.0099703769424	True
7	0.05	-0.0296723948285	True
8	0.05	-0.0337135799699	True
9	0.05	-0.00875305144	True

Units: Hz; S m^{-1}; dimensionless correction. Denominator: sigma_aligned at matching ϕ,f. All shape/volume/area preservation flags retained.

Full records: Table_S4g.csv.

Table S4h. Bulk dissipative-power partition

Table S4h, column panel 1/3. First column is repeated for alignment.

Row	phi_ECS	frequency_Hz	P_ECS_W	P_intra_W
1	0.05	100000	$1.52942458547 \times 10^{-13}$	$7.15666813971 \times 10^{-15}$
2	0.05	1000000	$3.27007632594 \times 10^{-13}$	$3.890004502 \times 10^{-13}$
3	0.05	3000000	$3.83778017002 \times 10^{-13}$	$1.56438862262 \times 10^{-12}$
4	0.1	100000	$3.00588581148 \times 10^{-13}$	$6.76183616853 \times 10^{-15}$
5	0.1	1000000	$4.57417208351 \times 10^{-13}$	$4.41070348559 \times 10^{-13}$
6	0.1	3000000	$5.66232535557 \times 10^{-13}$	$1.56672046895 \times 10^{-12}$
7	0.2	100000	$6.1425618898 \times 10^{-13}$	$5.86125560377 \times 10^{-15}$
8	0.2	1000000	$7.18671962982 \times 10^{-13}$	$4.4064092205 \times 10^{-13}$
9	0.2	3000000	$8.82138585484 \times 10^{-13}$	$1.52296624483 \times 10^{-12}$

Table S4h, column panel 2/3. First column is repeated for alignment.

Row	phi_ECS	P_ECS_fraction	P_intra_fraction	P_membrane_fraction
1	0.05	0.955298518563	0.0447014814372	Not available
2	0.05	0.456709414952	0.543290585048	Not available
3	0.05	0.196994450678	0.803005549322	Not available
4	0.1	0.977999586831	0.0220004131686	Not available
5	0.1	0.509096876004	0.490903123996	Not available
6	0.1	0.265468828596	0.734531171404	Not available
7	0.2	0.990548152362	0.00945184763783	Not available
8	0.2	0.619911994648	0.380088005352	Not available
9	0.2	0.366777603356	0.633222396644	Not available

Table S4h, column panel 3/3. First column is repeated for alignment.

Row	phi_ECS	membrane_partition_status	partition_basis
1	0.05	NOT_AVAILABLE_FROM_CURRENT_FORMULATION	BULK_DISSIPATIVE_POWER_ECS_PLUS_INTRACELLULAR
2	0.05	NOT_AVAILABLE_FROM_CURRENT_FORMULATION	BULK_DISSIPATIVE_POWER_ECS_PLUS_INTRACELLULAR
3	0.05	NOT_AVAILABLE_FROM_CURRENT_FORMULATION	BULK_DISSIPATIVE_POWER_ECS_PLUS_INTRACELLULAR
4	0.1	NOT_AVAILABLE_FROM_CURRENT_FORMULATION	BULK_DISSIPATIVE_POWER_ECS_PLUS_INTRACELLULAR
5	0.1	NOT_AVAILABLE_FROM_CURRENT_FORMULATION	BULK_DISSIPATIVE_POWER_ECS_PLUS_INTRACELLULAR
6	0.1	NOT_AVAILABLE_FROM_CURRENT_FORMULATION	BULK_DISSIPATIVE_POWER_ECS_PLUS_INTRACELLULAR
7	0.2	NOT_AVAILABLE_FROM_CURRENT_FORMULATION	BULK_DISSIPATIVE_POWER_ECS_PLUS_INTRACELLULAR
8	0.2	NOT_AVAILABLE_FROM_CURRENT_FORMULATION	BULK_DISSIPATIVE_POWER_ECS_PLUS_INTRACELLULAR
9	0.2	NOT_AVAILABLE_FROM_CURRENT_FORMULATION	BULK_DISSIPATIVE_POWER_ECS_PLUS_INTRACELLULAR

Units: Hz; W; fractions dimensionless. Denominator: P_ECS + P_intra only. Membrane power is unavailable, not zero.

Full records: Table_S4h.csv.

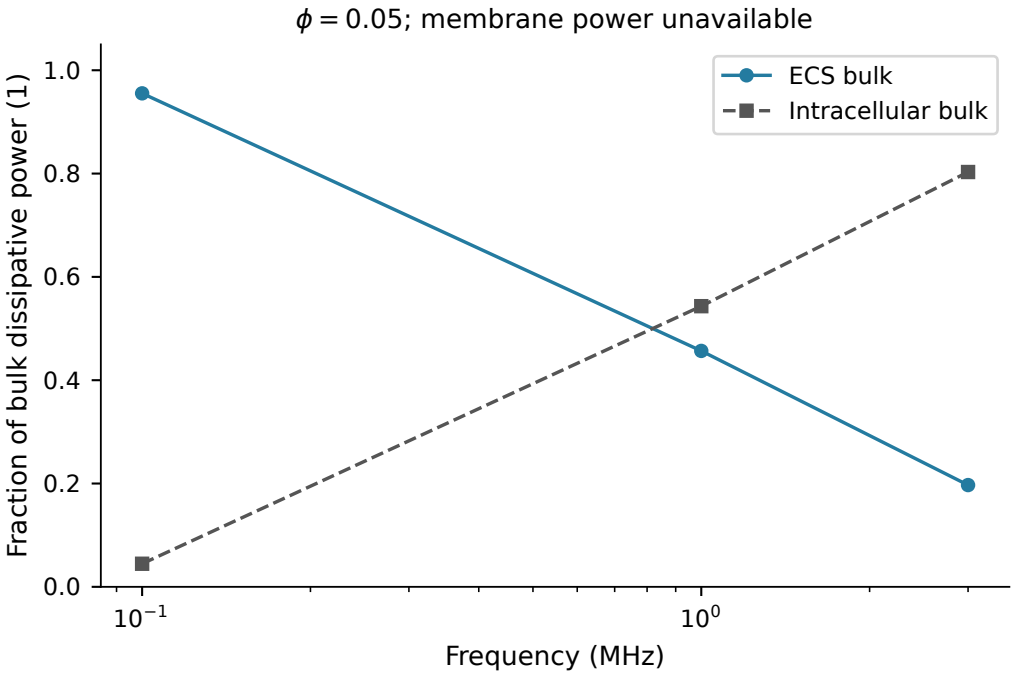


Figure S3. Existing bulk dissipative-power partition at ϕ=0.05. The denominator contains only ECS and intracellular bulk power; unavailable membrane power is not assigned zero. Equal nominal bulk properties condition the high-frequency trend.

S5. Prescribed electrical stress scenarios and the matched reversal

The eleven prescribed scenarios multiply intracellular conductivity, extracellular conductivity, membrane capacitance and membrane conductance by the factors below, with unchanged bulk permittivities and geometry. They are dimensionless stress scenarios, not a physiological parameter distribution or confidence interval. $R_{\text{total}} = \frac{\sigma_{\text{eff}}(\phi,f,E)}{\sigma_{\text{eff}}(0.20,f,E_0)}$; $R_{\text{matched}} = \frac{\sigma_{\text{eff}}(\phi,f,E)}{\sigma_{\text{eff}}(0.20,f,E)}$.

Table S5a. Electrical multiplier definitions

Table S5a, column panel 1/2. First column is repeated for alignment.

Row	scenario	r_i	r_e	r_C
1	E0	1	1	1
2	E1	0.75	1	1
3	E2	1.25	1	1
4	E3	1	0.75	1
5	E4	1	1.25	1
6	E5	1	1	0.75
7	E6	1	1	1.25
8	E7	1	1	1
9	E8	1	1	1
10	E9	0.75	0.75	0.75
11	E10	1.25	1.25	1.25

Table S5a, column panel 2/2. First column is repeated for alignment.

Row	scenario	r_G
1	E0	1
2	E1	1
3	E2	1
4	E3	1
5	E4	1
6	E5	1
7	E6	1
8	E7	0.75
9	E8	1.25
10	E9	0.75
11	E10	1.25

Units: Dimensionless multipliers. Denominator: E0 benchmark parameters. Eleven discrete scenarios only.

Full records: Table_S5a.csv.

Direct 5 MHz replacements for Table S5b

The four rows below supersede the corresponding interpolated conductivity rows in the historical Table S5b ledger. The companion Table_S5b.csv contains the replacements and per-row provenance; Table_S5b_historical.csv preserves the original export. All other rows retain their stated origin. At 5 MHz the total denominator here is the newly direct E0 conductivity at $\phi = 0.20$; no original direct E0 value existed at this frequency. The matched denominator is the same electrical state at $\phi = 0.20$. Table S10d provides the full interpolation/direct comparison.

Scenario	ϕ	R_{total}	R_{matched}
E0	0.05	0.910768860405	0.910768860405
E0	0.20	1.000000000000	1.000000000000
E3	0.05	0.889868011623	0.952117348585
E3	0.20	0.934620100081	1.000000000000

Historical Table S5b. Total and matched-electrical ratios; four 5 MHz rows superseded above

Table S5b, column panel 1/2. First column is repeated for alignment.

Row	scenario	phi_ECS	frequency_Hz	R_sigma_total	R_sigma_matched_electrical_baseline	provenance
1	E0	0.05	100000	0.25715537618	0.25715537618	DIRECT_RVE_FEM
2	E0	0.05	300000	0.428497714135	0.428497714135	INTERPOLATED_FROM_RVE
3	E0	0.05	1000000	0.616272343325	0.616272343325	DIRECT_RVE_FEM
4	E0	0.05	2000000	0.73894483597	0.73894483597	INTERPOLATED_FROM_RVE
5	E0	0.05	3000000	0.810703644038	0.810703644038	DIRECT_RVE_FEM
6	E0	0.05	5000000	0.881530223015	0.881530223015	INTERPOLATED_FROM_RVE
7	E0	0.05	10000000	0.977635902218	0.977635902218	DIRECT_RVE_FEM
8	E0	0.1	100000	0.496440870332	0.496440870332	DIRECT_RVE_FEM

Table S5b continued

Row	scenario	phi_ECS	frequency_Hz	R_sigma_total	R_sigma_matched_electrical_baseline	provenance
9	E0	0.1	300000	0.629458603414	0.629458603414	INTERPOLATED_FROM_RVE
10	E0	0.1	1000000	0.775233172637	0.775233172637	DIRECT_RVE_FEM
11	E0	0.1	2000000	0.845700739072	0.845700739072	INTERPOLATED_FROM_RVE
12	E0	0.1	3000000	0.886921622954	0.886921622954	DIRECT_RVE_FEM
13	E0	0.1	5000000	0.928336217492	0.928336217492	INTERPOLATED_FROM_RVE
14	E0	0.1	10000000	0.984532320629	0.984532320629	DIRECT_RVE_FEM
15	E0	0.15	100000	0.742938988757	0.742938988757	DIRECT_RVE_FEM
16	E0	0.15	300000	0.813422667353	0.813422667353	INTERPOLATED_FROM_RVE
17	E0	0.15	1000000	0.890665961509	0.890665961509	DIRECT_RVE_FEM
18	E0	0.15	2000000	0.926542382981	0.926542382981	INTERPOLATED_FROM_RVE
19	E0	0.15	3000000	0.947528744202	0.947528744202	DIRECT_RVE_FEM
20	E0	0.15	5000000	0.96635841676	0.96635841676	INTERPOLATED_FROM_RVE
21	E0	0.15	10000000	0.991908690351	0.991908690351	DIRECT_RVE_FEM
22	E0	0.2	100000	1	1	DIRECT_RVE_FEM
23	E0	0.2	300000	1	1	INTERPOLATED_FROM_RVE
24	E0	0.2	1000000	1	1	DIRECT_RVE_FEM
25	E0	0.2	2000000	1	1	INTERPOLATED_FROM_RVE
26	E0	0.2	3000000	1	1	DIRECT_RVE_FEM

Table S5b continued

Row	scenario	phi_ECS	frequency_Hz	R_sigma_total	R_sigma_matched_electrical_baseline	provenance
27	E0	0.2	5000000	1	1	INTERPOLATED_FROM_RVE
28	E0	0.2	10000000	1	1	DIRECT_RVE_FEM
29	E1	0.05	100000	0.260779855863	0.26001088917	DIRECT_RVE_FEM
30	E1	0.05	300000	0.453085978799	0.440330529196	INTERPOLATED_FROM_RVE
31	E1	0.05	1000000	0.66383488859	0.627755968668	DIRECT_RVE_FEM
32	E1	0.05	2000000	0.735485097956	0.746788889606	INTERPOLATED_FROM_RVE
33	E1	0.05	3000000	0.777397783603	0.82492176441	DIRECT_RVE_FEM
34	E1	0.05	5000000	0.781861224841	0.87194466126	INTERPOLATED_FROM_RVE
35	E1	0.05	10000000	0.787917737212	0.943985210732	DIRECT_RVE_FEM
36	E1	0.1	100000	0.500011699982	0.498537305643	DIRECT_RVE_FEM
37	E1	0.1	300000	0.655520006772	0.637065557062	INTERPOLATED_FROM_RVE
38	E1	0.1	1000000	0.825942069362	0.781052747796	DIRECT_RVE_FEM
39	E1	0.1	2000000	0.835225924016	0.848062648856	INTERPOLATED_FROM_RVE
40	E1	0.1	3000000	0.84065663085	0.892047759604	DIRECT_RVE_FEM
41	E1	0.1	5000000	0.824500128653	0.91949627702	INTERPOLATED_FROM_RVE
42	E1	0.1	10000000	0.802577121222	0.961548264653	DIRECT_RVE_FEM
43	E1	0.15	100000	0.746801388459	0.74459928051	DIRECT_RVE_FEM
44	E1	0.15	300000	0.841937692323	0.818235140698	INTERPOLATED_FROM_RVE
45	E1	0.15	1000000	0.946197879232	0.894772746112	DIRECT_RVE_FEM

Table S5b continued

Row	scenario	phi_ECS	frequency_Hz	R_sigma_total	R_sigma_matched_electrical_baseline	provenance
46	E1	0.15	2000000	0.913081472384	0.927114771975	INTERPOLATED_FROM_RVE
47	E1	0.15	3000000	0.89370961622	0.948343986865	DIRECT_RVE_FEM
48	E1	0.15	5000000	0.861715268681	0.960999221064	INTERPOLATED_FROM_RVE
49	E1	0.15	10000000	0.818301644228	0.98038743588	DIRECT_RVE_FEM
50	E1	0.2	100000	1.00295744034	1	DIRECT_RVE_FEM
51	E1	0.2	300000	1.02896789742	1	INTERPOLATED_FROM_RVE
52	E1	0.2	1000000	1.05747284251	1	DIRECT_RVE_FEM
53	E1	0.2	2000000	0.984863471045	1	INTERPOLATED_FROM_RVE
54	E1	0.2	3000000	0.942389711537	1	DIRECT_RVE_FEM
55	E1	0.2	5000000	0.896686750408	1	INTERPOLATED_FROM_RVE
56	E1	0.2	10000000	0.834671696393	1	DIRECT_RVE_FEM
57	E2	0.05	100000	0.25478566023	0.255305776283	DIRECT_RVE_FEM
58	E2	0.05	300000	0.408596342439	0.418762849437	INTERPOLATED_FROM_RVE
59	E2	0.05	1000000	0.577157972691	0.606673006727	DIRECT_RVE_FEM
60	E2	0.05	2000000	0.721395865772	0.725082286473	INTERPOLATED_FROM_RVE
61	E2	0.05	3000000	0.805769624407	0.789660061056	DIRECT_RVE_FEM
62	E2	0.05	5000000	0.944686547922	0.882821185284	INTERPOLATED_FROM_RVE
63	E2	0.05	10000000	1.13318506755	0.996221215256	DIRECT_RVE_FEM
64	E2	0.1	100000	0.49426620411	0.495275192554	DIRECT_RVE_FEM

Table S5b continued

Row	scenario	phi_ECS	frequency_Hz	R_sigma_total	R_sigma_matched_electrical_baseline	provenance
65	E2	0.1	300000	0.607533786974	0.622650164326	INTERPOLATED_FROM_RVE
66	E2	0.1	1000000	0.731664101905	0.769080358618	DIRECT_RVE_FEM
67	E2	0.1	2000000	0.834948659126	0.839215348426	INTERPOLATED_FROM_RVE
68	E2	0.1	3000000	0.895366252004	0.877465404265	DIRECT_RVE_FEM
69	E2	0.1	5000000	0.996977729606	0.931687937007	INTERPOLATED_FROM_RVE
70	E2	0.1	10000000	1.13485591334	0.997690112154	DIRECT_RVE_FEM
71	E2	0.15	100000	0.741427085892	0.742940625267	DIRECT_RVE_FEM
72	E2	0.15	300000	0.790226496036	0.809888549676	INTERPOLATED_FROM_RVE
73	E2	0.15	1000000	0.843705929396	0.886851845072	DIRECT_RVE_FEM
74	E2	0.15	2000000	0.919624167315	0.92432355877	INTERPOLATED_FROM_RVE
75	E2	0.15	3000000	0.964033489619	0.944759793883	DIRECT_RVE_FEM
76	E2	0.15	5000000	1.03709218979	0.969175392892	INTERPOLATED_FROM_RVE
77	E2	0.15	10000000	1.13622666873	0.998895189453	DIRECT_RVE_FEM
78	E2	0.2	100000	0.997962772093	1	DIRECT_RVE_FEM
79	E2	0.2	300000	0.975722519293	1	INTERPOLATED_FROM_RVE
80	E2	0.2	1000000	0.951349353428	1	DIRECT_RVE_FEM
81	E2	0.2	2000000	0.994915858835	1	INTERPOLATED_FROM_RVE
82	E2	0.2	3000000	1.02040063078	1	DIRECT_RVE_FEM

Table S5b continued

Row	scenario	phi_ECS	frequency_Hz	R_sigma_total	R_sigma_matched_electrical_baseline	provenance
83	E2	0.2	5000000	1.07007688949	1	INTERPOLATED_FROM_RVE
84	E2	0.2	10000000	1.13748337236	1	DIRECT_RVE_FEM
85	E3	0.05	100000	0.201445191243	0.267225689411	DIRECT_RVE_FEM
86	E3	0.05	300000	0.371247981165	0.458249433225	INTERPOLATED_FROM_RVE
87	E3	0.05	1000000	0.557335414624	0.63925723095	DIRECT_RVE_FEM
88	E3	0.05	2000000	0.696402625732	0.774759852814	INTERPOLATED_FROM_RVE
89	E3	0.05	3000000	0.77775172931	0.850313379867	DIRECT_RVE_FEM
90	E3	0.05	5000000	0.856743425384	0.923089328491	INTERPOLATED_FROM_RVE
91	E3	0.05	10000000	0.963928478117	1.01852955446	DIRECT_RVE_FEM
92	E3	0.1	100000	0.378095858852	0.501560379384	DIRECT_RVE_FEM
93	E3	0.1	300000	0.530150588185	0.654390646912	INTERPOLATED_FROM_RVE
94	E3	0.1	1000000	0.696787863932	0.799207566519	DIRECT_RVE_FEM
95	E3	0.1	2000000	0.78407719572	0.872299314082	INTERPOLATED_FROM_RVE
96	E3	0.1	3000000	0.835138181529	0.913053797286	DIRECT_RVE_FEM
97	E3	0.1	5000000	0.887073076866	0.955767697289	INTERPOLATED_FROM_RVE
98	E3	0.1	10000000	0.957544338683	1.01178378977	DIRECT_RVE_FEM
99	E3	0.15	100000	0.562211043423	0.74579707138	DIRECT_RVE_FEM
100	E3	0.15	300000	0.671481707949	0.828842519554	INTERPOLATED_FROM_RVE
101	E3	0.15	1000000	0.791231786987	0.907533646556	DIRECT_RVE_FEM

Table S5b continued

Row	scenario	phi_ECS	frequency_Hz	R_sigma_total	R_sigma_matched_electrical_baseline	provenance
102	E3	0.15	2000000	0.846264479069	0.941483732282	INTERPOLATED_FROM_RVE
103	E3	0.15	3000000	0.87845654025	0.960413614855	DIRECT_RVE_FEM
104	E3	0.15	5000000	0.909571240033	0.980008110129	INTERPOLATED_FROM_RVE
105	E3	0.15	10000000	0.951791256854	1.00570482851	DIRECT_RVE_FEM
106	E3	0.2	100000	0.753839167513	1	DIRECT_RVE_FEM
107	E3	0.2	300000	0.810143895985	1	INTERPOLATED_FROM_RVE
108	E3	0.2	1000000	0.871848432275	1	DIRECT_RVE_FEM
109	E3	0.2	2000000	0.898862561351	1	INTERPOLATED_FROM_RVE
110	E3	0.2	3000000	0.91466481385	1	DIRECT_RVE_FEM
111	E3	0.2	5000000	0.92812623756	1	INTERPOLATED_FROM_RVE
112	E3	0.2	10000000	0.946392251356	1	DIRECT_RVE_FEM
113	E4	0.05	100000	0.313770197491	0.251790357015	DIRECT_RVE_FEM
114	E4	0.05	300000	0.482590772858	0.405679755067	INTERPOLATED_FROM_RVE
115	E4	0.05	1000000	0.66760179417	0.592061171448	DIRECT_RVE_FEM
116	E4	0.05	2000000	0.775701407789	0.706838096985	INTERPOLATED_FROM_RVE
117	E4	0.05	3000000	0.838935628098	0.776951101304	DIRECT_RVE_FEM
118	E4	0.05	5000000	0.903049103427	0.846624401509	INTERPOLATED_FROM_RVE
119	E4	0.05	10000000	0.990045668581	0.94395519749	DIRECT_RVE_FEM
120	E4	0.1	100000	0.615385482992	0.493826793314	DIRECT_RVE_FEM

Table S5b continued

Row	scenario	phi_ECS	frequency_Hz	R_sigma_total	R_sigma_matched_electrical_baseline	provenance
121	E4	0.1	300000	0.725203085158	0.609626678558	INTERPOLATED_FROM_RVE
122	E4	0.1	1000000	0.845552554946	0.749876409221	DIRECT_RVE_FEM
123	E4	0.1	2000000	0.902168068504	0.822077611694	INTERPOLATED_FROM_RVE
124	E4	0.1	3000000	0.935286020895	0.866182671984	DIRECT_RVE_FEM
125	E4	0.1	5000000	0.966522829103	0.906132134597	INTERPOLATED_FROM_RVE
126	E4	0.1	10000000	1.00890853673	0.96193992587	DIRECT_RVE_FEM
127	E4	0.15	100000	0.925103773832	0.742365627302	DIRECT_RVE_FEM
128	E4	0.15	300000	0.954702673911	0.802550667556	INTERPOLATED_FROM_RVE
129	E4	0.15	1000000	0.987140205423	0.875443103224	DIRECT_RVE_FEM
130	E4	0.15	2000000	1.00311654555	0.914064333254	INTERPOLATED_FROM_RVE
131	E4	0.15	3000000	1.01246210543	0.937656622864	DIRECT_RVE_FEM
132	E4	0.15	5000000	1.01929621623	0.955608112288	INTERPOLATED_FROM_RVE
133	E4	0.15	10000000	1.02856952676	0.980685620451	DIRECT_RVE_FEM
134	E4	0.2	100000	1.24615652963	1	DIRECT_RVE_FEM
135	E4	0.2	300000	1.18958554582	1	INTERPOLATED_FROM_RVE
136	E4	0.2	1000000	1.12758921943	1	DIRECT_RVE_FEM
137	E4	0.2	2000000	1.09742444712	1	INTERPOLATED_FROM_RVE
138	E4	0.2	3000000	1.07977918648	1	DIRECT_RVE_FEM

Table S5b continued

Row	scenario	phi_ECS	frequency_Hz	R_sigma_total	R_sigma_matched_electrical_baseline	provenance
139	E4	0.2	5000000	1.06664667569	1	INTERPOLATED_FROM_RVE
140	E4	0.2	10000000	1.04882696892	1	DIRECT_RVE_FEM
141	E5	0.05	100000	0.247726207003	0.249053672221	DIRECT_RVE_FEM
142	E5	0.05	300000	0.354989772588	0.388126169708	INTERPOLATED_FROM_RVE
143	E5	0.05	1000000	0.472540265326	0.57145806443	DIRECT_RVE_FEM
144	E5	0.05	2000000	0.572775652671	0.682438989702	INTERPOLATED_FROM_RVE
145	E5	0.05	3000000	0.631409595513	0.745851031896	DIRECT_RVE_FEM
146	E5	0.05	5000000	0.741600650502	0.840619859031	INTERPOLATED_FROM_RVE
147	E5	0.05	10000000	0.891120595342	0.957603955689	DIRECT_RVE_FEM
148	E5	0.1	100000	0.489532331922	0.492155539018	DIRECT_RVE_FEM
149	E5	0.1	300000	0.544147031034	0.594940246794	INTERPOLATED_FROM_RVE
150	E5	0.1	1000000	0.603999458615	0.730435873649	DIRECT_RVE_FEM
151	E5	0.1	2000000	0.678191280094	0.808037439884	INTERPOLATED_FROM_RVE
152	E5	0.1	3000000	0.721590713519	0.852377255761	DIRECT_RVE_FEM
153	E5	0.1	5000000	0.799365650744	0.906097695826	INTERPOLATED_FROM_RVE
154	E5	0.1	10000000	0.904899664598	0.972411032637	DIRECT_RVE_FEM
155	E5	0.15	100000	0.737600815706	0.741553322144	DIRECT_RVE_FEM
156	E5	0.15	300000	0.726262933676	0.794055695163	INTERPOLATED_FROM_RVE
157	E5	0.15	1000000	0.713837711636	0.863266787916	DIRECT_RVE_FEM

Table S5b continued

Row	scenario	phi_ECS	frequency_Hz	R_sigma_total	R_sigma_matched_electrical_baseline	provenance
158	E5	0.15	2000000	0.761920215299	0.907797074715	INTERPOLATED_FROM_RVE
159	E5	0.15	3000000	0.790046676883	0.933240694133	DIRECT_RVE_FEM
160	E5	0.15	5000000	0.844278303238	0.957007127449	INTERPOLATED_FROM_RVE
161	E5	0.15	10000000	0.917866034856	0.986344777985	DIRECT_RVE_FEM
162	E5	0.2	100000	0.994669963279	1	DIRECT_RVE_FEM
163	E5	0.2	300000	0.914624676959	1	INTERPOLATED_FROM_RVE
164	E5	0.2	1000000	0.826902785591	1	DIRECT_RVE_FEM
165	E5	0.2	2000000	0.839306753151	1	INTERPOLATED_FROM_RVE
166	E5	0.2	3000000	0.846562609035	1	DIRECT_RVE_FEM
167	E5	0.2	5000000	0.882206912595	1	INTERPOLATED_FROM_RVE
168	E5	0.2	10000000	0.930573218759	1	DIRECT_RVE_FEM
169	E6	0.05	100000	0.268776724179	0.267050223527	DIRECT_RVE_FEM
170	E6	0.05	300000	0.502837805814	0.462590355444	INTERPOLATED_FROM_RVE
171	E6	0.05	1000000	0.759346111562	0.646104669904	DIRECT_RVE_FEM
172	E6	0.05	2000000	0.887095901549	0.778027775714	INTERPOLATED_FROM_RVE
173	E6	0.05	3000000	0.961824738166	0.859030253361	DIRECT_RVE_FEM
174	E6	0.05	5000000	0.990412721918	0.911089892512	INTERPOLATED_FROM_RVE
175	E6	0.05	10000000	1.02920419872	0.986935161697	DIRECT_RVE_FEM
176	E6	0.1	100000	0.505231015877	0.501985639325	DIRECT_RVE_FEM

Table S5b continued

Row	scenario	phi_ECS	frequency_Hz	R_sigma_total	R_sigma_matched_electrical_baseline	provenance
177	E6	0.1	300000	0.712421788091	0.655399105575	INTERPOLATED_FROM_RVE
178	E6	0.1	1000000	0.939482833764	0.799377565708	DIRECT_RVE_FEM
179	E6	0.1	2000000	0.992899966225	0.870823268239	INTERPOLATED_FROM_RVE
180	E6	0.1	3000000	1.02414698561	0.914691845217	DIRECT_RVE_FEM
181	E6	0.1	5000000	1.02780044656	0.945483208828	INTERPOLATED_FROM_RVE
182	E6	0.1	10000000	1.03275788417	0.990342898595	DIRECT_RVE_FEM
183	E6	0.15	100000	0.750931778518	0.7461081309	DIRECT_RVE_FEM
184	E6	0.15	300000	0.901103864884	0.828978951721	INTERPOLATED_FROM_RVE
185	E6	0.15	1000000	1.06567794604	0.906753174957	DIRECT_RVE_FEM
186	E6	0.15	2000000	1.07140416256	0.939675401535	INTERPOLATED_FROM_RVE
187	E6	0.15	3000000	1.0747537845	0.959890070573	DIRECT_RVE_FEM
188	E6	0.15	5000000	1.05893611103	0.974125196722	INTERPOLATED_FROM_RVE
189	E6	0.15	10000000	1.03747286554	0.994864237413	DIRECT_RVE_FEM
190	E6	0.2	100000	1.00646507848	1	DIRECT_RVE_FEM
191	E6	0.2	300000	1.08700451684	1	INTERPOLATED_FROM_RVE
192	E6	0.2	1000000	1.17526795105	1	DIRECT_RVE_FEM
193	E6	0.2	2000000	1.14018538828	1	INTERPOLATED_FROM_RVE
194	E6	0.2	3000000	1.11966340464	1	DIRECT_RVE_FEM

Table S5b continued

Row	scenario	phi_ECS	frequency_Hz	R_sigma_total	R_sigma_matched_electrical_baseline	provenance
195	E6	0.2	5000000	1.08706366963	1	INTERPOLATED_FROM_RVE
196	E6	0.2	10000000	1.04282858557	1	DIRECT_RVE_FEM
197	E7	0.05	100000	0.256806035632	0.256900003696	DIRECT_RVE_FEM
198	E7	0.05	300000	0.428241065699	0.428351172109	INTERPOLATED_FROM_RVE
199	E7	0.05	1000000	0.616117276478	0.616202244466	DIRECT_RVE_FEM
200	E7	0.05	2000000	0.738926340438	0.738983317388	INTERPOLATED_FROM_RVE
201	E7	0.05	3000000	0.810765037603	0.810798720719	DIRECT_RVE_FEM
202	E7	0.05	5000000	0.881582674887	0.881614000547	INTERPOLATED_FROM_RVE
203	E7	0.05	10000000	0.977676220969	0.977702986382	DIRECT_RVE_FEM
204	E7	0.1	100000	0.496200903185	0.496382468381	DIRECT_RVE_FEM
205	E7	0.1	300000	0.629306290801	0.629468093725	INTERPOLATED_FROM_RVE
206	E7	0.1	1000000	0.775176920915	0.775283824626	DIRECT_RVE_FEM
207	E7	0.1	2000000	0.845675065313	0.845740273418	INTERPOLATED_FROM_RVE
208	E7	0.1	3000000	0.886913836156	0.886950682863	DIRECT_RVE_FEM
209	E7	0.1	5000000	0.928330476515	0.928363463285	INTERPOLATED_FROM_RVE
210	E7	0.1	10000000	0.984529355657	0.984556308685	DIRECT_RVE_FEM
211	E7	0.15	100000	0.743230829517	0.743502785594	DIRECT_RVE_FEM
212	E7	0.15	300000	0.813702290399	0.81391150396	INTERPOLATED_FROM_RVE
213	E7	0.15	1000000	0.890932195124	0.891055062505	DIRECT_RVE_FEM

Table S5b continued

Row	scenario	phi_ECS	frequency_Hz	R_sigma_total	R_sigma_matched_electrical_baseline	provenance
214	E7	0.15	2000000	0.926759876122	0.926831336495	INTERPOLATED_FROM_RVE
215	E7	0.15	3000000	0.947717725993	0.947757098789	DIRECT_RVE_FEM
216	E7	0.15	5000000	0.966529223138	0.966563567242	INTERPOLATED_FROM_RVE
217	E7	0.15	10000000	0.992054834231	0.99208199328	DIRECT_RVE_FEM
218	E7	0.2	100000	0.999634223189	1	DIRECT_RVE_FEM
219	E7	0.2	300000	0.999742952938	1	INTERPOLATED_FROM_RVE
220	E7	0.2	1000000	0.999862110227	1	DIRECT_RVE_FEM
221	E7	0.2	2000000	0.999922898191	1	INTERPOLATED_FROM_RVE
222	E7	0.2	3000000	0.999958456871	1	DIRECT_RVE_FEM
223	E7	0.2	5000000	0.999964467828	1	INTERPOLATED_FROM_RVE
224	E7	0.2	10000000	0.999972624188	1	DIRECT_RVE_FEM
225	E8	0.05	100000	0.257274197561	0.257262079093	DIRECT_RVE_FEM
226	E8	0.05	300000	0.428536377617	0.428532785211	INTERPOLATED_FROM_RVE
227	E8	0.05	1000000	0.616223161501	0.61624414651	DIRECT_RVE_FEM
228	E8	0.05	2000000	0.738970179239	0.738998487398	INTERPOLATED_FROM_RVE
229	E8	0.05	3000000	0.81077258169	0.810805657679	DIRECT_RVE_FEM
230	E8	0.05	5000000	0.88158548995	0.88161747702	INTERPOLATED_FROM_RVE
231	E8	0.05	10000000	0.977672619146	0.977702106864	DIRECT_RVE_FEM
232	E8	0.1	100000	0.496655891441	0.496632497302	DIRECT_RVE_FEM

Table S5b continued

Row	scenario	phi_ECS	frequency_Hz	R_sigma_total	R_sigma_matched_electrical_baseline	provenance
233	E8	0.1	300000	0.629591435698	0.629586157855	INTERPOLATED_FROM_RVE
234	E8	0.1	1000000	0.77527593392	0.775302335349	DIRECT_RVE_FEM
235	E8	0.1	2000000	0.845714638767	0.845747036048	INTERPOLATED_FROM_RVE
236	E8	0.1	3000000	0.886918639702	0.886954822119	DIRECT_RVE_FEM
237	E8	0.1	5000000	0.928331867383	0.928365550578	INTERPOLATED_FROM_RVE
238	E8	0.1	10000000	0.984526115809	0.984555810235	DIRECT_RVE_FEM
239	E8	0.15	100000	0.743665510188	0.743630481076	DIRECT_RVE_FEM
240	E8	0.15	300000	0.813978065344	0.813971241793	INTERPOLATED_FROM_RVE
241	E8	0.15	1000000	0.891033824763	0.891064168239	DIRECT_RVE_FEM
242	E8	0.15	2000000	0.926798997138	0.926834500564	INTERPOLATED_FROM_RVE
243	E8	0.15	3000000	0.947720281809	0.947758944667	DIRECT_RVE_FEM
244	E8	0.15	5000000	0.966529427653	0.966564496793	INTERPOLATED_FROM_RVE
245	E8	0.15	10000000	0.992051848229	0.99208176964	DIRECT_RVE_FEM
246	E8	0.2	100000	1.00004710553	1	DIRECT_RVE_FEM
247	E8	0.2	300000	1.00000838304	1	INTERPOLATED_FROM_RVE
248	E8	0.2	1000000	0.999965946923	1	DIRECT_RVE_FEM
249	E8	0.2	2000000	0.999961693887	1	INTERPOLATED_FROM_RVE
250	E8	0.2	3000000	0.999959206021	1	DIRECT_RVE_FEM

Table S5b continued

Row	scenario	phi_ECS	frequency_Hz	R_sigma_total	R_sigma_matched_electrical_baseline	provenance
251	E8	0.2	5000000	0.999963717745	1	INTERPOLATED_FROM_RVE
252	E8	0.2	10000000	0.999969839773	1	DIRECT_RVE_FEM
253	E9	0.05	100000	0.192779426447	0.257080250775	DIRECT_RVE_FEM
254	E9	0.05	300000	0.321096123755	0.428300814424	INTERPOLATED_FROM_RVE
255	E9	0.05	1000000	0.46171881248	0.616037841533	DIRECT_RVE_FEM
256	E9	0.05	2000000	0.552758951864	0.738515342226	INTERPOLATED_FROM_RVE
257	E9	0.05	3000000	0.606014019464	0.810315608447	DIRECT_RVE_FEM
258	E9	0.05	5000000	0.657396205434	0.880454696536	INTERPOLATED_FROM_RVE
259	E9	0.05	10000000	0.727117487372	0.975994452693	DIRECT_RVE_FEM
260	E9	0.1	100000	0.372321014299	0.496507233624	DIRECT_RVE_FEM
261	E9	0.1	300000	0.471852598177	0.629390506881	INTERPOLATED_FROM_RVE
262	E9	0.1	1000000	0.580929586845	0.775092110369	DIRECT_RVE_FEM
263	E9	0.1	2000000	0.632784691329	0.845433984011	INTERPOLATED_FROM_RVE
264	E9	0.1	3000000	0.663117982923	0.886670661976	DIRECT_RVE_FEM
265	E9	0.1	5000000	0.692658095875	0.927681158738	INTERPOLATED_FROM_RVE
266	E9	0.1	10000000	0.7327415315	0.983543488394	DIRECT_RVE_FEM
267	E9	0.15	100000	0.557585928922	0.743566536523	DIRECT_RVE_FEM
268	E9	0.15	300000	0.610153245938	0.813865733111	INTERPOLATED_FROM_RVE
269	E9	0.15	1000000	0.667761940775	0.890946206942	DIRECT_RVE_FEM

Table S5b continued

Row	scenario	phi_ECS	frequency_Hz	R_sigma_total	R_sigma_matched_electrical_baseline	provenance
270	E9	0.15	2000000	0.693593665003	0.92667800521	INTERPOLATED_FROM_RVE
271	E9	0.15	3000000	0.708704255005	0.947625139285	DIRECT_RVE_FEM
272	E9	0.15	5000000	0.721453349054	0.966246814715	INTERPOLATED_FROM_RVE
273	E9	0.15	10000000	0.738752791728	0.99161227609	DIRECT_RVE_FEM
274	E9	0.2	100000	0.749880342289	1	DIRECT_RVE_FEM
275	E9	0.2	300000	0.749697672619	1	INTERPOLATED_FROM_RVE
276	E9	0.2	1000000	0.749497484328	1	DIRECT_RVE_FEM
277	E9	0.2	2000000	0.748473214108	1	INTERPOLATED_FROM_RVE
278	E9	0.2	3000000	0.747874054438	1	DIRECT_RVE_FEM
279	E9	0.2	5000000	0.746655345267	1	INTERPOLATED_FROM_RVE
280	E9	0.2	10000000	0.745001659964	1	DIRECT_RVE_FEM
281	E10	0.05	100000	0.321300837576	0.257081596439	DIRECT_RVE_FEM
282	E10	0.05	300000	0.535681341412	0.428526676904	INTERPOLATED_FROM_RVE
283	E10	0.05	1000000	0.770621637509	0.616334327457	DIRECT_RVE_FEM
284	E10	0.05	2000000	0.92514095219	0.73927566706	INTERPOLATED_FROM_RVE
285	E10	0.05	3000000	1.01552895692	0.811092977941	DIRECT_RVE_FEM
286	E10	0.05	5000000	1.10580410501	0.882314924646	INTERPOLATED_FROM_RVE
287	E10	0.05	10000000	1.22829984812	0.978730456669	DIRECT_RVE_FEM
288	E10	0.1	100000	0.620535804576	0.496507685731	DIRECT_RVE_FEM

Table S5b continued

Row	scenario	phi_ECS	frequency_Hz	R_sigma_total	R_sigma_matched_electrical_baseline	provenance
289	E10	0.1	300000	0.787045222205	0.629609149267	INTERPOLATED_FROM_RVE
290	E10	0.1	1000000	0.969523438184	0.77541370128	DIRECT_RVE_FEM
291	E10	0.1	2000000	1.05860854756	0.845928977958	INTERPOLATED_FROM_RVE
292	E10	0.1	3000000	1.11071999592	0.887121123443	DIRECT_RVE_FEM
293	E10	0.1	5000000	1.16403354445	0.928775869433	INTERPOLATED_FROM_RVE
294	E10	0.1	10000000	1.23637552209	0.985165292661	DIRECT_RVE_FEM
295	E10	0.15	100000	0.929310431592	0.743566718169	DIRECT_RVE_FEM
296	E10	0.15	300000	1.01752715837	0.81398678305	INTERPOLATED_FROM_RVE
297	E10	0.15	1000000	1.11420415809	0.891127677974	DIRECT_RVE_FEM
298	E10	0.15	2000000	1.15996893292	0.92692557239	INTERPOLATED_FROM_RVE
299	E10	0.15	3000000	1.18673961004	0.947837240673	DIRECT_RVE_FEM
300	E10	0.15	5000000	1.21163262767	0.966754912313	INTERPOLATED_FROM_RVE
301	E10	0.15	10000000	1.24541034786	0.992364397313	DIRECT_RVE_FEM
302	E10	0.2	100000	1.24980100492	1	DIRECT_RVE_FEM
303	E10	0.2	300000	1.25005366126	1	INTERPOLATED_FROM_RVE
304	E10	0.2	1000000	1.25033054818	1	DIRECT_RVE_FEM
305	E10	0.2	2000000	1.25141539673	1	INTERPOLATED_FROM_RVE
306	E10	0.2	3000000	1.25204999246	1	DIRECT_RVE_FEM

Table S5b continued

Row	scenario	phi_ECS	frequency_Hz	R_sigma_total	R_sigma_matched_electrical_baseline	provenance
307	E10	0.2	5000000	1.25329865122	1	INTERPOLATED_FROM_RVE
308	E10	0.2	10000000	1.25499297559	1	DIRECT_RVE_FEM

Table S5b, column panel 2/2. First column is repeated for alignment.

Row	scenario	total_sign_reversal_vs_fixed_normal	structural_sign_reversal_at_fixed_electrical_parameters
1	E0	False	False
2	E0	False	False
3	E0	False	False
4	E0	False	False
5	E0	False	False
6	E0	False	False
7	E0	False	False
8	E0	False	False
9	E0	False	False
10	E0	False	False
11	E0	False	False
12	E0	False	False
13	E0	False	False
14	E0	False	False
15	E0	False	False
16	E0	False	False
17	E0	False	False

Table S5b continued

Row	scenario	total_sign_reversal_vs_fixed_normal	structural_sign_reversal_at_fixed_electrical_parameters
18	E0	False	False
19	E0	False	False
20	E0	False	False
21	E0	False	False
22	E0	False	False
23	E0	False	False
24	E0	False	False
25	E0	False	False
26	E0	False	False
27	E0	False	False
28	E0	False	False
29	E1	False	False
30	E1	False	False
31	E1	False	False
32	E1	False	False
33	E1	False	False
34	E1	False	False
35	E1	False	False
36	E1	False	False
37	E1	False	False
38	E1	False	False
39	E1	False	False
40	E1	False	False
41	E1	False	False
42	E1	False	False
43	E1	False	False
44	E1	False	False

Table S5b continued

Row	scenario	total_sign_reversal_vs_fixed_normal	structural_sign_reversal_at_fixed_electrical_parameters
45	E1	False	False
46	E1	False	False
47	E1	False	False
48	E1	False	False
49	E1	False	False
50	E1	False	False
51	E1	False	False
52	E1	False	False
53	E1	False	False
54	E1	False	False
55	E1	False	False
56	E1	False	False
57	E2	False	False
58	E2	False	False
59	E2	False	False
60	E2	False	False
61	E2	False	False
62	E2	False	False
63	E2	True	False
64	E2	False	False
65	E2	False	False
66	E2	False	False
67	E2	False	False
68	E2	False	False
69	E2	False	False
70	E2	True	False
71	E2	False	False

Table S5b continued

Row	scenario	total_sign_reversal_vs_fixed_normal	structural_sign_reversal_at_fixed_electrical_parameters
72	E2	False	False
73	E2	False	False
74	E2	False	False
75	E2	False	False
76	E2	True	False
77	E2	True	False
78	E2	False	False
79	E2	False	False
80	E2	False	False
81	E2	False	False
82	E2	False	False
83	E2	False	False
84	E2	False	False
85	E3	False	False
86	E3	False	False
87	E3	False	False
88	E3	False	False
89	E3	False	False
90	E3	False	False
91	E3	False	True
92	E3	False	False
93	E3	False	False
94	E3	False	False
95	E3	False	False
96	E3	False	False
97	E3	False	False
98	E3	False	True

Table S5b continued

Row	scenario	total_sign_reversal_vs_fixed_normal	structural_sign_reversal_at_fixed_electrical_parameters
99	E3	False	False
100	E3	False	False
101	E3	False	False
102	E3	False	False
103	E3	False	False
104	E3	False	False
105	E3	False	True
106	E3	False	False
107	E3	False	False
108	E3	False	False
109	E3	False	False
110	E3	False	False
111	E3	False	False
112	E3	False	False
113	E4	False	False
114	E4	False	False
115	E4	False	False
116	E4	False	False
117	E4	False	False
118	E4	False	False
119	E4	False	False
120	E4	False	False
121	E4	False	False
122	E4	False	False
123	E4	False	False
124	E4	False	False
125	E4	False	False

Table S5b continued

Row	scenario	total_sign_reversal_vs_fixed_normal	structural_sign_reversal_at_fixed_electrical_parameters
126	E4	True	False
127	E4	False	False
128	E4	False	False
129	E4	False	False
130	E4	True	False
131	E4	True	False
132	E4	True	False
133	E4	True	False
134	E4	False	False
135	E4	False	False
136	E4	False	False
137	E4	False	False
138	E4	False	False
139	E4	False	False
140	E4	False	False
141	E5	False	False
142	E5	False	False
143	E5	False	False
144	E5	False	False
145	E5	False	False
146	E5	False	False
147	E5	False	False
148	E5	False	False
149	E5	False	False
150	E5	False	False
151	E5	False	False
152	E5	False	False

Table S5b continued

Row	scenario	total_sign_reversal_vs_fixed_normal	structural_sign_reversal_at_fixed_electrical_parameters
153	E5	False	False
154	E5	False	False
155	E5	False	False
156	E5	False	False
157	E5	False	False
158	E5	False	False
159	E5	False	False
160	E5	False	False
161	E5	False	False
162	E5	False	False
163	E5	False	False
164	E5	False	False
165	E5	False	False
166	E5	False	False
167	E5	False	False
168	E5	False	False
169	E6	False	False
170	E6	False	False
171	E6	False	False
172	E6	False	False
173	E6	False	False
174	E6	False	False
175	E6	True	False
176	E6	False	False
177	E6	False	False
178	E6	False	False
179	E6	False	False

Table S5b continued

Row	scenario	total_sign_reversal_vs_fixed_normal	structural_sign_reversal_at_fixed_electrical_parameters
180	E6	True	False
181	E6	True	False
182	E6	True	False
183	E6	False	False
184	E6	False	False
185	E6	True	False
186	E6	True	False
187	E6	True	False
188	E6	True	False
189	E6	True	False
190	E6	False	False
191	E6	False	False
192	E6	False	False
193	E6	False	False
194	E6	False	False
195	E6	False	False
196	E6	False	False
197	E7	False	False
198	E7	False	False
199	E7	False	False
200	E7	False	False
201	E7	False	False
202	E7	False	False
203	E7	False	False
204	E7	False	False
205	E7	False	False
206	E7	False	False

Table S5b continued

Row	scenario	total_sign_reversal_vs_fixed_normal	structural_sign_reversal_at_fixed_electrical_parameters
207	E7	False	False
208	E7	False	False
209	E7	False	False
210	E7	False	False
211	E7	False	False
212	E7	False	False
213	E7	False	False
214	E7	False	False
215	E7	False	False
216	E7	False	False
217	E7	False	False
218	E7	False	False
219	E7	False	False
220	E7	False	False
221	E7	False	False
222	E7	False	False
223	E7	False	False
224	E7	False	False
225	E8	False	False
226	E8	False	False
227	E8	False	False
228	E8	False	False
229	E8	False	False
230	E8	False	False
231	E8	False	False
232	E8	False	False
233	E8	False	False

Table S5b continued

Row	scenario	total_sign_reversal_vs_fixed_normal	structural_sign_reversal_at_fixed_electrical_parameters
234	E8	False	False
235	E8	False	False
236	E8	False	False
237	E8	False	False
238	E8	False	False
239	E8	False	False
240	E8	False	False
241	E8	False	False
242	E8	False	False
243	E8	False	False
244	E8	False	False
245	E8	False	False
246	E8	False	False
247	E8	False	False
248	E8	False	False
249	E8	False	False
250	E8	False	False
251	E8	False	False
252	E8	False	False
253	E9	False	False
254	E9	False	False
255	E9	False	False
256	E9	False	False
257	E9	False	False
258	E9	False	False
259	E9	False	False
260	E9	False	False

Table S5b continued

Row	scenario	total_sign_reversal_vs_fixed_normal	structural_sign_reversal_at_fixed_electrical_parameters
261	E9	False	False
262	E9	False	False
263	E9	False	False
264	E9	False	False
265	E9	False	False
266	E9	False	False
267	E9	False	False
268	E9	False	False
269	E9	False	False
270	E9	False	False
271	E9	False	False
272	E9	False	False
273	E9	False	False
274	E9	False	False
275	E9	False	False
276	E9	False	False
277	E9	False	False
278	E9	False	False
279	E9	False	False
280	E9	False	False
281	E10	False	False
282	E10	False	False
283	E10	False	False
284	E10	False	False
285	E10	True	False
286	E10	True	False
287	E10	True	False

Table S5b continued

Row	scenario	total_sign_reversal_vs_fixed_normal	structural_sign_reversal_at_fixed_electrical_parameters
288	E10	False	False
289	E10	False	False
290	E10	False	False
291	E10	True	False
292	E10	True	False
293	E10	True	False
294	E10	True	False
295	E10	False	False
296	E10	True	False
297	E10	True	False
298	E10	True	False
299	E10	True	False
300	E10	True	False
301	E10	True	False
302	E10	False	False
303	E10	False	False
304	E10	False	False
305	E10	False	False
306	E10	False	False
307	E10	False	False
308	E10	False	False

Units: Hz; dimensionless ratios and flags. Denominator: R_total fixed E0 normal; R_matched same E normal. 31 total reversals and three matched reversals are distinct.

Full records: Table_S5b.csv.

Table S5c. Existing refined E3 endpoint

E3, 10 MHz	sigma at phi 0.20 (S m^{-1})	sigma at phi 0.05 (S m^{-1})	Matched structural change
Medium	0.8078992764685715	0.8228692901093781	+1.852955446%
Fine	0.8077355581436308	0.8231551725403141	+1.908992893%

The endpoint sign persists after existing refinement; the change between ratios is 0.000560374468, not a new uncertainty interval. The maximum conductivity refinement change in the recorded targeted check is 0.345359054%. The reversal is an electrical-state-dependent result, not a dismissed numerical anomaly or established biological mechanism.

Table S5d. Propagated discrete material endpoints

Table S5d, column panel 1/3. First column is repeated for alignment.

Row	frequency_Hz	scenario_min	R_sigma_min	head_min_abs_delta
1	2000000	E9	0.632784691329	$1.84746364027 \times 10^{-9}$
2	3000000	E9	0.663117982923	$2.76536533382 \times 10^{-9}$
3	5000000	E9	0.692658095875	$4.85328497812 \times 10^{-9}$

Table S5d, column panel 2/3. First column is repeated for alignment.

Row	frequency_Hz	R_sigma_nominal	head_nominal_abs_delta	scenario_max
1	2000000	0.845700739072	$7.76281019633 \times 10^{-10}$	E10
2	3000000	0.886921622954	$9.28227118049 \times 10^{-10}$	E10
3	5000000	0.928336217492	$1.13165420738 \times 10^{-9}$	E10

Table S5d, column panel 3/3. First column is repeated for alignment.

Row	frequency_Hz	R_sigma_max	head_max_abs_delta
1	2000000	1.05860854756	$2.94860148998 \times 10^{-10}$
2	3000000	1.11071999592	$9.08867861131 \times 10^{-10}$
3	5000000	1.16403354445	$2.59027983545 \times 10^{-9}$

Units: Hz; dimensionless ratio/response. Denominator: Fixed E0 ϕ.20 material; same-frequency normal voltage. The minimum material ratio can give the maximum response; no continuous-box bound.

Full records: Table_S5d.csv.

At 5 MHz the largest propagated endpoint is $4.85328497812 \times 10^{-9}$ at ϕ=0.10; the same-ϕ nominal response is $1.13165420738 \times 10^{-9}$. Neither is the nominal ϕ=0.05 headline.

S6. IT'IS/Gabriel provenance

The original database archive and mapping/validation records are retained under D:/codex/data/tissue_properties/ITIS_V5_0/. Official V5.0 release: 2025-08-21; original retrieval recorded as 2026-09-20. Database DOI 10.13099/VIP21000-05-0; dielectric-model reference Gabriel et al. [7], DOI 10.1088/0031-9155/41/11/003.

Table S6a. Verified tissue mapping

Macro role	Database tissue	Confirmed dielectric source
Scalp	Scalp	Skin, then Gabriel Skin (Dry)
Skull	Skull (Cortical)	Bone (Cortical)
CSF	Cerebrospinal Fluid	Direct CSF model
Primary brain	Brain (Grey Matter)	Direct grey-matter model
Comparator only	Brain (White Matter)	Direct white-matter model

Table S6b. Full conductivity and relative-permittivity input

tissue_model	frequency_Hz	conductivity_S_m	relative_permittivity
Scalp	100000	0.000451288718791	1119.21263729
Scalp	200000	0.00105480184038	1104.78659327
Scalp	300000	0.00193433445451	1090.54022909
Scalp	500000	0.00436466629366	1061.99613445
Scalp	700000	0.00751155648905	1033.37636486
Scalp	1000000	0.0132371451497	990.755213952
Scalp	1500000	0.0245592794246	922.097225674
Scalp	2000000	0.0371026021037	857.958321875
Scalp	3000000	0.063141434878	745.659944658
Scalp	4000000	0.0882357564128	653.826109541
Scalp	5000000	0.111344212712	579.205510198
Scalp	7000000	0.151093762447	468.162838771
Scalp	10000000	0.197320818163	361.66188755
Skull_Cortical	100000	0.0207910253102	227.641786419
Skull_Cortical	200000	0.0210808750195	203.744984584
Skull_Cortical	300000	0.0214072802257	191.439775245
Skull_Cortical	500000	0.0221652563958	174.502439285
Skull_Cortical	700000	0.0230138951851	161.177849567
Skull_Cortical	1000000	0.0243530620399	144.509767609
Skull_Cortical	1500000	0.0265442807742	122.624052507
Skull_Cortical	2000000	0.0285402053712	106.051362018
Skull_Cortical	3000000	0.0318563883986	83.2507521048
Skull_Cortical	4000000	0.0344339575853	68.7349813928
Skull_Cortical	5000000	0.0364880727889	58.8850132259
Skull_Cortical	7000000	0.0395909412858	46.5990366505
Skull_Cortical	10000000	0.0428225211079	36.7718218084
CSF	100000	2.00000022865	108.999787641

Table S6b continued

tissue_model	frequency_Hz	conductivity_S_m	relative_permittivity
CSF	200000	2.00000091296	108.999518291
CSF	300000	2.00000205212	108.999176501
CSF	500000	2.00000569351	108.99826563
CSF	700000	2.00001115065	108.997045465
CSF	1000000	2.00002273783	108.994628243
CSF	1500000	2.00005111086	108.989023031
CSF	2000000	2.00009079578	108.981439224
CSF	3000000	2.00020402987	108.96032484
CSF	4000000	2.00036227529	108.931286188
CSF	5000000	2.00056532487	108.894346286
CSF	7000000	2.00110477213	108.796921488
CSF	10000000	2.0022420558	108.59279516
Brain_GreyMatter	100000	0.133666893671	3221.77862833
Brain_GreyMatter	200000	0.140636300099	2009.87167567
Brain_GreyMatter	300000	0.14524777831	1569.4147078
Brain_GreyMatter	500000	0.151870895216	1186.98304737
Brain_GreyMatter	700000	0.156951617907	1007.39390268
Brain_GreyMatter	1000000	0.163292450172	860.422091745
Brain_GreyMatter	1500000	0.172373168674	731.417250924
Brain_GreyMatter	2000000	0.18069271785	656.489673891
Brain_GreyMatter	3000000	0.196546184785	564.724617773
Brain_GreyMatter	4000000	0.211922302129	504.587589211
Brain_GreyMatter	5000000	0.226852803796	458.925358973
Brain_GreyMatter	7000000	0.254935326844	390.524862604
Brain_GreyMatter	10000000	0.291724547509	319.673062266
Brain_WhiteMatter	100000	0.0818464854696	2107.62814041
Brain_WhiteMatter	200000	0.0867663027788	1288.62103227
Brain_WhiteMatter	300000	0.0900324338615	982.400344495

Table S6b continued

tissue_model	frequency_Hz	conductivity_S_m	relative_permittivity
Brain_WhiteMatter	500000	0.094659649144	712.226724942
Brain_WhiteMatter	700000	0.0980888682007	584.241506725
Brain_WhiteMatter	1000000	0.10213916646	479.791153103
Brain_WhiteMatter	1500000	0.107416985234	390.145145344
Brain_WhiteMatter	2000000	0.111747797372	340.634701175
Brain_WhiteMatter	3000000	0.11905186381	285.391005432
Brain_WhiteMatter	4000000	0.125465777314	253.786798809
Brain_WhiteMatter	5000000	0.13143729029	232.369260054
Brain_WhiteMatter	7000000	0.142681398931	203.5600486
Brain_WhiteMatter	10000000	0.158455007438	175.724001272

Units: Hz; $\mathrm{S\,m^{-1}}$; epsilon_r dimensionless. Denominator: Same ITIS/Gabriel frequency-dependent dielectric model. Five tissues $\times$ thirteen frequencies; no low-frequency conductivity splice.

Full records: Table_S6b.csv.

The existing validation record reports positive finite properties, continuity over the band and 1 MHz agreement with the official online computation within 5×10^{-6} relative tolerance. These are archived checks, not a new online validation. The main head uses seven frequencies. Generic Brain/Cerebellum, grey/white averaging and low-frequency conductivity splicing are excluded.

S7. Head-scale numerical verification

S7.1. Problem, paired mesh and verified settings

Reference: 5 MHz, D = 3 mm, centroid depth = 1.5 mm, ϕ = 0.05, nominal R_σ = 0.8815302230145321. The micro input at 5 MHz is interpolated; the stored head solutions are direct FEM calculations. The brain/CSF/skull/scalp radii are 6.0/6.3/6.7/7.2 mm. Transmit and receive loops have radius 7.2 mm at z = −10/+10 mm; transmitter current is 0.010 A in a wire cross-section of radius 0.1 mm. The ideal receiver is non-loading. Production air radius is 120 mm.

The axisymmetric A_ϕ problem retains conduction and displacement current as stated in Methods 2.7. Geometry is built with the feasible lesion partitions before paired solves. A material indicator changes conductivity within the designated sphere; the normal case sets the perturbation ratio to one. Normal and lesion cases therefore use identical partitions and the same mesh within each comparison pair. Refinement/domain variants use new meshes but retain pairing within each variant. This cancellation control is not itself a discretization-error bound.

Source settings are D:/codex/results/stage3PMB_multiscale_forward/05_forward_runs/Stage3PMBHead.java and Stage3PMBJobA.java, and 03_head_geometry/stage3PMB_geometry_config.yaml in the same stage root. Free triangular meshes use nominal maximum sizes of 2 mm in air, 0.30 mm in head and 0.04 mm in coil, with 0.005 mm minimum; mesh multipliers are 1.6/1/0.65 for coarse/medium/fine.

Saved metadata was inspected read-only in the existing Stage3PMBJobA.mph ZIP entry dmodel.xml, without launching COMSOL or solving. It confirms InductionCurrents physics mf, order_magneticvectorpotential and order_magneticvectorpotentialExpr = 2, MagneticInsulation node mi1 with EXTERIOR default selection, and AxialSymmetry node axi1 with SYMMETRYAXIS selection. Magnetic insulation and regularity at r = 0 are thus verified settings, not guesses from a version default. Serialized Direct_linsolver defaults identify MUMPS; the alternate saved-run source and log explicitly identify PARDISO at sol1/s1/dDef. Local COMSOL 6.4 documentation provides consistent formulation context but is not the sole evidence for these metadata findings.

S7.2. Raw complex receiver voltages

Table S7a. Historical interpolated-input reference ledger, superseded for the current 5 MHz paired response by S11. All entries are volts at 5 MHz; digits are retained from existing exports, not claims of physical accuracy. Reference rows originate in Stage3PMBJobA_values.log; variants originate in Stage3PMBJobV_values.log and Stage3PMBJobPResume_values.log, all under 05_forward_runs.

Pair / state	Re(V_RX), V	Im(V_RX), V
Production normal	$-6.5359409906693030 \times 10^{-9}$	-0.00014951448530076364
Production lesion	$-6.5356612826942400 \times 10^{-9}$	-0.00014951448530081682
Coarse normal	$-6.5377199191762420 \times 10^{-9}$	-0.00014942612207370675
Coarse lesion	$-6.5374397094397850 \times 10^{-9}$	-0.00014942612207375730
Fine normal	$-6.5359339550561550 \times 10^{-9}$	-0.00014949778306384540
Fine lesion	$-6.5356541168970330 \times 10^{-9}$	-0.00014949778306389905
Air 60 mm normal	$-6.4099460324480530 \times 10^{-9}$	-0.00014334689021888830
Air 60 mm lesion	$-6.4096717953953500 \times 10^{-9}$	-0.00014334689021894390
Air 90 mm normal	$-6.5075907411758540 \times 10^{-9}$	-0.00014819804316371550
Air 90 mm lesion	$-6.5073118109239910 \times 10^{-9}$	-0.00014819804316376875
PARDISO normal	$-6.5359409906712240 \times 10^{-9}$	-0.00014951448530079430
PARDISO lesion	$-6.5356612826961700 \times 10^{-9}$	-0.00014951448530084680

Table S7a continued

Pair / state	Re(V_RX), V	Im(V_RX), V
Half current normal	$-3.2679704953346800 \times 10^{-9}$	$-7.4757242650382390 \times 10^{-5}$
Half current lesion	$-3.2678306413471482 \times 10^{-9}$	$-7.4757242650407840 \times 10^{-5}$
Double current normal	$-1.3071881981338673 \times 10^{-8}$	-0.00029902897060152530
Double current lesion	$-1.3071322565388449 \times 10^{-8}$	-0.00029902897060163266

The reference $\Delta V = V_{\text{lesion}} - V_{\text{normal}}$ is $(2.797079750631774 \times 10^{-13} - \text{j}\ 5.318011656041399 \times 10^{-17})$ V. With $\delta = \Delta V / V_{\text{normal}}$, $\delta = 2.739055068050333 \times 10^{-13} + \text{j}\ 1.8707751044371822 \times 10^{-9}$ and $|\delta| = 1.8707751244888244 \times 10^{-9}$. The recorded phase change is $1.870775104439787 \times 10^{-9}$ rad. The relative amplitude change $2.7400304247748863 \times 10^{-13}$ is a different quantity and was not independently demonstrated to be resolved.

The predominant quadrature normalized response arises mainly from the small real-voltage difference, not subtraction of the entire signal exclusively from the approximately 1.5×10^{-4} V imaginary baseline. This observation addresses the component-wise subtraction mechanism; it is not a proof based on machine precision or residual alone.

S7.3. Mesh and air-domain sequences

Table S7b. Historical interpolated-input complex normalized responses from 09_validation/head_validation.json, with mesh element counts from the corresponding exported logs.

Table S7b, column panel 1/2. First column is repeated for alignment.

Row	Check	Elements	Re(delta)	Im(delta)
1	Coarse, scale 1.6, air 120 mm	10128	$2.5625463852674803 \times 10^{-13}$	$1.8752393105316656 \times 10^{-9}$
2	Medium, scale 1, air 120 mm	21952	$2.739055068050333 \times 10^{-13}$	$1.8707751044371822 \times 10^{-9}$
3	Fine, scale 0.65, air 120 mm	48411	$2.7697121319728657 \times 10^{-13}$	$1.8718549211712765 \times 10^{-9}$
4	Air 60 mm, scale 1	9502	$3.022708986135925 \times 10^{-13}$	$1.9131008298963023 \times 10^{-9}$
5	Air 90 mm, scale 1	14740	$2.767458960800774 \times 10^{-13}$	$1.8821453219537952 \times 10^{-9}$
6	Air 120 mm, scale 1	21952	$2.739055068050333 \times 10^{-13}$	$1.8707751044371822 \times 10^{-9}$

Table S7b, column panel 2/2. First column is repeated for alignment.

Row	Check	abs(delta)
1	Coarse, scale 1.6, air 120 mm	$1.8752393280404814 \times 10^{-9}$
2	Medium, scale 1, air 120 mm	$1.8707751244888244 \times 10^{-9}$
3	Fine, scale 0.65, air 120 mm	$1.8718549416624618 \times 10^{-9}$
4	Air 60 mm, scale 1	$1.9131008537757794 \times 10^{-9}$
5	Air 90 mm, scale 1	$1.882145342299804 \times 10^{-9}$
6	Air 120 mm, scale 1	$1.8707751244888244 \times 10^{-9}$

The air sequence changes both domain extent and its associated mesh; it is the actual tested domain comparison, not an isolated analytic boundary error. The medium/fine

magnitude-relative metric retained in the historical JSON is 0.0576870114%, using the fine magnitude as denominator. Table 1 instead uses the magnitude of the complex difference divided by the production reference magnitude; its mesh value is 0.05772%. These are explicitly different metrics, not inconsistent rounded versions of one metric.

Table S7c. Historical interpolated-input direct complex differences and common reference denominator:

Comparison	abs(delta_check − delta_ref)	100 × difference / abs(delta_ref)
mesh	$1.0798210860071615 \times 10^{-12}$	0.05772051765453182%
air_domain	$1.1370217871391235 \times 10^{-11}$	0.6077811128955471%
alternate_solver	$4.532178643872372 \times 10^{-15}$	0.0002422620754651 5014%

For the historical interpolated-input reference, the largest tested difference is $1.1370217871391235 \times 10^{-11}$. The reference response divided by this value is 164.5329179835602, a local separation factor. No extrapolation to an infinite air domain, asymptotic order, statistical confidence interval or global error bound is made. The response is numerically resolved relative to the tested convergence differences at the verified reference condition.

S7.4. Alternate factorization and current scaling

PARDISO gives $\Delta V = 2.797079750540784 \times 10^{-13} - \mathrm{j}\, 5.250249020261055 \times 10^{-17}$ V, $\delta = 2.6937332816858217 \times 10^{-13} + \mathrm{j}\, 1.87077510417782 \times 10^{-9}$, and $|\delta| = 1.870775123571383 \times 10^{-9}$. The complex difference from MUMPS is $4.532178643872372 \times 10^{-15}$, or $2.4226207546515013 \times 10^{-6}$ of the reference response. This compares independent direct factorizations of the same discrete physical problem, not independent physical models.

Table S7d. Current scaling checks from existing validation records; relative errors are dimensionless fractions, not percentages.

Current	Scale	Raw voltage relative scaling error	Normalized delta relative difference
0.005 A	0.5	$7.660538902644995 \times 10^{-15}$	$8.14000573474508 \times 10^{-6}$
0.010 A	1	Reference	Reference
0.020 A	2	$6.5503158646359165 \times 10^{-15}$	$1.7442869518873904 \times 10^{-6}$

Raw error is the maximum of abs(V_check/(scale V_production) − 1) over the normal and lesion voltages; normalized error compares each paired δ to the production δ. The raw voltages above preserve the underlying observations. Current invariance of δ supports the linear forward extraction but does not establish hardware performance.

S7.5. Solver tolerance, residuals and execution provenance

The historical logs contain 78 completed/exported solver rows with maximum reported linear residual 4×10^{-13}. The configured reported_linear_residual_acceptance = 1×10^{-8} is a recorded acceptance threshold, not evidence that a particular relative solver tolerance was applied. The effective numerical relative-tolerance value is **not explicitly verified from saved model metadata**.

A historical JobV source statement attempted to set rtol = 1×10^{-10} on the stationary solver. The matching run log reports an unknown-property error at that statement; it occurred after the retained mesh, air, current and benchmark exports. It

therefore cannot establish an applied 1×10^{-10} tolerance or a completed additional MUMPS pair. The independently completed PARDISO pair is evidenced instead by Stage3PMBJobPResume.java and Stage3PMBJobPResume_values.log, which explicitly reports INDEPENDENT_DIRECT_SOLVER=pardiso. No rerun or repair was performed for this production.

The historical ledger has 79 attempted head frequency solutions, 78 directly exported and one recovered pilot. The recovered 100 kHz/40 mm air pilot is excluded from production and from the reference convergence claim. These are pre-existing counts, not V2 simulations. That historical production added no simulations. The subsequent major revision performed 201 unique direct RVE frequency solutions (140 electrical, 45 local sensitivity, 16 crossing/refinement), and no head FEM solves. The present reconciliation adds 8 RVE frequency solutions and 8 paired-reference head frequency solutions (4 normal/lesion configurations); analytical reevaluations and duplicate exports are excluded from these counts. Small residuals and shared meshes are supporting diagnostics, not estimates of total forward error.

S7.6. Independent baseline benchmarks

Table S7e. Air-coil voltage at 5 MHz.

Quantity	Re(V), V	Im(V), V
FEM air-coil	0	-0.00014951253521355410
Independent loop quadrature	0	-0.00015043944756608685

Relative complex-voltage difference = 0.006161365037754329 (0.6161365038%). The reference is independent loop-vector-potential quadrature in unbounded vacuum with an ideal filament; the FEM includes finite wire cross-section and an outer boundary. The recorded acceptance threshold was 0.01. This is a baseline coupling test, not the lesion δ error.

Table S7f. Homogeneous nonmagnetic sphere, radius 7.2 mm, at 5 MHz. FEM total voltage = $-4.1650123076841900 \times 10^{-9}$ **− j 0.00014951487358430722 V. Secondary response is (**$V_{\text{sphere}} - V_{\text{air}}$**)/**$V_{\text{air}}$**.**

Secondary response	Real part	Imaginary part
FEM	$1.5639964567475633 \times 10^{-5}$	$-2.7857278332784298 \times 10^{-5}$
Independent reference	$1.562221528212473 \times 10^{-5}$	$-2.7765027601358274 \times 10^{-5}$

Relative complex secondary-response error = 0.0029487688239767653 (0.2948768824%). The reference uses 24 terms in regular/outgoing multipole matching, a magnetoquasistatic exterior and full complex material properties inside the sphere. It is not an exact radiating-wave solution validating every layered-head case. Its recorded acceptance threshold was 0.03. The maximum recorded head-size/tissue-wavelength ratio, 0.020685769891448838, supplies a scale check; displacement current remains in the head operator.

S7.7. Scope and source index

The nominal 5 MHz/D3/depth1.5/phi0.05 reference response is locally supported by these comparisons. The largest propagated electrical-stress endpoint has separate recorded coarse/medium/fine magnitudes $4.864866307385834 \times 10^{-9}$, $4.853284978124659 \times 10^{-9}$ and $4.856086307663936 \times 10^{-9}$; this does not replace the nominal headline or establish a global stress bound. Neither the baseline benchmarks nor the D3 local difference scale

certifies D1, every sampled frequency, the tiny amplitude component or instrumental detectability.

All S7 inputs are under D:/codex/results/stage3PMB_multiscale_forward/:

- 05_forward_runs/Stage3PMBJobA_values.log: production normal_5000000 and rve_phi0.05_5000000.
- 05_forward_runs/Stage3PMBJobV_values.log: air_small/air_medium, mesh_coarse/mesh_fine, current_half/current_double, air_coil and homogeneous_sphere records.
- 05_forward_runs/Stage3PMBJobV_run.log: failed historical rtol assignment, not an applied tolerance.
- 05_forward_runs/Stage3PMBJobPResume_values.log and Stage3PMBJobPResume.java: alternate PARDISO pair.
- 05_forward_runs/Stage3PMBJobA.mph, dmodel.xml: read-only physics/order/boundary/solver-default inspection.
- 05_forward_runs/Stage3PMBHead.java and Stage3PMBJobA.java: geometry, material functions, receiver extraction and study.
- 03_head_geometry/stage3PMB_geometry_config.yaml: reference dimensions and mesh configuration.
- 09_validation/head_validation.json: all tabulated paired metrics, comparisons and ledger.
- 09_validation/stage3PMB_quasistatic_metrics.csv: 35 existing scale-check rows, five tissues at seven frequencies.

Unknown tolerance remains explicitly unknown; the supported numerical claim is local.

Table S7g. Electrically-small scale checks

tissue	frequency_Hz	conductivity_S_m	relative_permittivity	wavelength_m	head_diameter_over_wavelength	conduction_over_displacement
Scalp	100000	0.000451288718791	1119.21263729	89.5529258152	0.000160798766416	0.0724791804211
Scalp	300000	0.00193433445451	1090.54022909	30.218160458	0.000476534632874	0.106277180366
Scalp	1000000	0.0132371451497	990.755213952	9.45740696318	0.00152261608875	0.240159276357
Scalp	2000000	0.0371026021037	857.958321875	5.02673424794	0.00286468297104	0.388668714473
Scalp	3000000	0.063141434878	745.659944658	3.55335008938	0.00405251372305	0.507368826116
Scalp	5000000	0.111344212712	579.205510198	2.36704581438	0.00608353244053	0.691092788929
Scalp	10000000	0.197320818163	361.66188755	1.43886709823	0.0100078735678	0.980712170113
Skull_Cortical	100000	0.0207910253102	227.641786419	67.2733855274	0.000214051959584	16.4170576702
Skull_Cortical	300000	0.0214072802257	191.439775245	36.6326278994	0.000393092192009	6.70007193346
Skull_Cortical	1000000	0.0243530620399	144.509767609	17.2298117513	0.000835760727272	3.02919878712
Skull_Cortical	2000000	0.0285402053712	106.051362018	10.8232316989	0.00133047137865	2.41870136371
Skull_Cortical	3000000	0.0318563883986	83.2507521048	8.27756626048	0.0017396417675	2.29275959202
Skull_Cortical	5000000	0.0364880727889	58.8850132259	5.956207751	0.00241764569034	2.22765302086
Skull_Cortical	10000000	0.0428225211079	36.7718218084	3.8372219008	0.00375271495166	2.09328560514
CSF	100000	2.00000022865	108.999787641	7.06999552744	0.00203677639457	3298.19094669
CSF	300000	2.00000205212	108.999176501	4.08062455377	0.00352887157597	1099.40414873
CSF	1000000	2.00002273783	108.994628243	2.2326682176	0.00644968199328	329.838419228
CSF	2000000	2.00009079578	108.981439224	1.57631740234	0.00913521602859	164.944780912
CSF	3000000	2.00020402987	108.96032484	1.28507364977	0.0112055834329	109.990722708
CSF	5000000	2.00056532487	108.894346286	0.992318193628	0.014511474336	66.0463470667
CSF	10000000	2.0022420558	108.59279516	0.6961307254	0.0206857698914	33.1426300442
Brain_GreyMatter	100000	0.133666893671	3221.77862833	25.5833308093	0.000562866505044	7.45760816222
Brain_GreyMatter	300000	0.14524777831	1569.4147078	13.8495208831	0.0010397471596	5.54526016944
Brain_GreyMatter	1000000	0.163292450172	860.422091745	6.77236961875	0.00212628678153	3.41134744745
Brain_GreyMatter	2000000	0.18069271785	656.489673891	4.31980485619	0.00333348391406	2.47374060058
Brain_GreyMatter	3000000	0.196546184785	564.724617773	3.26741144924	0.00440715845669	2.08534562361

Table S7g continued

tissue	frequency_Hz	conductivity_S_m	relative_permittivity	wavelength_m	head_diameter_over_wavelength	conduction_over_displacement
Brain_GreyMatter	5000000	0.226852803796	458.925358973	2.27050038975	0.00634221428238	1.77706573278
Brain_GreyMatter	10000000	0.291724547509	319.673062266	1.38741586184	0.0103790077626	1.64035684535
Brain_WhiteMatter	100000	0.0818464854696	2107.62814041	32.5459592575	0.000442451239064	6.98035401091
Brain_WhiteMatter	300000	0.0900324338615	982.400344495	17.5755964346	0.00081931785664	5.49111616832
Brain_WhiteMatter	1000000	0.10213916646	479.791153103	8.69528218029	0.00165607046458	3.82658597452
Brain_WhiteMatter	2000000	0.111747797372	340.634701175	5.6631847891	0.00254273885389	2.94843453438
Brain_WhiteMatter	3000000	0.11905186381	285.391005432	4.35370233738	0.00330752974919	2.49945927189
Brain_WhiteMatter	5000000	0.13143729029	232.369260054	3.07796512021	0.00467841558874	2.03348662149
Brain_WhiteMatter	10000000	0.158455007438	175.724001272	1.87664864758	0.00767325307194	1.6208629166

Units: Units encoded in original columns. Denominator: Tissue wavelength under each frequency-dependent property pair. 35 rows; displacement current retained.

Full records: Table_S7g.csv.

S8. Additional geometry and material checks

The reference lesion is spherical and on-axis. Feasibility requires abs(6−depth)+D/2 $\leq$ 6, with lengths in millimetres. The D3/depth1.5 sphere is tangent and contained. Non-contained combinations are excluded without clipping or relocation. D1 values remain exploratory / not independently numerically certified. D2/D3 scans also do not inherit the separate phi0.05 reference-case certificate.

Table S8a. Historical forward ledger; the $\phi = 0.05$, 5 MHz row is superseded by S11. Complete feasible size and depth responses

Table S8a, column panel 1/2. First column is repeated for alignment.

Row	analysis	frequency_Hz	diameter_mm	depth_mm
1	size	2000000	1	1.5
2	size	2000000	2	1.5
3	size	2000000	3	1.5
4	depth	2000000	3	1.5
5	depth	2000000	3	3
6	depth	2000000	3	5
7	size	3000000	1	1.5
8	size	3000000	2	1.5
9	size	3000000	3	1.5
10	depth	3000000	3	1.5
11	depth	3000000	3	3
12	depth	3000000	3	5
13	size	5000000	1	1.5
14	size	5000000	2	1.5
15	size	5000000	3	1.5
16	depth	5000000	3	1.5
17	depth	5000000	3	3
18	depth	5000000	3	5

Table S8a, column panel 2/2. First column is repeated for alignment.

Row	analysis	phi_ECS	abs_DeltaV_over_V	interpretation
1	size	0.1	$3.2253078421 \times 10^{-12}$	Exploratory / not independently numerically certified
2	size	0.1	$1.02838778724 \times 10^{-10}$	Sampled finite geometry comparison; no universal law
3	size	0.1	$7.76281019633 \times 10^{-10}$	Sampled finite geometry comparison; no universal law
4	depth	0.1	$7.76281019633 \times 10^{-10}$	Sampled finite geometry comparison; no universal law
5	depth	0.1	$7.36703714387 \times 10^{-10}$	Sampled finite geometry comparison; no universal law
6	depth	0.1	$7.03590506258 \times 10^{-10}$	Sampled finite geometry comparison; no universal law

Table S8a continued

Row	analysis	phi_ECS	abs_DeltaV_over_V	interpretation
7	size	0.1	$3.85661582694 \times 10^{-12}$	Exploratory / not independently numerically certified
8	size	0.1	$1.2296804699 \times 10^{-10}$	Sampled finite geometry comparison; no universal law
9	size	0.1	$9.28227118049 \times 10^{-10}$	Sampled finite geometry comparison; no universal law
10	depth	0.1	$9.28227118049 \times 10^{-10}$	Sampled finite geometry comparison; no universal law
11	depth	0.1	$8.80904862722 \times 10^{-10}$	Sampled finite geometry comparison; no universal law
12	depth	0.1	$8.41311299499 \times 10^{-10}$	Sampled finite geometry comparison; no universal law
13	size	0.1	$4.70182795625 \times 10^{-12}$	Exploratory / not independently numerically certified
14	size	0.1	$1.49917374721 \times 10^{-10}$	Sampled finite geometry comparison; no universal law
15	size	0.1	$1.13165420738 \times 10^{-9}$	Sampled finite geometry comparison; no universal law
16	depth	0.1	$1.13165420738 \times 10^{-9}$	Sampled finite geometry comparison; no universal law
17	depth	0.1	$1.07396653345 \times 10^{-9}$	Sampled finite geometry comparison; no universal law
18	depth	0.1	$1.02569923808 \times 10^{-9}$	Sampled finite geometry comparison; no universal law

Units: mm; Hz; dimensionless response. Denominator: Same-frequency matching normal voltage. No fit or universal size/depth exponent.

Full records: Table_S8a.csv.

Table S8b. Separate material-property checks

Table S8b, column panel 1/2. First column is repeated for alignment.

Row	case	frequency_Hz	abs_delta	response_over_primary
1	Grey primary	3000000	$9.28227118049 \times 10^{-10}$	1
2	White comparator	3000000	$5.6224104272 \times 10^{-10}$	0.605714950347
3	Independent epsilon prescription	3000000	$9.9151733657 \times 10^{-10}$	1.06818397921

Table S8b, column panel 2/2. First column is repeated for alignment.

Row	case	lesion_epsilon_ratio
1	Grey primary	1
2	White comparator	1
3	Independent epsilon prescription	1.08858203366

Units: Hz; dimensionless response and ratios. Denominator: Grey Matter primary response. Single-frequency checks; epsilon ratio is independent of conductivity ratio, not negligible.

Full records: Table_S8b.csv.

Table S8c. All matched conductivity-only comparisons

Table S8c, column panel 1/3. First column is repeated for alignment.

Row	frequency_Hz	diameter_mm	depth_mm	RVE_id
1	100000	3	1.5	rve_phi0.1_100000
2	300000	3	1.5	rve_phi0.1_300000
3	1000000	3	1.5	rve_phi0.1_1000000
4	2000000	3	1.5	rve_phi0.1_2000000
5	3000000	3	1.5	rve_phi0.1_3000000
6	5000000	3	1.5	rve_phi0.1_5000000
7	10000000	3	1.5	rve_phi0.1_10000000
8	3000000	1	1.5	size_D1_3000000
9	3000000	2	1.5	size_D2_3000000
10	3000000	3	3	depth_d3_3000000
11	3000000	3	5	depth_d5_3000000

Table S8c, column panel 2/3. First column is repeated for alignment.

Row	frequency_Hz	comparator_id	RVE_abs_response	MODEL_10PCT_abs_response
1	100000	comparator_100000	$9.37031590324 \times 10^{-11}$	$1.86081897003 \times 10^{-11}$
2	300000	comparator_300000	$2.24774770196 \times 10^{-10}$	$6.06611767188 \times 10^{-11}$
3	1000000	comparator_1000000	$5.10951464802 \times 10^{-10}$	$2.27325122302 \times 10^{-10}$
4	2000000	comparator_2000000	$7.76281019633 \times 10^{-10}$	$5.03100931961 \times 10^{-10}$
5	3000000	comparator_3000000	$9.28227118049 \times 10^{-10}$	$8.20870570136 \times 10^{-10}$
6	5000000	comparator_5000000	$1.13165420738 \times 10^{-9}$	$1.57911593345 \times 10^{-9}$
7	10000000	comparator_10000000	$6.28250181878 \times 10^{-10}$	$4.06169643191 \times 10^{-9}$
8	3000000	comparator_D1	$3.85661582694 \times 10^{-12}$	$3.4105687504 \times 10^{-12}$
9	3000000	comparator_D2	$1.2296804699 \times 10^{-10}$	$1.08745854236 \times 10^{-10}$
10	3000000	comparator_d3	$8.80904862722 \times 10^{-10}$	$7.79021494449 \times 10^{-10}$
11	3000000	comparator_d5	$8.41311299499 \times 10^{-10}$	$7.44007228279 \times 10^{-10}$

Table S8c, column panel 3/3. First column is repeated for alignment.

Row	frequency_Hz	Response_RVE_over_Response_10pct
1	100000	5.0355870475
2	300000	3.70541394603
3	1000000	2.24766827189

Table S8c continued

Row	frequency_Hz	Response_RVE_over_Response_10pct
4	2000000	1.54299260907
5	3000000	1.13078377008
6	5000000	0.716637824624
7	10000000	0.154676793899
8	3000000	1.130783781
9	3000000	1.13078376968
10	3000000	1.13078377041
11	3000000	1.13078377134

Units: Hz; mm; dimensionless response/ratio. Denominator: abs(delta_RVE)/abs(delta_10pct). The seven-frequency spectrum and five 3 MHz geometries share one row. No accuracy ranking or normalized spatial-shape novelty.

Full records: Table_S8c.csv.

Table S8d. Geometry feasibility and exclusions

Table S8d, column panel 1/3. First column is repeated for alignment.

Row	lesion_diameter_mm	centroid_depth_mm	centroid_z_mm	volume_mm3
1	1	0.5	5.5	0.523598775598
2	1	1.5	4.5	0.523598775598
3	1	3	3	0.523598775598
4	1	5	1	0.523598775598
5	2	0.5	5.5	4.18879020479
6	2	1.5	4.5	4.18879020479
7	2	3	3	4.18879020479
8	2	5	1	4.18879020479
9	3	0.5	5.5	14.1371669412
10	3	1.5	4.5	14.1371669412
11	3	3	3	14.1371669412
12	3	5	1	14.1371669412
13	4	0.5	5.5	33.5103216383
14	4	1.5	4.5	33.5103216383
15	4	3	3	33.5103216383
16	4	5	1	33.5103216383
17	5	0.5	5.5	65.4498469498
18	5	1.5	4.5	65.4498469498
19	5	3	3	65.4498469498
20	5	5	1	65.4498469498

Table S8d, column panel 2/3. First column is repeated for alignment.

Row	lesion_diameter_mm	minimum_brain_clearance_mm	geometry_status	warning
1	1	0	TANGENT_REQUIRES_BOOLEAN_VALIDATION	LESION_GEOMETRY_WARNING
2	1	1	CONTAINED	Not available
3	1	2.5	CONTAINED	Not available
4	1	4.5	CONTAINED	Not available

Table S8d continued

Row	lesion_diameter_mm	minimum_brain_clearance_mm	geometry_status	warning
5	2	-0.5	INFEASIBLE_OUTSIDE_BRAIN	LESION_GEOMETRY_WARNING
6	2	0.5	CONTAINED	Not available
7	2	2	CONTAINED	Not available
8	2	4	CONTAINED	Not available
9	3	-1	INFEASIBLE_OUTSIDE_BRAIN	LESION_GEOMETRY_WARNING
10	3	0	TANGENT_REQUIRES_BOOLEAN_VALIDATION	LESION_GEOMETRY_WARNING
11	3	1.5	CONTAINED	Not available
12	3	3.5	CONTAINED	Not available
13	4	-1.5	INFEASIBLE_OUTSIDE_BRAIN	LESION_GEOMETRY_WARNING
14	4	-0.5	INFEASIBLE_OUTSIDE_BRAIN	LESION_GEOMETRY_WARNING
15	4	1	CONTAINED	Not available
16	4	3	CONTAINED	Not available
17	5	-2	INFEASIBLE_OUTSIDE_BRAIN	LESION_GEOMETRY_WARNING
18	5	-1	INFEASIBLE_OUTSIDE_BRAIN	LESION_GEOMETRY_WARNING
19	5	0.5	CONTAINED	Not available
20	5	2.5	CONTAINED	Not available

Table S8d, column panel 3/3. First column is repeated for alignment.

Row	lesion_diameter_mm	requested_design_groups	action
1	1	Not available	NOT_SOLVED_MISSING_MACRO_PROPERTIES
2	1	9B	NOT_SOLVED_MISSING_MACRO_PROPERTIES
3	1	Not available	NOT_SOLVED_MISSING_MACRO_PROPERTIES
4	1	Not available	NOT_SOLVED_MISSING_MACRO_PROPERTIES
5	2	Not available	NOT_SOLVED_MISSING_MACRO_PROPERTIES
6	2	9B	NOT_SOLVED_MISSING_MACRO_PROPERTIES
7	2	Not available	NOT_SOLVED_MISSING_MACRO_PROPERTIES
8	2	Not available	NOT_SOLVED_MISSING_MACRO_PROPERTIES
9	3	9C	NOT_SOLVED_MISSING_MACRO_PROPERTIES
10	3	9A;9D;9B;9C	NOT_SOLVED_MISSING_MACRO_PROPERTIES
11	3	9C	NOT_SOLVED_MISSING_MACRO_PROPERTIES

Table S8d continued

Row	lesion_diameter_mm	requested_design_groups	action
12	3	9C	NOT_SOLVED_MISSING_MACRO_PROPERTIES
13	4	Not available	NOT_SOLVED_MISSING_MACRO_PROPERTIES
14	4	9B	NOT_SOLVED_MISSING_MACRO_PROPERTIES
15	4	Not available	NOT_SOLVED_MISSING_MACRO_PROPERTIES
16	4	Not available	NOT_SOLVED_MISSING_MACRO_PROPERTIES
17	5	Not available	NOT_SOLVED_MISSING_MACRO_PROPERTIES
18	5	9B	NOT_SOLVED_MISSING_MACRO_PROPERTIES
19	5	Not available	NOT_SOLVED_MISSING_MACRO_PROPERTIES
20	5	Not available	NOT_SOLVED_MISSING_MACRO_PROPERTIES

Units: mm; geometric status. Denominator: Containment rule in S8. D4/D5 at depth1.5 and D3 at depth0.5 are not assigned responses.

Full records: Table_S8d.csv.

At 3 MHz the comparator ratios across sampled geometries range from 1.130783769679912 to 1.1307837810006602. Thus the demonstrated distinction is spectral, not a change in normalized spatial-response shape. The comparator changes conductivity only and is not a full reproduction of the dual-property model of González et al. [8].

S9. Matched finite sensitivities and RVE reproducibility

The common family-B baseline is $(\phi_0, \kappa_0) = (0.10, 0.60)$. For each parameter p, the other parameter is fixed and

$$S_p^{(h)} = \frac{\sigma_B(p_0(1+h)) - \sigma_B(p_0(1-h))}{2h\sigma_B(\phi_0, \kappa_0)}, \qquad Q^{(h)} = |S_\phi^{(h)}|/|S_\kappa^{(h)}|. \tag{S5}$$

The $h = 0.50$ calculation uses the original bottleneck CSV, cross-checked against Table S4f to relative tolerance 5×10^{-14} (publication-export rounding). New direct FEM geometry runs provide $h = 0.10$ and 0.05: $\phi = 0.09/0.11$ and $0.095/0.105$ at $\kappa = 0.60$; $\kappa = 0.54/0.66$ and $0.57/0.63$ at $\phi = 0.10$, plus the repeated baseline. Nine geometries at five frequencies give 45 new frequency solutions. No interpolated values enter these sensitivities. Baseline values, the four paired conductivities and the denominators are included in matched_sensitivity_all.csv.

The repeated baseline differs from the original by at most 1.76×10^{-5} relatively, reflecting a new mesh/solve rather than a changed material baseline. Each finite-step calculation uses its own common baseline; the old $h = 0.50$ calculation retains the original denominator. The rank and sign pattern persist across the three steps, but non-monotonic step dependence and independently generated meshes preclude claiming convergence to an infinitesimal derivative. No mesh error bound is assigned to these derivative-like estimates.

Table S9a. Signed matched sensitivities. All S and Q values are dimensionless; f is in MHz.

h	f	σ_0 (S m^{-1})	S_ϕ	S_κ	Q
0.05	0.001	0.067271	1.041058	0.064468	16.1485
0.05	0.1	0.069727	0.989134	0.057771	17.1216
0.05	1	0.213972	0.324111	-0.045086	7.1887
0.05	3	0.503620	0.161711	-0.037999	4.2557
0.05	10	0.844687	0.017422	-0.006278	2.7753
0.10	0.001	0.067271	1.027859	0.069833	14.7188
0.10	0.1	0.069727	0.976416	0.062024	15.7426
0.10	1	0.213972	0.320744	-0.045833	6.9981
0.10	3	0.503620	0.162178	-0.035513	4.5668
0.10	10	0.844687	0.020093	-0.006469	3.1062
0.50	0.001	0.067272	1.026600	0.072884	14.0853
0.50	0.1	0.069728	0.971549	0.064811	14.9904
0.50	1	0.213973	0.345794	-0.045151	7.6587
0.50	3	0.503621	0.166835	-0.035710	4.6719
0.50	10	0.844686	0.019992	-0.006807	2.9370

The old unequal finite comparisons are reproduced below as secondary descriptive effects. The ECS endpoint change 0.20 to 0.05 and the maximum selected topology correction do not share perturbation magnitude or family. Their ratios are not normalized sensitivities and no longer support the main ranking. The area-preserving arrangement comparison remains a discrete comparison without an imposed continuous coordinate.

The RVE is a terminal-driven electroquasistatic model with total current conservation, positive passive admittivity under $\exp(+j\omega t)$, and a finite complex surface-admittance membrane. Main section 2.3 supplies the derivation and boundary/interface conditions. The serialized production topology-A model explicitly records quadratic potential order and BiCGStab, with stored iterative relative-residual setting 0.01. That configured setting is not a measured error bound; actual residuals and mesh checks must be considered separately. The topology-B builder uses COMSOL's generated frequency solver sequence; its source and execution logs are included, without assigning an unverified factorization name. Head-scale MUMPS/PARDISO comparisons concern a different formulation.

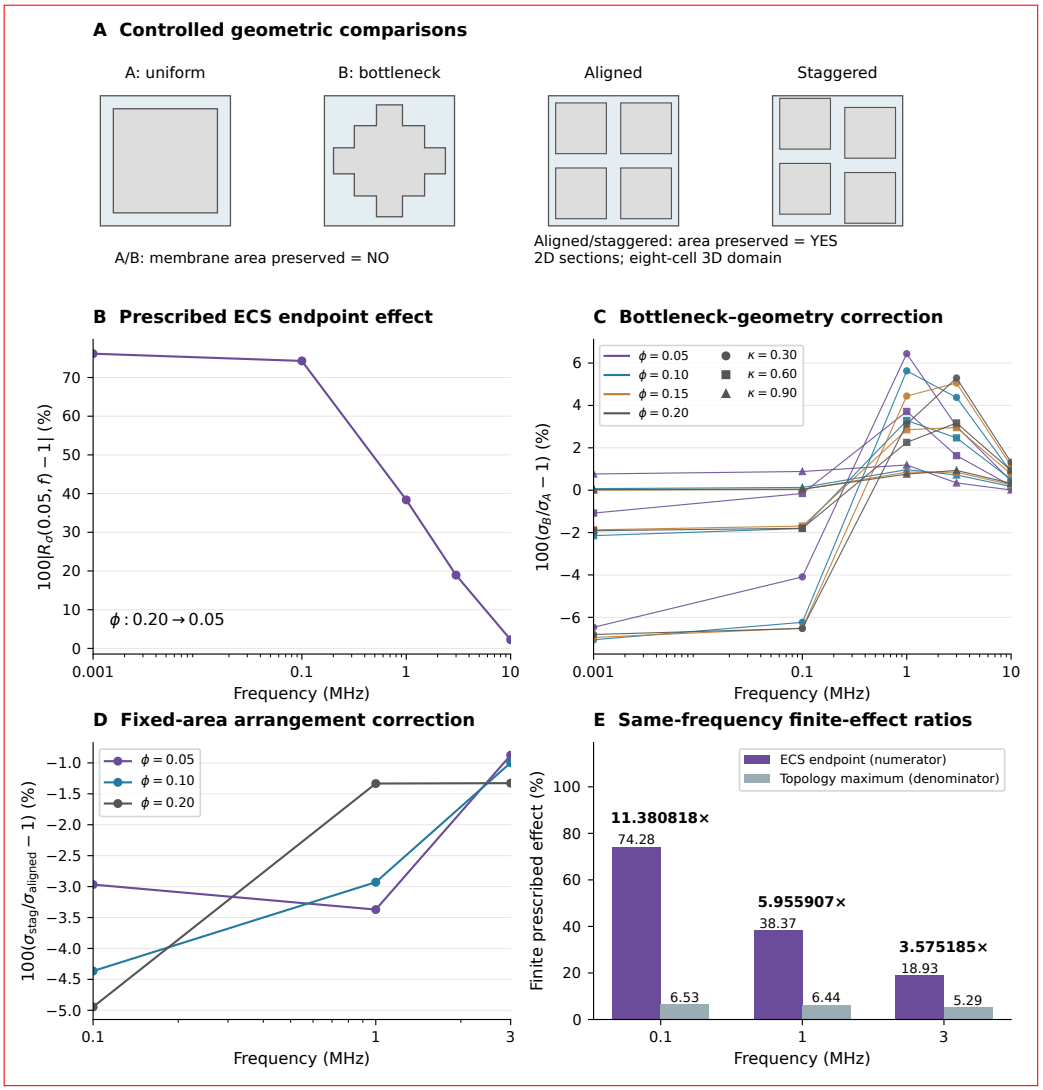


Figure S4. Original unequal finite-effect comparison, retained for traceability only. Panel E's 11.380818, 5.955907 and 3.575185 ratios are secondary endpoint-effect ratios, not the revised matched sensitivities. The principal analysis is Table S9a and revised main Figure 3.

Production meshes use free tetrahedra and four membrane boundary layers; the saved refined A meshes use six layers. At $\phi = 0.20/0.05$, production element counts are 35,176/560,681 and refined counts 40,496/646,711. Geometry construction and material selection are identical between each production/refined pair. For A, $g_A = (L - L(1 - \phi)^{1/3})/2$; for B, $g_{neck} = \kappa g_A$. At the compressed $\phi = 0.05$ endpoint, $g_A = 0.07359$ μm, and $g_{neck} = 0.02208$ μm for $\kappa = 0.30$. Thin-interface validity is less secure at these smallest gaps and at corners than the small global thickness/size ratio alone suggests. The calculations solve the interface model; they do not validate it against a volumetrically resolved membrane at each corner.

The retained scripts are stage2B_model_builder.java, RevisionLocal.java and new_results.py. The builder differs from the original only in output destination and visibility of the reused method; no geometric or electrical equations were changed. Raw console records retain geometry volumes, membrane area, mesh counts and passive-sign checks. rve_scale_checks.csv supplies the independent $|k|L$ and thickness/gap calculations. All new solves ran sequentially in COMSOL 6.4 with four threads after a documented resource check.

S10. Staged electrical robustness and directly resolved crossing brackets

For each electrical state E, $C(f,E) = \sigma(0.05,f,E)/\sigma(0.20,f,E) - 1$. The separate fixed-reference ratio divides by the *original stored* $\sigma(0.20,f,E_0)$. These are retained as different columns, never inferred from each other. The factorial and membrane branches below supply 140 new direct frequency solves (14 parameter sets, two structural endpoints and five frequencies). Conductivities are in $\mathrm{S\,m^{-1}}$; $r_C = C_m/C_{m0}$ and $r_G = G_m/G_{m0}$, with $C_{m0} = 0.0088541878\ \mathrm{F\,m^{-2}}$ and $G_{m0} = 20\ \mathrm{S\,m^{-2}}$. Both bulk relative permittivities remain 80.

N4 repeats the nominal parameters with new solves; original E0 reused the archived solution. Their maximum conductivity difference across the two endpoints/five frequencies is 0.0472%. This repeat difference is disclosed, not treated as bitwise recovery or a solver error bound. R_{total} always retains the original E0 denominator; new R_{matched} pairs use the new same-state solutions.

Table S10a. Exact newly solved electrical parameter sets. N4 reproduces the nominal electrical state; N3 reproduces E3.

Case	σ_i	σ_e	r_C	r_G
N0	0.75	0.75	1	1
N1	0.75	1	1	1
N2	0.75	1.25	1	1
N3	1	0.75	1	1
N4	1	1	1	1
N5	1	1.25	1	1
N6	1.25	0.75	1	1
N7	1.25	1	1	1
N8	1.25	1.25	1	1
N9	1	0.75	0.75	1
N10	1	0.75	1.25	1
N11	1	0.75	1	0.1
N12	1	0.75	1	10
N13	0.3	1.5	1.2	1

Table S10b. Direct matched structural response $100C$ (percent). Positive values denote an increase after compression under the same electrical state.

Case	0.001 MHz	0.1 MHz	1 MHz	3 MHz	10 MHz
N0	-76.13741	-72.90085	-34.51067	-12.85835	-1.24471
N1	-76.16480	-73.99891	-37.22440	-17.50782	-5.60148
N2	-76.18124	-74.58206	-39.78244	-21.19493	-9.25040
N3	-76.13568	-73.27743	-36.07428	-14.96866	+1.85296
N4	-76.16347	-74.29189	-38.37768	-18.91978	-2.22975
N5	-76.18016	-74.82096	-40.79388	-22.30489	-5.60448
N6	-76.13397	-73.50629	-37.24385	-17.52781	+3.53575
N7	-76.16215	-74.46942	-39.33270	-21.03399	-0.37788
N8	-76.17909	-74.96547	-41.72391	-24.01661	-3.56919
N9	-76.13581	-74.48963	-39.62824	-21.75869	-0.13490
N10	-76.13551	-71.80031	-33.18006	-9.99049	+2.78184
N11	-76.22903	-73.36142	-36.08409	-14.96997	+1.85310
N12	-75.21581	-72.44918	-35.97645	-14.95561	+1.85148
N13	-76.19368	-72.81881	-40.53446	-31.50806	-29.40069

S10.1. Evidence for parameter choices and limits of biological interpretation

The 0.75–1.25 $\mathrm{S\,m^{-1}}$ factorial is an independently varied neighborhood of the nominal benchmark, not a measured tissue interval. The conductance factors 0.1/10 are deliberately

broad diagnostic stress factors. Neither has a physiological probability measure. The capacitance branches span 0.00664064–0.01106773 F m^{-2}; they test coupling strength around the original membrane benchmark.

Preparation-specific context comes from Zhou et al. [16]: dielectrophoresis crossover fitting in isolated mouse hippocampal cells gave neuronal cytoplasmic conductivity 0.75–0.95 S m^{-1} and effective membrane capacitance 0.010–0.012 F m^{-2} (their Table 4). Their glial discussion examined 0.3–0.4 S m^{-1}, with an approximately 0.35 S m^{-1} estimate. These are preparation/model-dependent estimates, not paired normal/ischemic values. N13's $\sigma_i = 0.30$ and $C_m = 0.0106250$ have that order-of-magnitude context; $\sigma_e = 1.50$ and the retained bulk permittivity are analyst assumptions, not values established by that paper. N13 is therefore an illustrative stronger-contrast case, not a calibrated neuron or glial tissue state.

Bedard et al. [19] studied 1–10 kHz impedance in primary cultures and acute slices, while Yang et al. [20] measured ex-vivo rabbit bulk tissue over 10 Hz–1 MHz. Neither provides a matched four-parameter distribution for 10 MHz ischemic tissue. The present evidence supports conditional positive and negative examples and sensitivity to membrane coupling. It does not establish whether a reversal occurs in vivo or persists throughout a physiological uncertainty region. This remains a specific biological limitation, not an inferred negative experimental result.

The companion electrical_new_raw.csv retains all 140 conductivities/permittivities. electrical_new_response.csv retains all 70 matched comparisons, their fixed-reference ratios, and real/imaginary parts of γ_i/γ_e and Ly_m/γ_e. The original E0–E10 scenarios are separately recalculated in existing_electrical_recalculated.csv; no interpolated original head-grid values are counted as new FEM solutions.

S10.2. Additional direct frequencies and mesh comparison

After the first grid identified the E3 crossing, four additional frequencies (5, 7, 8 and 9 MHz) were solved at each structural endpoint on both saved meshes: 16 new frequency solutions. The electrical parameters remain $(\sigma_i, \sigma_e, r_C, r_G) = (1, 0.75, 1, 1)$. The frequency parameter was updated in both study and solver sequences. Original MPH files were loaded read-only; outputs were captured in separate revision logs.

Table S10c. Direct crossing checks. Conductivities are in S m^{-1}. These points, rather than a fitted interpolant, determine the sign brackets.

Mesh	f (MHz)	$\sigma_{0.20}$	$\sigma_{0.05}$	100C (%)
medium	5	0.654112644	0.622791996	-4.788265
medium	7	0.738798966	0.734306330	-0.608100
medium	8	0.767387298	0.771330982	+0.513911
medium	9	0.789914213	0.800142848	+1.294905
fine	5	0.653958026	0.623026030	-4.729967
fine	7	0.738638689	0.734569177	-0.550948
fine	8	0.767225293	0.771603254	+0.570623
fine	9	0.789751070	0.800422618	+1.351255

The fine mesh directly brackets a sign change between 7 and 8 MHz. The medium mesh directly brackets a sign change between 7 and 8 MHz. No exact crossing frequency is claimed, and no interpolation of this bracket is supplied as a new solution. The old 10 MHz refined E3 result (+1.90899%) and the new near-crossing checks address numerical persistence only at the selected parameter state. Main Figure 7D marks intervals between opposite-sign conductivity nodes; it does not infer a continuously validated multidimensional phase boundary. No new head FEM calculations were run for these added electrical states.

S10.3. Interpolation reconciliation and targeted numerical checks

At 5 MHz, historical E3 interpolation gave $R_{matched} = 0.923089328491$ ($C = -7.691067\%$). The source algorithm interpolated each total ratio linearly in log frequency between 3 and 10 MHz, then divided the interpolated endpoint ratios. Direct E3 production/fine solutions give $C = -4.788265\%/-4.729967\%$. Identical topology-A geometry and electrical assignments, the same matched-denominator definition and the small direct mesh difference identify frequency interpolation as the dominant discrepancy, rather than rounding. Original interpolated ratios have no uniquely prescribed absolute conductivity at 5 MHz; no artificial absolute values are assigned to them. Current direct R_{total} uses the new direct E0 reference $\sigma(0.20) = 0.6998700793410687$ S/m. The 10 MHz historical denominator is unchanged.

Table S10d. E3 5 MHz reconciliation. Conductivity in S/m. Historical absolute entries are undefined by the original ratio interpolation. Full precision and denominator identities are in E3_5MHz_comparison.csv.

Method	$\sigma_{.20}$	$\sigma_{.05}$	$R_{matched}$	C (%)
Historical interpolation	–	–	0.9230893285	-7.691067
Direct, medium	0.654112644	0.622791996	0.9521173486	-4.788265
Direct, fine	0.653958026	0.623026030	0.9527003338	-4.729967

Two targeted direct E0 solves gave $\sigma(0.05) = 0.6374198745930665$ S/m and $R_\sigma = 0.9107688604050634$, replacing the historical 0.8815302230145321 only at this structural/frequency point. The corresponding paired head update is reported in S11. Other interpolated microscopic inputs remain explicitly marked.

Table S10e. N9 at 10 MHz. All four signs are negative; stricter settings materially improve agreement between meshes. Conductivity in S/m.

Mesh / solver	$\sigma_{.20}$	$\sigma_{.05}$	$R_{matched}$	C (%)
medium / production archived	0.7493543568	0.7483435144	0.9986510489	-0.1348951
fine / production	0.7491931066	0.7486120470	0.9992244195	-0.0775580
fine / strict	0.7493104122	0.7479933138	0.9982422526	-0.1757747
medium / strict	0.7493111062	0.7479931071	0.9982410522	-0.1758948

Production BiCGStab settings were stationary tolerance 0.001 and iterative residual acceptance 0.01; the latter is not a conductivity error percentage. Stricter solves used 10^{-7} and 10^{-6}, respectively. Production endpoint meshes had 35,176/560,681 elements and four membrane boundary layers; fine meshes had 40,496/646,711 and six layers. Strict endpoint linear residuals were $2.3 \times 10^{-11}/9.2 \times 10^{-11}$ (production mesh) and $8.9 \times 10^{-11}/1.3 \times 10^{-10}$ (fine mesh). All runs completed. Strict mesh-to-mesh C changed by $1.20041484 \times 10^{-6}$, or 0.0001200415 percentage points. The N9 negative sign persists in these tests, while its production-setting magnitude is solver-sensitive. This is a discretization/solver check, not validation of the thin-membrane physical reduction.

S10.4. *Parameter provenance and evidence status*

Table S10f. Compartment parameter provenance. Values are not a joint physiological distribution.

Parameter	Benchmark / tested values	Evidence status
σ_i (S/m)	1; factorial .75/1/1.25; illustrative .30	Zhou et al. [16]: neuronal .75–.95 inferred from primary mouse-cell DEP crossover fitting; glial .3–.4 context. Factorial endpoints remain stress choices.
σ_e (S/m)	1; .75/1/1.25; illustrative 1.50	Analyst-selected. No verified acute-ischemia compartment interval; suspension-medium and tissue ECS conductivities are not interchangeable.
C_m (F/m^2)	.00885419; .00664064–.01106773; illustrative .01062503	Zhou et al. [16]: inferred .010–.012 in isolated mouse hippocampal cells. Does not justify every stress endpoint or an ischemic range.
G_m (S/m^2)	20; 2–200	Assumed passive benchmark and stress factors. No verified disease-specific measurement assigned.

Zhou et al. used measured DEP crossover behavior in varying suspension media and model fitting, not a matched in-tissue impedance spectrum. The accessible primary record verifies the inferred intervals; a complete numeric experimental drive-frequency range was not independently recoverable from the accessible primary record and is not assumed to equal the model's 1 kHz–10 MHz band. Bedard et al. [19] measured impedance in primary cultures, acute slices and artificial CSF over 1–10 kHz. Their electrode-path dependence and mean-field interpretation do not supply a transferable MHz ECS conductivity interval. Rabbit bulk data [20] cover 10 Hz–1 MHz without uniquely identifying compartments. These preparations are not pooled. The evidence status and unresolved frequency metadata are stated in Table S10f.

S11. Independent layered-sphere benchmark and raw-voltage audit

S11.1. Radial matching and receiver observable

The additional independent reference uses an axisymmetric vector potential $A_\phi = \sum_{\ell\geq 1} a_\ell(r) P_\ell^1(\cos\theta)$. In a nonmagnetic homogeneous layer,

$$a_\ell'' + \frac{2}{r}a_\ell' + \left[k^2 - \frac{\ell(\ell+1)}{r^2}\right]a_\ell = 0, \qquad k^2 = -\mathrm{j}\omega\mu_0(\sigma + \mathrm{j}\omega\varepsilon_0\varepsilon_r). \tag{S6}$$

Regular core solutions use $j_\ell(kr)$; each shell uses a combination of j_ℓ and y_ℓ. At each interface, a_ℓ and $(a_\ell + ra_\ell')/\mu_0$ are continuous. The latter expresses tangential magnetic-field continuity. Defining $Y_\ell = (a_\ell + ra_\ell')/a_\ell$, radial transfer proceeds through normalized two-by-two Bessel matrices. In the source-free exterior region between the sphere and the source, use the surface-normalized basis

$$a_\ell^{\mathrm{ext}}(r) = A_\ell(r/R)^\ell + D_\ell(R/r)^{\ell+1}. \tag{S7}$$

Both coefficients have vector-potential units. At $r = R$, $a = A_\ell + D_\ell$ and $a + ra' = (\ell+1)A_\ell - \ell D_\ell$, so

$$Y_\ell(R) = \frac{(\ell+1)A_\ell - \ell D_\ell}{A_\ell + D_\ell}, \qquad q_\ell = \frac{D_\ell}{A_\ell} = \frac{\ell + 1 - Y_\ell(R)}{Y_\ell(R) + \ell}. \tag{S8}$$

Thus Y_ℓ and q_ℓ are dimensionless. If the unnormalized basis $\widetilde{A}_\ell r^\ell + \widetilde{D}_\ell r^{-\ell-1}$ is used instead, $\widetilde{D}_\ell/\widetilde{A}_\ell = R^{2\ell+1}q_\ell$, with units of length$^{2\ell+1}$. The implementation projects the incident amplitude at R and multiplies it by $q_\ell(R/r)^{\ell+1}$ for the scattered field. Its numerical algorithm therefore already uses the normalized convention; this clarification changes no computed coefficient or voltage. The primary loop field is evaluated directly at the receiver, outside the incident regular expansion's source-free convergence region. Incident coefficients are projected from the independent filament-loop vector-potential quadrature on the outer spherical surface, using 160-point Gauss–Legendre angular integration. The field is evaluated at the receiver location and converted with $V = -\mathrm{j}\omega 2\pi r_{RX} A_\phi$. The 24-term result is the reported reference; 12/32 terms test truncation. This is a newly implemented radial spherical expansion, not a claimed reproduction of every full-wave feature of Liu and Crozier [15]'s DP/DGF formulation.

The matched parameters are radii 6.0/6.3/6.7/7.2 mm; Grey Matter/CSF/cortical skull/scalp complex properties from the same processed IT'IS table as COMSOL; Tx/Rx loop radius 7.2 mm at $z = -10/+10$ mm; Tx current 0.010 A; and $\exp(+\mathrm{j}\omega t)$. The independent exterior is unbounded, whereas FEM uses magnetic insulation at 120 mm. The reference loop is a filament, whereas the FEM transmitter has radius 0.1 mm circular wire section. Interior complex properties retain conduction and displacement current; the reference omits exterior vacuum displacement current. The independent check is therefore carefully matched but not algebraically identical to the finite-domain FEM problem.

Setting all four layers to the same brain material recovers the separately implemented homogeneous-sphere reference with maximum relative secondary difference 4.80×10^{-9} over seven frequencies. Differences between 24 and 32 terms are at floating-point scale. These checks establish implementation consistency, not experimental truth. Receiver $A_\phi = V/(-\mathrm{j}\omega 2\pi r_{RX})$ and $E_\phi = -\mathrm{j}\omega A_\phi$ are exported alongside the complex voltages. They check the complex field at the receiver, not an internal field map.

Only the existing 5 MHz FEM air run permits the explicitly matched secondary comparison. At other frequencies, this revision reports total voltage and the independent reference's secondary response, without fabricating a missing FEM air run. The approx-

Table S11a. Seven-frequency total receiver-voltage comparison, real and imaginary parts in volts. Full precision is retained in the CSV.

f (MHz)	Re FEM	Im FEM	Re reference	Im reference
0.1	$-2.069389 \times 10^{-12}$	-2.990244×10^{-6}	$-2.075285 \times 10^{-12}$	-3.008789×10^{-6}
0.3	$-1.899252 \times 10^{-11}$	-8.970734×10^{-6}	$-1.904657 \times 10^{-11}$	-9.026368×10^{-6}
1	$-2.194898 \times 10^{-10}$	-2.990247×10^{-5}	$-2.201141 \times 10^{-10}$	-3.008792×10^{-5}
2	$-9.218755 \times 10^{-10}$	-5.980509×10^{-5}	$-9.244989 \times 10^{-10}$	-6.017596×10^{-5}
3	-2.171578×10^{-9}	-8.970793×10^{-5}	-2.177762×10^{-9}	-9.026420×10^{-5}
5	-6.535941×10^{-9}	-1.495145×10^{-4}	-6.554567×10^{-9}	-1.504414×10^{-4}
10	-3.006894×10^{-8}	-2.990375×10^{-4}	-3.015456×10^{-8}	-3.008895×10^{-4}

Table S11b. Total complex discrepancy $|V_{FEM} - V_{ref}|/|V_{ref}|$ and absolute voltage difference.

f (MHz)	Relative (%)	Absolute (V)
0.1	0.6163484	1.854462×10^{-8}
0.3	0.6163477	5.563381×10^{-8}
1	0.6163399	1.854438×10^{-7}
2	0.6163141	3.708730×10^{-7}
3	0.6162715	5.562725×10^{-7}
5	0.6161356	9.269231×10^{-7}
10	0.6155024	1.851982×10^{-6}

Table S11c. Distinct 5 MHz complex metrics. Air entries have units volts; sphere/layered entries are dimensionless secondary responses $(V_{tissue} - V_{air})/V_{air}$. Each implementation uses its own air reference.

Metric	Re FEM	Im FEM	Re reference	Im reference
Air	0	-1.495125×10^{-4}	0	-1.504394×10^{-4}
Sphere	1.563996×10^{-5}	-2.785728×10^{-5}	1.562222×10^{-5}	-2.776503×10^{-5}
Layered	1.304297×10^{-5}	-4.371500×10^{-5}	1.303378×10^{-5}	-4.356947×10^{-5}

Table S11d. Errors of the correctly matched metrics in Table S11c. Absolute-difference units follow that table.

Metric	Relative (%)	Absolute difference
Air total voltage	0.6161365	9.269124×10^{-7}
Homogeneous secondary	0.2948769	9.394272×10^{-8}
Layered secondary	0.3206540	1.458246×10^{-7}

imately 0.616% total-voltage discrepancy contains baseline coupling differences. The 0.294877% homogeneous and 0.3207% layered secondary errors concern material-induced baseline response. Neither is a lesion-difference error bar; the very small lesion quantity instead requires the current paired convergence checks in S11e–f (historical checks in S7). MUMPS/PARDISO remains an alternate factorization check of one physical model.

S11.2. Historical interpolated-input lesion voltage

For the superseded interpolated-input calculation, the raw 5 MHz normal voltage is $-6.5359409906693030 \times 10^{-9} - \mathrm{j}\,1.4951448530076364 \times 10^{-4}$ V, and the lesion voltage is $-6.5356612826942400 \times 10^{-9} - \mathrm{j}\,1.4951448530081682 \times 10^{-4}$ V. Double-precision round-trip CSV parsing is necessary because a tiny amplitude change is obtained by subtracting nearly equal magnitudes. The raw-log values were cross-checked before recalculation.

S11.3. Direct-input 5 MHz paired head update

The historical interpolation produced $|\delta| = 1.8707751244888244 \times 10^{-9}$ and $|\Delta V| =$ 0.279708 pV. Direct RVE input yields the current quantities in Table S11e, approximately 24.68% smaller in complex magnitude. The updated nominal grid has its largest sampled response at 3 MHz ($1.5538780759535157 \times 10^{-9}$). The local checks below certify only separation from the tested differences at the updated 5 MHz reference, not the sampled 3 MHz maximum.

Table S11e. Current direct-input 5 MHz paired reference. Historical interpolated-input values remain in S7 and the comparison CSV.

Quantity	Value
$\lvert V_{normal}\rvert$ (V)	0.000149514485444
$\lvert\Delta V\rvert$ (V)	$2.10675350905 \times 10^{-13}$
$\lvert\delta\rvert$	$1.40906314382 \times 10^{-9}$
Phase change (rad)	$1.40906312752 \times 10^{-9}$
Relative amplitude change	$2.14273043753 \times 10^{-13}$
Local numerical separation factor	164.53285513

The relative amplitude change is reported for definition/traceability, not as independently numerically resolved. The current local separation factor 164.532855 compares $|\delta|$ with selected numerical differences only; it does not include a receiver bandwidth, sensor noise, coupling drift, positioning error or background interference. No conclusion of experimental detectability or impossibility is drawn.

Table S11f. Updated paired complex differences at the direct-input 5 MHz reference. Full complex voltages and current records are in head_direct5_raw.csv and head_direct5_comparison.csv.

Check	$\lvert\delta_{check} - \delta_{medium}\rvert$	Relative difference (%)
air90	$8.56402292844 \times 10^{-12}$	0.607781345
fine	$8.13347778886 \times 10^{-13}$	0.0577225927
pardiso	$1.86725760641 \times 10^{-14}$	0.00132517667

S11.4. Files and reproducibility

The revision archive includes original-source copies, the independent recalculate.py implementation, raw COMSOL console logs, the archived and targeted Java drivers, the minimally adjusted topology-B builder, all derived CSVs, plotting scripts and source/reference audits. The 140 electrical-grid, 45 local-sensitivity and 16 direct crossing frequency solutions total 201 new RVE solutions. Independent analytical evaluations are counted separately and were followed by eight targeted RVE solutions (two direct E0 and six N9

checks) and eight head frequency solutions (normal/lesion pairs in four numerical configurations) for the direct-input 5 MHz update. Thus 209 new RVE frequency solutions and eight head frequency solutions are documented across the revision and final reconciliation. Repeated exports and analytical evaluations are not counted as FEM solves. Native existing MPH files remain at their original recorded project paths; their hashes and source paths are included in the audit, and the commercial COMSOL license is required to rerun those models. The clean manuscript sources contain all prose in a single main TeX file, and the supplementary sources likewise form one TeX file. No original simulation output was overwritten.

References

1. Perez-Pinzon, M.A.; Tao, L.; Nicholson, C. Extracellular potassium, volume fraction, and tortuosity in rat hippocampal CA1, CA3, and cortical slices during ischemia. *Journal of Neurophysiology* **1995**, *74*, 565–573. https://doi.org/10.1152/jn.1995.74.2.565.
2. Pauly, H.; Schwan, H.P. Über die Impedanz einer Suspension von kugelförmigen Teilchen mit einer Schale. *Zeitschrift für Naturforschung B* **1959**, *14*, 125–131. https://doi.org/10.1515/znb-1959-0213.
3. Garnett, J.C.M. XII. Colours in metal glasses and in metallic films. *Philosophical Transactions of the Royal Society of London. Series A, Containing Papers of a Mathematical or Physical Character* **1904**, *203*, 385–420. https://doi.org/10.1098/rsta.1904.0024.
4. Bruggeman, D.A.G. Berechnung verschiedener physikalischer Konstanten von heterogenen Substanzen. I. Dielektrizitätskonstanten und Leitfähigkeiten der Mischkörper aus isotropen Substanzen. *Annalen der Physik* **1935**, *416*, 636–664. https://doi.org/10.1002/andp.19354160705.
5. Markel, V.A. Introduction to the Maxwell Garnett approximation: tutorial. *Journal of the Optical Society of America A* **2016**, *33*, 1244–1256. https://doi.org/10.1364/JOSAA.33.001244.
6. Poignard, C. About the transmembrane voltage potential of a biological cell in time-harmonic regime. *ESAIM: Proceedings* **2009**, *26*, 162–179. https://doi.org/10.1051/proc/2009012.
7. Gabriel, S.; Lau, R.W.; Gabriel, C. The dielectric properties of biological tissues: III. Parametric models for the dielectric spectrum of tissues. *Physics in Medicine and Biology* **1996**, *41*, 2271–2293. https://doi.org/10.1088/0031-9155/41/11/003.
8. González, C.A.; Villanueva, C.; Vera, C.; Flores, O.; Reyes, R.D.; Rubinsky, B. The detection of brain ischaemia in rats by inductive phase shift spectroscopy. *Physiological Measurement* **2009**, *30*, 809–819. https://doi.org/10.1088/0967-3334/30/8/006.
9. Gonzalez, C.A.; Valencia, J.A.; Mora, A.; Gonzalez, F.; Velasco, B.; Porras, M.A.; Salgado, J.; Polo, S.M.; Hevia-Montiel, N.; Cordero, S.; et al. Volumetric Electromagnetic Phase-Shift Spectroscopy of Brain Edema and Hematoma. *PLoS ONE* **2013**, *8*, e63223. https://doi.org/10.1371/journal.pone.0063223.
10. Morris, A.; Griffiths, H.; Gough, W. A numerical model for magnetic induction tomographic measurements in biological tissues. *Physiological Measurement* **2001**, *22*, 113–119. https://doi.org/10.1088/0967-3334/22/1/315.
11. Simard, J.M.; Kent, T.A.; Chen, M.; Tarasov, K.V.; Gerzanich, V. Brain oedema in focal ischaemia: molecular pathophysiology and theoretical implications. *The Lancet Neurology* **2007**, *6*, 258–268. https://doi.org/10.1016/S1474-4422(07)70055-8.
12. Syková, E.; Nicholson, C. Diffusion in Brain Extracellular Space. *Physiological Reviews* **2008**, *88*, 1277–1340. https://doi.org/10.1152/physrev.00027.2007.
13. Zolgharni, M.; Ledger, P.D.; Armitage, D.W.; Holder, D.S.; Griffiths, H. Imaging cerebral haemorrhage with magnetic induction tomography: numerical modelling. *Physiological Measurement* **2009**, *30*, S187–S200. https://doi.org/10.1088/0967-3334/30/6/S13.
14. Zolgharni, M.; Ledger, P.D.; Griffiths, H. Forward modelling of magnetic induction tomography: a sensitivity study for detecting haemorrhagic cerebral stroke. *Medical & Biological Engineering & Computing* **2009**, *47*, 1301–1313. https://doi.org/10.1007/s11517-009-0541-1.
15. Liu, F.; Crozier, S. Electromagnetic fields inside a lossy, multilayered spherical head phantom excited by MRI coils: models and methods. *Physics in Medicine and Biology* **2004**, *49*, 1835–1851. https://doi.org/10.1088/0031-9155/49/10/001.
16. Zhou, T.; Ming, Y.; Perry, S.F.; Tatic-Lucic, S. Estimation of the physical properties of neurons and glial cells using dielectrophoresis crossover frequency. *Journal of Biological Physics* **2016**, *42*, 571–586. https://doi.org/10.1007/s10867-016-9424-5.
17. Berre, N.; Rognes, M.E.; Massing, A. Cut Finite Element Discretizations of Cell-by-Cell EMI Electrophysiology Models. *SIAM Journal on Scientific Computing* **2024**, *46*, B527–B553. https://doi.org/10.1137/23M1580632.
18. Gratiy, S.L.; Halnes, G.; Denman, D.; Hawrylycz, M.J.; Koch, C.; Einevoll, G.T.; Anastassiou, C.A. From Maxwell's equations to the theory of current-source density analysis. *European Journal of Neuroscience* **2017**, *45*, 1013–1023. https://doi.org/10.1111/ejn.13534.
19. Bedard, C.; Piette, C.; Venance, L.; Destexhe, A. Extracellular and intracellular components of the impedance of neural tissue. *Biophysical Journal* **2022**, *121*, 869–885. https://doi.org/10.1016/j.bpj.2022.02.022.

20. Yang, L.; Zhang, G.; Song, J.; Dai, M.; Xu, C.; Dong, X.; Fu, F. Ex-Vivo Characterization of Bioimpedance Spectroscopy of Normal, Ischemic and Hemorrhagic Rabbit Brain Tissue at Frequencies from 10 Hz to 1 MHz. *Sensors* **2016**, *16*, 1942. https://doi.org/10.3390/s16111942.
21. Scharfetter, H.; Lackner, H.K.; Rosell, J. Magnetic induction tomography: hardware for multi-frequency measurements in biological tissues. *Physiological Measurement* **2001**, *22*, 131–146. https://doi.org/10.1088/0967-3334/22/1/317.
22. Gabriel, C.; Gabriel, S.; Corthout, E. The dielectric properties of biological tissues: I. Literature survey. *Physics in Medicine and Biology* **1996**, *41*, 2231–2249. https://doi.org/10.1088/0031-9155/41/11/001.
23. Gabriel, S.; Lau, R.W.; Gabriel, C. The dielectric properties of biological tissues: II. Measurements in the frequency range 10 Hz to 20 GHz. *Physics in Medicine and Biology* **1996**, *41*, 2251–2269. https://doi.org/10.1088/0031-9155/41/11/002.
24. Baumgartner, C.; Hasgall, P.A.; Di Gennaro, F.; Neufeld, E.; Lloyd, B.; Gosselin, M.C.; Payne, D.; Klingenböck, A.; Kuster, N. IT'IS Database for thermal and electromagnetic parameters of biological tissues, 2025. Version 5.0, 21 August 2025. IT'IS Foundation, https://doi.org/10.13099/VIP21000-05-0.